SEMMELWEIS EGYETEM

DOKTORI ISKOLA

Ph.D. értekezések

2407.

HADJADJ LEILA

A vérkeringési rendszer normális és kóros működésének mechanizmusai

című program

Programvezető: Dr. Benyó Zoltán, egyetemi tanár

Témavezető: Dr. Várbíró Szabolcs, egyetemi docens

Effect of hyperandrogenism and vitamin D deficiency on metabolic parameters and coronary artery function in female rats

PhD thesis

Leila Hadjadj MD

Doctoral School of Basic and Translational Medicine

Semmelweis University

Supervisor:
Szabolcs Várbíró, MD, Ph.D, Med. Habil.

Official reviewers:
Zsolt Nagy MD, Ph.D
Gergely Gősi MD, Ph.D

Head of the Final Examination Committee:
István Pénzes MD, Ph.D, DSc

Members of the Final Examination Committee:
Ádám László MD, Ph.D, Med. Habil.
Péter Studinger MD, Ph.D

Budapest
202

CONTENTS

Abbreviations

A_{cs} – Cross-sectional area of the arteriole

AE – Androgen excess

Akt – Protein kinase B, serine/threonine-specific protein kinase

AMH – Anti-Müllerian hormone

ANOVA – Analysis of variance

Ca free – Calcium-free solution

CV risk – Cardiovascular risk

cJUN – Transcription factor JUN

DHT – 5-dihidrotestosterone

DHEAS – Dehydroepiandrosterone sulphate

dP – Intraluminal pressure change in the arteriole

dR_o – Change in a vessel's outer radius due to intraluminal pressure change

E_{inc} – Incremental elastic modulus of the arteriole

eNOS – Endothelial nitric oxide synthase

ET-1 – Endothelin 1

FFA – Free fatty acid

FSH – Follicle-stimulating hormone

GnRH – Gonadotropin-releasing hormone

h – Wall thickness of the arteriole

HDL-C – High-density lipoprotein cholesterol

HOMA IR – Homeostatic assessment for insulin resistance

HSD – Hydroxysteroid dehydrogenase

ICAM 1 – Intercellular adhesion molecule 1

IGF-1 – Insulin-like growth factor 1

IGFBP-1 – Insulin-like growth factor 1 binding protein

IGT – Impaired glucose tolerance

IR – Insulin resistance

IRS-1 – Insulin receptor substrate 1

IVSD(d) – Thickness of interventricular septum measured in a cross-sectional image at the level of the papillary muscles in diastole

LDL-C – Low-density lipoprotein cholesterol

LH – Luteinizing hormone

$LogE_{inc}$ – Incremental elastic modulus of the vessel wall

LVAd – Left ventricular area in diastole

LVAs – Left ventricular area in systole

LVIDd – Left ventricular internal diameter in diastole

LVIDs – Left ventricular internal diameter in systole

LVLd – Left ventricular length in diastole

LVLs – Left ventricular length in systole

MAPK – Mitogen-activated protein kinase

MetS – Metabolic syndrome

nKR – Normal Krebs solution

NO – Nitric oxide

OGTT – Oral glucose tolerance test

P – Intraluminal pressure

P450c17alpha - 17-alpha hydroxylase

PCOS – Polycystic ovarian syndrome

PI3-K – Phosphatidylinositol 3-kinase

R_{Ade} – Radius of the arteriole if adenosine was added to the organ chamber

R_i – Inner radius of the arteriole

R_{Ins} – Radius of the arteriole if insulin was added to the organ chamber

R_o – Outer radius of the arteriole

R_{u46619} – Radius of the arteriole if thromboxane A_2 agonist was added to the organ chamber

RXR – Retinoid X receptor

SEM - Standard error of the mean

SHBG – Sex hormone-binding globulins

T – Testosterone

T1D – Type 1 diabetes mellitus

T2D – Type 2 diabetes mellitus

T_{Ade} – Adenosin-induced relaxation of the arteriole

T_{Full} – Full contraction of the arteriole

Tg_{stress} – Tangential wall stress of the arteriole

T_{ins} – Insulin-induced relaxation of the arteriole

T_{nKR} – Spontaneous (myogenic) tone of the arteriole

U46619 – Potent thromboxane A_2 agonist

VCAM-1 – Vascular cell adhesion molecule 1

VD – Vitamin D

VDD – Vitamin deficiency

VDR – Vitamin D receptor

1 Introduction

1.1 Background

Polycystic ovary syndrome (PCOS) is reported to be the most common endocrine disorder affecting women of reproductive age. According to the National Institutes of Health, the prevalence of PCOS is estimated to be 8–12%, but some recent screenings suggest even larger numbers [1].

In addition to androgen excess (AE), oligomenorrhea, infertility, and insulin resistance (IR), PCOS is frequently accompanied by a higher prevalence of metabolic disorders and cardiovascular risk factors. Different PCOS phenotypes differ significantly in their cardiometabolic risk profile depending on the presence and severity of AE. Although PCOS diagnosis and care have improved significantly during the last three decades, longer-time-scale data regarding cardiovascular morbidity, mortality, and the possible beneficial effects of different interventions are still missing.

Although the pathophysiology of PCOS is not fully understood, possible connections between cardiometabolic complications, IR, genetic polymorphisms, and environmental factors have been identified recently. According to some estimations, 30–40% of the world's population is reported to have IR, and the proportion is even greater (75%) among PCOS women [2]. Normally, female gender has a positive impact on IR, body fat composition, and cardiometabolic risk. This is supported by the fact that estrogen replacement after menopause has beneficial effects on insulin sensitivity and keeps cardiovascular risk low [3]. A higher-than-normal serum concentration of sexual steroids of the opposite gender increases the prevalence of coronary disease, stroke, and hypertension, as proven by data from individuals that underwent female-to-male sex-change interventions [4].

Vitamin D deficiency (VDD) affects approximately 30–50% of the world's population. Exposure to sunlight or dietary supplementation (fortified foods and dietary

supplements, which are widely accepted in the United States) could help achieve sufficient vitamin D (VD) serum levels. Recently, an inverse relationship was found between VD serum levels and the occurrence of coronary heart disease. Previous studies reported that hyperinsulinemia, VDD, and AE coexist in PCOS women [5, 6], and the prevalence of VDD in women with AE is predicted to be 67–85% worldwide.

1.2 Polycystic ovarian syndrome

1.2.1 Definition

The first description of PCOS dates back to 1721, when Vallisneri described a young, moderately obese, and infertile woman with “two larger than normal ovaries, bumpy, shiny, just like pigeon eggs” [7]. In 1935, Stein and Leventhal presented the cases of seven fertile reproductive-aged women with similar endocrine conditions and ovarian morphology. They identified infertility, amenorrhea, hirsutism, enlarged ovaries with multiple cysts, and thickened ovarian tunica as leading symptoms and proposed PCOS as a name for this condition. They also began to perform wedge biopsies on their patients, which was demonstrated to be an effective treatment; later on, 90% reported normal menstruation cycles and 65% became pregnant [8].

During the last two decades, the definition of PCOS has changed and improved. The first commonly used diagnostic criteria were proposed in 1990 by the National Institutes of Health. This definition regarded oligo-anovulation and any signs of AE (either biochemical or clinical) as sufficient for diagnosis only if other endocrine disorders had already been excluded as the underlying cause. In 2003, the European Society of Human Reproduction and Embryology and the American Society of Reproductive Medicine organized a consensus workshop to refine and reconsider the definition of PCOS. The results were summarized in the Rotterdam criteria, which introduced ultrasound diagnosis of polycystic ovaries as a new provision. It also redefined the terms of AE, changing its description to an excess of androgen activity.

Although oligo-anovulation remained a lead criterion, two of the three above-mentioned conditions were sufficient for diagnosis [9].

As the Rotterdam criteria broadened the spectrum of patients and focused more on women with AE, it was widely criticized. Therefore, in 2006, the Androgen Excess PCOS Society discussed the topic again and proposed the currently accepted definition. Today, an excess of androgen activity, oligo-anovulation and/or polycystic ovaries, and exclusion of other diseases or conditions that could cause an excess of androgen activity are necessary to diagnose PCOS [10]. Based on these criteria, four different phenotypes of PCOS have been described [11, 12]:

- The hyperandrogenic form with oligo-anovulation and polycystic ovarian morphology, which is the "classic" PCOS phenotype.
- The hyperandrogenic form with oligo-anovulation without relevant signs of polycystic ovarian morphology.
- Hyperandrogenism with polycystic ovarian morphology but no relevant ovulation disturbances.
- Oligo-anovulation with polycystic ovarian morphology.

1.2.2 Diagnosis

Signs of AE should be judged based upon the presence of hirsutism and elevated levels of circulating androgens, mainly testosterone (T) and its active metabolite, 5-dihidrotestosterone (DHT). In cases of hirsutism, excessive terminal (coarse) hair is found in a male pattern. This differs from hypertrichosis, in which there is no typical pattern and excessive growth of hair follicles all over the body. High levels of circulating androgen enhance cytokine and specific growth factor production and trigger the conversion of T to DHT by 5α-reductase in the pilosebaceous unit, leading less visible vellus hair to turn into terminal hair [12]. The modified Ferriman-Gallwey scale is used for clinical evaluation [13]. In addition, hirsutism shows racial differences; Caucasian or African women develop it much more frequently than East Asian women [14, 15].

Analysis of circulating androgen levels requires sensitive methods, such as liquid chromatography and tandem mass spectrometry, immunochemiluminescence, or radioimmunoassay [16]. One standard method is to use high-quality T and steroid-binding globulin (SHBG) assays, which provide the total T and calculated free T. Ideally, these tests should be performed in the follicular phase, and reference hormone values should be obtained from women with regular menses [17, 18]. Another candidate hormone for AE measurement is dehydroepiandrosterone, which well represents adrenal hyperandrogenism. Although dehydroepiandrosterone itself is a weak androgen, it serves as a substrate for further androgen synthesis. The serum level of its precursor, dehydroepiandrosterone sulphate (DHEAS), is higher in PCOS women and is associated with elevated prevalence of IR [19]. According to some recent data, 75% of the adult PCOS female population has increased levels of all three biomarkers (T, androstenedione, and DHEAS), but serum T levels are the most frequently tested overall [20].

Anti-Müllerian hormone (AMH) is not an androgen, but a member of the transforming growth factor-β superfamily, which recently became of interest in relation to PCOS. Preantral or small antral follicle release of AMH clearly correlates with their number as well as the secretory activity of granulosa cells. Above all, AMH acts in opposition to follicle-stimulating hormone (FSH) in the ovarian tissue and shifts steroid synthesis towards androgenesis [21, 22]. Neurons that secrete gonadotropin-releasing hormone (GnRH) dispose AMH receptors on their surface. If the serum level of AMH is high, both GnRH neuronal firing and the pulsatility of gonadotropin secretion are more intense, which increases the secretion of luteinizing hormone (LH) and results in AE [23]. Although the level of AMH is relatively stable during the menstrual cycle, it is limited as a biomarker of PCOS. AMH secretion is age-dependent, reaching its peak in the individual's early 20s and declining slowly until menopause [24]. In this context, age-specific normal values of AMH levels are probably needed.

Oligomenorrhea is present in 85% of the whole PCOS population [10]. It is not always easy to determine the right diagnosis; on one hand, chronic anovulation could occur among normal fertile females, but on the other hand, some PCOS women could have normal ovulatory patterns. According to the criteria, oligo-anovulation leads menstrual cycles to last longer than 35 days and occur fewer than eight times a year

[25]. Low serum progesterone levels (lower than 3–4 ng/ml) from the midluteal phase of the cycle could help to prove the diagnosis [26].

Previously, polycystic ovarian morphology was defined after ultrasound examination based upon the presence of 10 or more follicles measuring 2–8 mm in diameter. Typically, follicles are arranged around the dense core of the stroma or are randomly scattered in the enlarged stroma [27]. Later on, this definition was changed due to modifications made by the Rotterdam criteria. The current definition requires the presence of 12 or more follicles measuring 2–9 mm in diameter in each ovary and/or increased ovarian volume (>10 ml) in at least one ovary. Furthermore, smaller follicle size (diameter of 2–5 mm) correlates strongly with serum T, DHT, and DHEAS levels and the severity of IR [28]. As PCOS may alter ovarian aging, some studies indicate the importance of adolescent ultrasound examinations. Early enlargement of the ovaries could be detected right after menarche, which provides the opportunity to implement early goal-oriented therapy [29]. Multiple follicles can often be detected at this age, whilst total ovarian volume correlates better with PCOS prevalence in adulthood. Other studies focusing on the number of follicles suggested raising the threshold from 12 to 25 and argued that PCOS morphology is commonly found in normal women without AE and oligo-anovulation [30].

1.2.3 Pathophysiology of PCOS

The underlying pathomechanism of PCOS is still under debate. Androgen overproduction, which is due to disturbed gonadotropin, FSH, and LH secretion, is the cornerstone of PCOS. Under normal circumstances, female androgen production takes place in the adrenal glands and the ovaries. Figures 1A and 1B show the different steps of adrenal and ovarian sex hormone genesis. Circulating levels of androgens could be the result of direct secretion or enzymatic conversion of 17-ketosteroids into androstenedione, mainly in the liver, skin, and adipose tissue. In the adrenal glands, androgen production is regulated by autocrine and paracrine signaling, whilst the control of the hypothalamic–pituitary axis dominates in the ovaries.

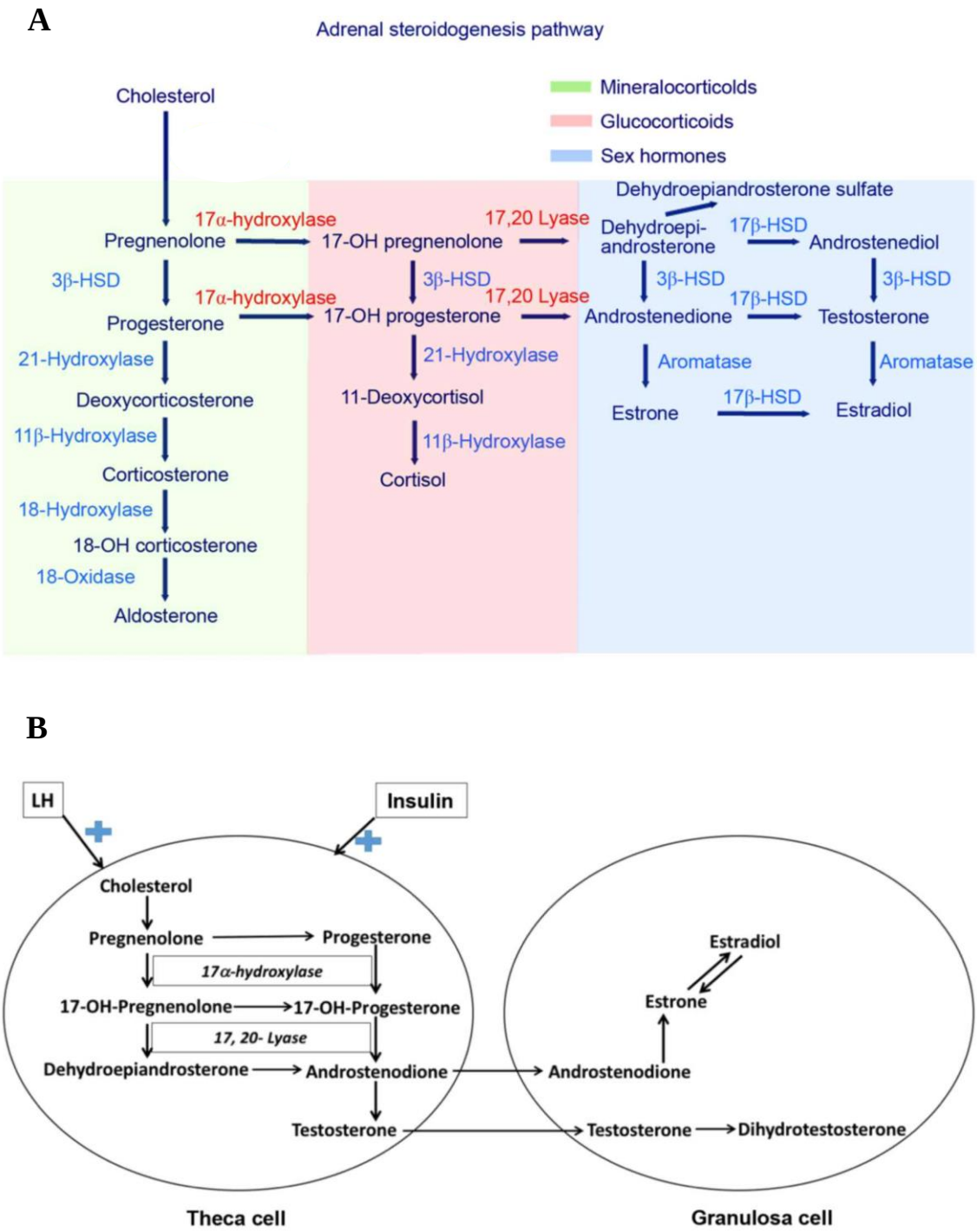

Figure 1 Different steps of adrenal and ovarian sex hormone genesis. A. Adrenal steroid hormone genesis in a human. Different types of steroid hormones are labelled with different colors. The first step is the conversion of cholesterol into pregnenolone, which is catalyzed by the 17α-hydroxylase/17,20-lyase enzyme. Androstenedione is the substrate of 17β-hydroxysteroid dehydrogenase and aromatase that leads to the formation of T and estrone. This figure is taken from the article "17α-hydroxylase/17,20-lyase deficiency in congenital adrenal hyperplasia: A case

report" [31]. **B.** Sexual steroid hormone biosynthesis in an ovary. In the ovarian theca cells, androgen formation is stimulated by LH and modulated by cytochrome P450c17, which engages in both 17-hydroxylase and 17,20-lyase activities. The formed androstenedione is taken up by granulosa cells and helps the formation of estrogens. Androstenedione in theca cells is converted to T, which leads to hyperandrogenism. Insulin enhances androgen synthesis in the theca cells. This figure is taken from the article "Association of polycystic ovary syndrome with metabolic syndrome and gestational diabetes: Aggravated complication of pregnancy" [32]. HSD, hydroxysteroid dehydrogenase; LH, luteinizing hormone.

In PCOS, ovarian androgen synthesis is the main cause of AE, but adrenal androgen production is reported to be elevated in 30–50% of PCOS women. Additionally, these women show enhanced 17-ketosteroid responses to adrenocorticotropic hormone [7, 12].

Androgens play a key role in the early gonadotropin independent phase of the menstrual cycle by initiating the growth of primordial follicles and recruiting small preantral follicles. A similar mechanism can be observed in girls during premenarche, when adrenal androgen synthesis helps induce gonadarche and menarche. Moreover, girls with "hyperpuberty" are at higher risk for subsequent development of PCOS [33, 34].

During the normal follicular phase of the menstrual cycle, LH triggers the androgenic precursor output of the ovarian theca cells and FSH regulates their conversion into estrogens (estradiol) at the granulosa cells. This hormonal balance promotes normal folliculogenesis in fertile females.

The main feature of PCOS is follicular arrest, which is provoked by an imbalance of LH, FSH, and sexual steroids. Increased follicular activation, a higher proportion of primordial follicles, and a corresponding increase in activated growing (primary) follicles are also typical features. Activated follicles show a lower rate of atresia and fail to mature. These characteristics of PCOS could be explained by the observed high "steady state" LH serum levels and lack of FSH peaks during the follicular phase. As a

consequence, theca cell hyperplasia occurs as well. At the level of the hypothalamic–pituitary axis, gonadotropin release increases and GnRH pulse secretion occurs at a rapid frequency, which keeps LH levels high [35].

In 1993, Crawley summarized possible theories for the development of AE [7, 36]:

- The *top-down theory* claims that the hypothalamic–pituitary axis is responsible for AE due to central dysregulation of GnRH firing, which leads to LH overproduction. The end effect is follicular theca cell hyperplasia and aromatase upon activation. In rats and mice, imbalance of GnRH secretion resulted in changes at the level of LH and FSH synthesis [37].
- The *bottom-up hypothesis* presumes the failure of adrenal sexual steroid synthesis. In this case, failure of peripheral androstenedione conversion is responsible for pituitary LH overproduction and, thus, increased ovarian androgen synthesis [36].
- The *androgen theory* summarizes different explanations for the first occurrence of AE. According to the theory, upon sudden peripheral (ovarian, adrenal) androgen overproduction or exposure, PCOS is induced. The so-called “fetal AE” theory supports the notion of early encounter with high serum androgen levels that provoke the onset of PCOS in adulthood. This explanation is also supported by some non-primate models that successfully produced phenotypical changes close to those seen in humans affected by PCOS [38]. Other explanations focus on the dysfunction of specific enzymes, like 11β-hydroxysteroid dehydrogenase. It has two subtypes (type 1 and 2) that coordinate to inactivate and reactivate adrenal glucocorticoid. Activation of subtype 2 triggers 11β-hydroxy androstenedione, 11β-hydroxytestosterone, and 11β-hydroxyprogesterone production [39]. Dysfunction of cytochrome P450c17a also leads to disturbed androgen synthesis, as it is responsible for both 17α-hydroxylase and 17-20-desmolase activities in the ovarian and adrenal cells. As a single gene encodes this cytochrome P450 enzyme, mutation or dysfunction could be responsible for AE [40].

- The *insulin theory* proposes IR as a provoking factor for AE. The major actions of insulin are mediated via three different pathways. Its metabolic effects are regulated by the phosphatidyl-inositol 3-kinase (PI3-K) pathway, whilst the mitogenic effects of insulin are coordinated by mitogen-activated protein kinases (MAPKs). The protein kinase C pathway is responsible for phospholipase C activation, which enhances second messengers in several tissues. In ovarian theca cells, LH increases steroidogenesis via the cyclic adenosine monophosphate–protein kinase A pathway. Insulin could trigger the accumulation of cyclic adenosine monophosphate through the PI3-K and protein kinase C cascade and increases LH secretion, which could prove the existence of cross-talk between LH and insulin signaling in ovarian tissue [41].

Figure 2 shows the complex hormonal disturbances that affect the development of PCOS.

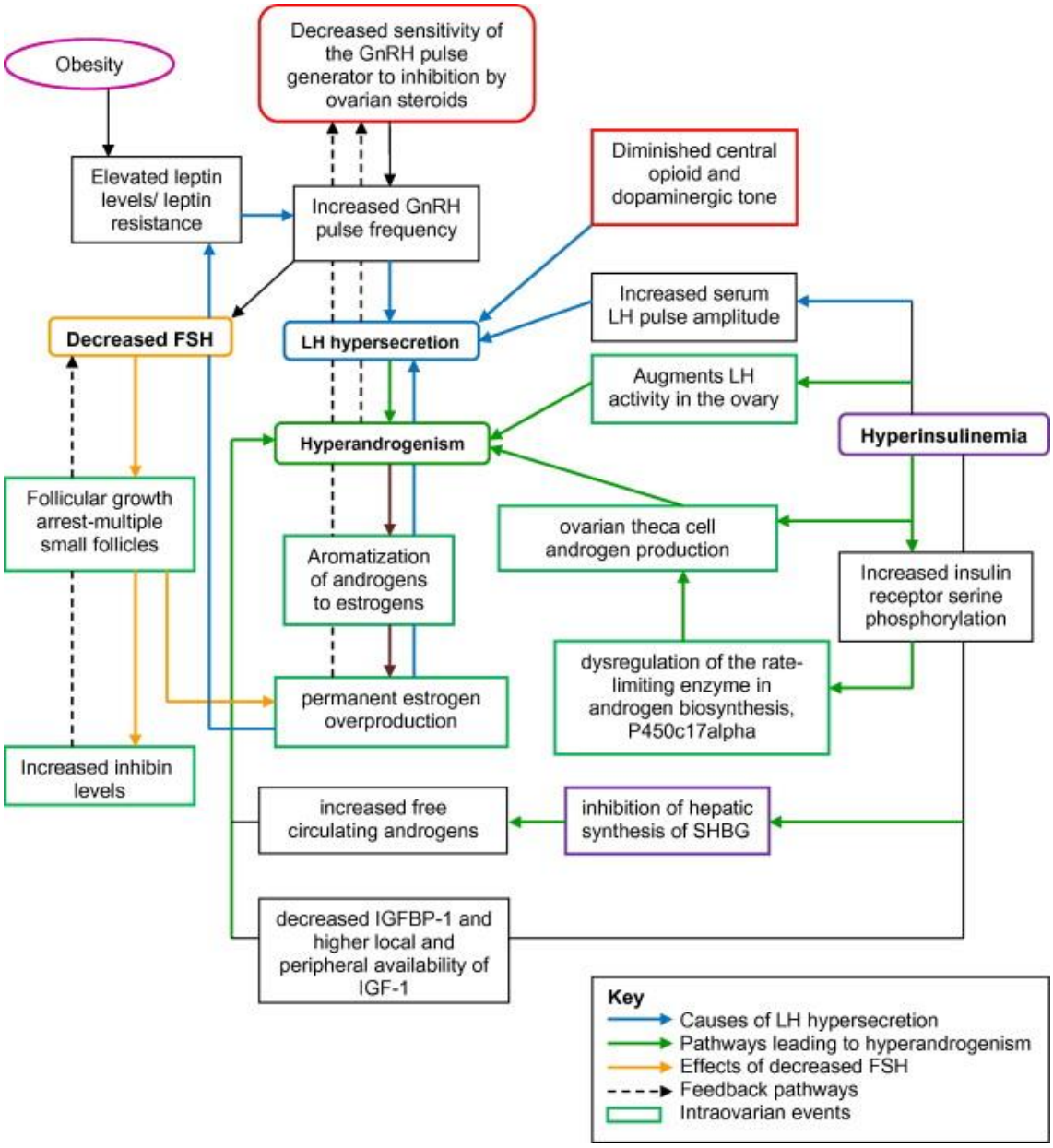

Figure 2. Endocrine disturbances in the background of PCOS. Decreased sensitivity of the GnRH pulse generator and increased GnRH firing frequency provoke LH hyper- and FSH hyposecretion and therefore lead to hyperandrogenism and ovarian arrest. Moreover, hyperinsulinemia results in further LH production and increases the level of circulating androgens by inhibiting the production of SHBG. Abbreviations: GnRH, gonadotropin-releasing hormone; LH, luteinizing hormone, FSH, follicle-stimulating hormone; SHBG, sex hormone-binding globulin; IGF-1, insulin-like growth factor 1; IGFBP-1, insulin-like growth factor 1 binding protein; P450c17alpha, 17-alpha hydroxylase. This figure is adopted from the article "Polycystic ovary syndrome and impact on health" [42].

1.3 Etiology of PCOS

Although the Rotterdam criteria suggest that PCOS is a well-characterized endocrine disorder, its symptoms are in fact highly variable and heterogeneous. Genetics, environmental background, nutrition, and ethnicity are important factors affecting its development. PCOS has the same prevalence among Caucasian women from the United States, Spain, and Australia (6–9%), but Southeastern Asian women—especially Chinese women (2.2%) have the lowest prevalence in the world [1]. The Hispanic PCOS population in the United States shows higher rates of hirsutism, metabolic syndrome (MetS), and obesity compared to Caucasians [43].

Lifestyle factors and eating habits also play an important role in the development of PCOS. The Western diet contains many processed foods, which are rich in advanced glycation end products. These glycotoxins enhance intracellular signal transduction, trigger pro-inflammatory gene transcription, macrophage activation, cytokine (e.g., interleukins 1, 6, and 8), chemokine release, and reactive oxygen species production (i.e., the Maillard reaction) [44, 45]. Additionally, the circulating level of glycotoxins is well correlated with central obesity, waist-to-hip ratio, and IR in PCOS women [44, 46].

Obesity is a common health problem that affects 50–80% of patients [47], strongly influencing their reproductive function and cardiometabolic health [43]. Approximately 75–80% of PCOS women suffer from IR, a significantly higher proportion than in the age- and body mass index-matched female population [48]. Non-alcoholic fatty liver disease is believed to be one of the major consequences of IR, and it shows a clear correlation with AE. Its estimated prevalence may exceed 40% among obese PCOS women [49].

PCOS is associated with a significant increase in risk factors such as cardiovascular disease, atherosclerosis, obesity, MetS, dyslipidemia, type 2 diabetes mellitus (T2D), and IR [12, 50]. Cognitive or mood disorders, like depression and anxiety, are more frequent among PCOS women compared to the healthy female population [51].

Figure 3 shows the complex etiology of PCOS.

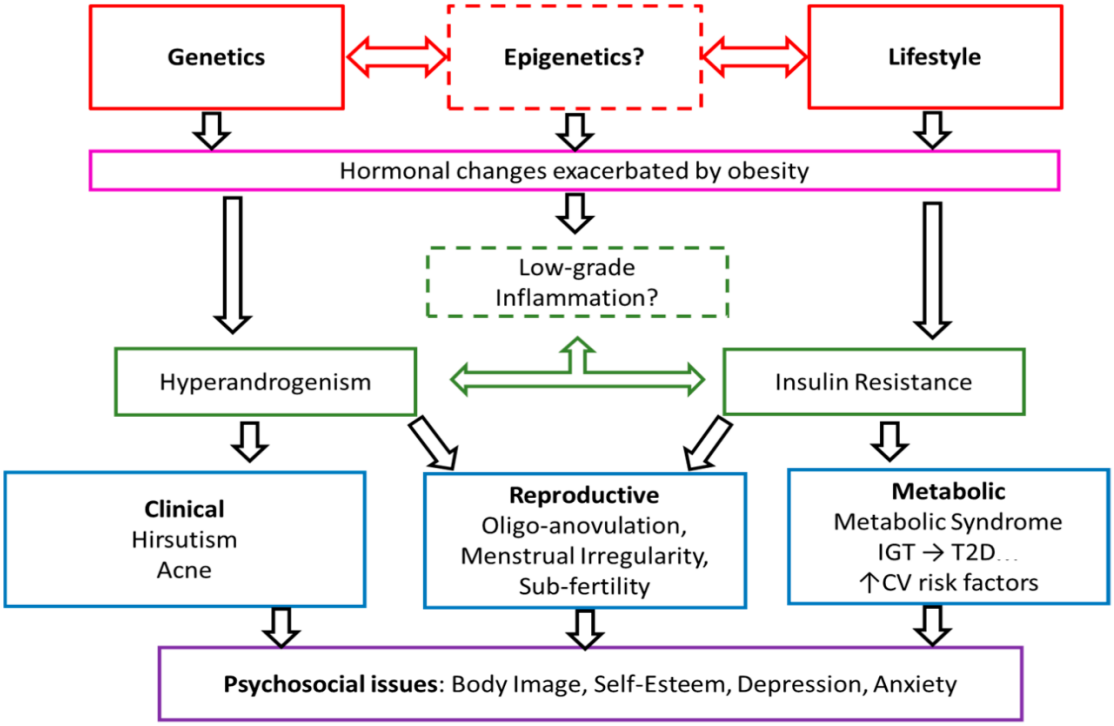

Figure 3. Complex etiology of PCOS. Genetics, epigenetics, and lifestyle could promote the development of hyperandrogenism, obesity, IR, and chronic inflammation. Hyperandrogenism and IR are responsible for further clinical, metabolic, reproductive and psychosocial consequences of these endocrine disturbances. Abbreviations: IGT, impaired glucose tolerance; T2D, type 2 diabetes mellitus; CV risk factors, cardiovascular risk factors. This figure is adopted from the article "The genetics of polycystic ovary syndrome: An overview of candidate gene systematic reviews and genome-wide association studies" [52].

1.3.1 Metabolic syndrome

The key elements of MetS are AE and IR, which join together all the necessary components of the syndrome. According to the definition utilized by the World Health

Organization, MetS is characterized by hyperglycemia (fasting glucose levels of 5.6 mmol/L or above), central obesity (increased waist circumference according to population- and country-specific definitions), elevated arterial blood pressure (130/85 mmHg or above), high total triglyceride (1.7 mmol/L or above), and a low high-density lipoprotein cholesterol (HDL-C) level (less than 1.29 mmol/L in women) [53, 54].

The prevalence of MetS is two to four times higher in the PCOS population than among healthy individuals. The presence of central obesity has a high impact on MetS prevalence [53]. If central obesity is combined with AE, the prevalence reaches approximately 29%, and if it is combined with polycystic morphology and AE, it reaches 35% [55]. The prevalence of IR is also around 30% in PCOS females, and it increases to 45–50% if centripetal obesity is present.

Higher triglyceride, lower HDL-C, and higher low-density lipoprotein cholesterol (LDL-C) levels are more common in PCOS patients than in the non-PCOS population [56]. Recently, some new biomarkers have been introduced to improve evaluation. For example, lipoprotein is a predictor of early-onset cardiovascular disease in PCOS women, even if they have normal lipid profiles [57]. In addition, reduced efflux capacity from macrophages, an indicator of HDL-C function, was decreased in the PCOS population [58].

Several rodent and non-primate models support the notion that fetal or adolescent exposure to androgens (mainly T or DHT) could provoke MetS [59, 60]. Furthermore, in a mouse model of letrozole-induced PCOS, antiandrogen therapy ameliorated symptoms of MetS and reduced body weight and adipocyte size [61]. Enlargement of adipocytes (hypertrophic obesity) is typical in PCOS patients. Apparently, this hypertrophy is due to disturbed lipolysis, reduced lipoprotein lipase activity, and altered storage capacity of adipocytes [62].

The most promising results for MetS were achieved if both AE and IR were treated at the same time. Flutamide is an androgen receptor antagonist that, together with metformin, has been reported to reduce plasma androgen indices and improve ovarian function. Metformin therapy induced hepatic estrogen receptor α expression,

while combination with flutamide decreased intestinal androgen receptor expression and increased estrogen receptor α expression. Hepatic and intestinal insulin and insulin receptor signaling were also improved by this "double" therapy [63].

Fasting blood sugar levels and dyslipidemia (characterized by a high triglyceride level and low HDL-C ratio) were found to be the strongest indicators of MetS onset. A study conducted in India reported that dyslipidemia was present in 90% of adolescent PCOS girls. Interestingly, more than 20% of these girls had already developed glucose intolerance, which indicates early onset of dysfunctional glucose metabolism and insulin sensitivity [64]. Insulin sensitivity and circulating SHBG levels also show a strong correlation, as IR is often associated with reduced SHBG levels and elevation of free androgens.

The development of MetS could be associated with failure of central regulation and energy metabolism. The role of decreased sympathetic tone has already been described in rodent models of neonatal androgenization, leptin resistance, and DHT-induced female AE. Central hyperleptinemia with peripheral leptin resistance (unresponsiveness to its anorexigenic effects) is often detected in MetS cases. In addition, energy intake is regulated by the firing activity of specialized fuel-sensing neurons of the hypothalamus. The hypothalamic expression of proopiomelanocortin neurons is found to be diminished in hyperandrogenic female mice. Moreover, chronic AE increases the adrenocorticotropic hormone sensitivity of proopiomelanocortin cell bodies and decreases fiber projection intensity, leading to increased energy intake and obesity. Reduced levels of α-melanocyte-stimulating hormone are also detected in AE cases [65].

1.3.2 Insulin resistance

1.3.2.1 Definition and diagnosis

Under normal circumstances, insulin regulates glucose homeostasis by enhancing glucose uptake in the target tissues (mainly adipocytes and skeletal and myocardial

muscle cells), decreasing hepatic glucose production, and modulating free fatty acid (FFA) release by lipolysis. The classic definition of IR is characterized by damage of all three pathways, which results in impaired glucose intake and metabolism with a compensatory increase in beta-cell insulin production and hyperinsulinemia. In the long term, hyperglycemia and hyperinsulinemia promote chronic inflammation and oxidative stress, which contribute to the development of arterial hypertension, dyslipidemia, visceral adiposity, endothelial dysfunction, a prothrombotic state, and T2D.

Among patients diagnosed with PCOS based on the Rotterdam criteria, 70% have impaired glucose tolerance or T2D, which are mainly diagnosed in their fourth decade of their life. Some recent data show that the prevalence of IR is almost the same among adolescents and young adults suffering from PCOS [64, 66], which suggests early onset of dysfunctional insulin signaling. Patients with AE and obesity are at the highest risk, although the lean PCOS phenotype seems to play no protective role in the development of dysglycemia. Elevated basal insulin secretion with insufficient insulin secretory responses to a glucose load are the main characteristics of IR in PCOS patients. Furthermore, in most cases, IR is selective and affects the metabolic—but not the mitogenic—signaling pathways [53, 67].

The hyperinsulinemic–euglycemic glucose clamp technique is the gold-standard method to assess metabolic IR *in vivo*. The clamp technique enables quantitative evaluation of the effect of insulin on whole-body glucose uptake, while euglycemia is maintained with the administration of different insulin concentrations and adjusted amounts of glucose infusion [68]. Insulin-mediated glucose disposal is used as an indicator of insulin sensitivity. It could be defined under steady-state conditions in which the amount of infused glucose equals the amount of glucose taken up by the peripheral tissues. Hepatic glucose production and renal elimination can be measured with the help of isotopic-labelled glucose infusion through the clamp [66].

Sequential multiple insulin dose euglycemic clamps provide the opportunity to investigate the concentration-dependent saturable actions of insulin *in vivo*. On one hand, any type of alteration in insulin receptor binding or phosphorylation could be assessed by insulin sensitivity, which is evaluated based on the concentration required for a half-maximal insulin response. On the other hand, the maximal biological effect of

insulin is defined by insulin responsiveness, which reflects post-receptor events such as glucose transporter translocation. Interestingly, there is no glucose load or dose-dependent difference in insulin sensitivity values between lean and obese PCOS women. This finding suggests that both phenotypes act similarly to compensate for sudden glucose uptake. In addition, basal endogenous glucose production and half-maximal insulin response are disturbed only in obese PCOS women, which may support the notion of a possible connection point between impaired lipid metabolism and IR [69].

The clamp technique could be used to measure insulin clearance, which is strongly related to insulin receptor activation. In hyperinsulinemia cases, longer elimination time and clearance of insulin should be expected. Interestingly, there is no significant difference between hyperinsulinemic PCOS patients and healthy individuals in terms of posthepatic insulin clearance. Nevertheless, the C-peptide ratio was elevated in PCOS patients, which suggests hepatic dysregulation of insulin extraction [70].

Another method for measuring whole-body insulin sensitivity in subjects without diabetes is the frequently sampled intravenous glucose tolerance test with minimal model analysis. The minimal model allows for evaluation of insulin sensitivity (i.e., the sensitivity index), which correlates well with glucose-uptake-stimulated insulin action and suppressed glucose production [71].

Although these techniques offer correct and complex results regarding whole-body insulin sensitivity, the oral glucose tolerance test (OGTT) and fasting glucose and insulin level measurements are still the most commonly used clinical techniques. OGTT values correlate well with the results for the euglycemic glucose clamp and frequently sampled intravenous glucose tolerance test, but they are insensitive to large changes in insulin sensitivity and inaccurate for evaluation of β-cell dysfunction [66].

1.3.2.2 Metabolic effects of insulin resistance in PCOS

The metabolic effects of IR are mainly detected in skeletal muscle and adipose tissue. Skeletal muscle tissue is responsible for primary peripheral glucose uptake,

which exceeds 70–85% of the whole-body glucose uptake under normal circumstances. If this capacity reaches its maximum, de novo lipogenesis takes place in the liver, which leads to an increased level of circulating FFAs. In the adipose tissue, failure of insulin signaling could provoke lipolysis, which also serves as a source of FFAs. Consequently, chronic inflammation and ectopic fat deposition occur, leading to vascular and metabolic complications.

In skeletal muscle, insulin receptor activation is followed by transmembrane translocation of glucose transporter 4 to promote glucose uptake. Recent studies found that reduced transcription of the β subunit can be detected in PCOS skeletal muscle cells. Although this mechanism provokes IR, it has some protective effects as well. If hyperinsulinemia persists, lower expression of the insulin receptor subunit would help to maintain the euglycemic state [72]. Additionally, glucose transporter 4 translocation problems could be associated with insulin downstream signaling failure. Some *in vitro* studies conducted with PCOS myotubes revealed that insulin receptor substrate 2-associated phosphatidyl-inositol 3-kinase (PI3-K) activity is decreased [73]. Moreover, essential changes in skeletal muscle morphology and reduced whole-body insulin sensitivity were found in a female rat model of T- and DHT-induced PCOS. These changes included a lower amount of insulin-sensitive fibers, a higher amount of less insulin-sensitive muscle fibers, reduction of capillary density, glycogen synthase dysfunction, and lower glucose transporter 4 protein expression [60].

Insulin resistance is responsible for specific changes in lipid homeostasis in PCOS cases. Insulin-induced suppression of lipid oxidation is reduced in PCOS females. Interestingly, no significant changes were detected between PCOS and healthy women regarding peripheral lipid uptake [73]. Furthermore, IR has selective effects on adipose tissue in different locations; adipocytes isolated from the subcutaneous fat of lean PCOS patients are reported to have decreased insulin and catecholamine-stimulated lipolysis capacity and bigger cell size, whilst adipocytes from visceral fatty tissue show increased lipid oxidation rate. A higher rate of visceral lipolysis can elevate the FFA concentration of portal blood flow and promote the development of hepatic IR in PCOS [66]. Not only lipolysis but also the endocrine function of adipocytes might play a role in insulin sensitivity. Adiponectins are adipocyte-derived hormones that positively affect whole-body insulin sensitivity, pancreatic β-cell viability, and secretory function

[74]. Leptin, known as the prototypical adipokine, is one protein that plays a regulatory role at the hypothalamic–pituitary axis. Infertility is one of the characteristics of congenital leptin deficiency, as leptin affects LH and GnRH secretion. In PCOS, low leptin serum levels are usually detected in association with hyperinsulinemia and AE [75]. In addition, a reduction in the adiponectin receptors of theca cells in PCOS ovaries (compared with normal ones) is frequently detected [76].

Fat accumulation may have an effect on hepatic glycogen synthase activity and pancreatic β-cell function. Non-alcoholic fatty liver disease and impaired glycogen synthase activity show a significant correlation with the prevalence of obesity in PCOS patients [49]. A high FFA concentration related to obesity has a negative impact on pancreatic β-cell insulin secretion and calcium channel distribution, which match well with the fat accumulation within the islets. In addition, intrapancreatic fat depots elevate the local amount of FFAs and trigger chronic inflammation and cytokine production [66]. In PCOS-related IR, chronic pancreatic islet inflammation (insulitis) could occur, which promotes β-cell dysfunction or apoptosis later on. Hyperinsulinemia and β-cell hyperplasia are the first consequences of insulitis and increased insulin demand due to IR, but some recent data suggest that mitochondrial dysfunction has a role in the pathophysiology of β-cell secretory failure [77]. Glucolipotoxicity could enhance the activation of reactive oxygen and nitrogen species, which leads to mitochondrial dysfunction and inhibition of the electron transport chain and, in turn, results in reduced energy production [44].

The complex consequences of impaired lipid metabolism are shown in Figure 4.

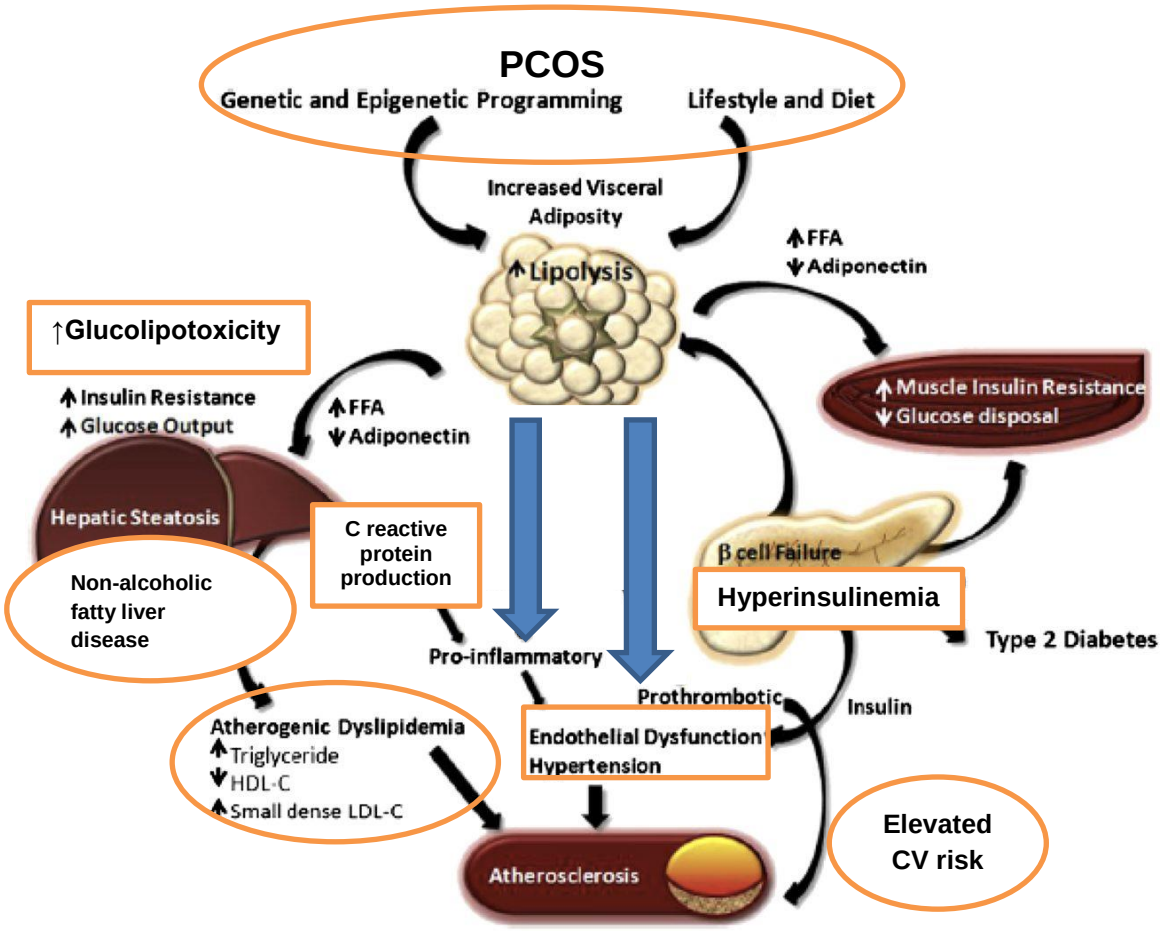

Figure 4. The effects of disturbed lipid metabolism on insulin resistance and cardiovascular complications in PCOS patients. In PCOS, impaired lipolysis results in free fatty acid overproduction and decreased adiponectin release. It also promotes pro-inflammation and thrombosis as well as IR of the liver and muscle cells. Atherogenic dyslipidemia due to hepatic failure, endothelial dysfunction, hypertension, and atherosclerosis are the end results. Abbreviations: FFA, free fatty acids; LDL-C, low-density lipoprotein cholesterol; CV risk, cardiovascular risk. This figure is adopted and modified from the article "Metabolic syndrome" [78].

1.3.2.1 The effects of insulin resistance on the female reproductive system

Insulin regulates several signaling mechanisms that are necessary to maintain normal function of the female reproductive system. In PCOS, hyperinsulinemia

dysregulates this physiological balance of signaling pathways, leading to AE and selective IR of the ovaries.

At the hypothalamus–hypophysis–adrenal axis, insulin triggers GnRH and LH secretion pulsatility and frequency by potentiating GnRH gene transcription. Insulin may increase hypothalamic corticotropin-releasing hormone secretion and, possibly, sensitize the adrenal cortex to adrenocorticotropic hormone stimulation. At the site of the adrenal glands, insulin promotes androgen secretion and consecutive AE.

The most important mitogenic effect of insulin is that it indirectly diminishes SHBG synthesis, which causes higher free androgen serum levels in PCOS patients. Not only hyperinsulinemia but also elevated concentrations of glucose and fructose are important indirect factors for SHBG decrease, as both monosaccharides downregulate hepatocyte protein synthesis by reducing hepatic nuclear factor 4-α activity [66, 79].

In ovarian tissue, theca cells and granulosa cells present insulin receptors and insulin-like growth factor-1 (IGF-1) receptors on their surfaces. The action of insulin was tested by direct administration of antibodies against both receptors, which led to a decrease in ovarian steroidogenesis [80]. Further investigations found that insulin modulates the activity of steroidogenic acute regulatory protein, which is a molecule involved in the transportation of cholesterol to the cholesterol side-chain cleavage enzyme and the rate-limiting enzyme of ovarian steroid synthesis. In addition to enhancing cholesterol side-chain cleavage enzyme activation, insulin increases the expression of 7-α-hydroxylase/17,20-lyase, 3-β-hydroxysteroid dehydrogenase, and aromatase [79]. It was recently reported that inositol phosphoglycans, which are second messengers in the metabolic signal transduction pathway of classic insulin receptor signaling, might have similar effects on the enzyme cascade of steroid genesis [79]. In this regard, hyperinsulinemia strongly shifts the balance towards overexpression of androgen-producing enzymes. Moreover, the hyperinsulinemic state represses IGF-1 binding protein synthesis, which increases the amount of available free IGF-1 and leads to further enhancement of ovarian insulin signaling. Together, these complex mechanisms lead to ovarian selective insulin resistance, which means that the insulin sensitivity of the ovarian tissue is unchanged or enhanced, although metabolic IR is present in all other insulin-sensitive tissues [81].

1.3.2.2 Hemodynamic consequences of insulin resistance

In addition to its above-mentioned actions, insulin has direct hemodynamic effects. Insulin improves regional blood flow, increases capillary recruitment, and aids peripheral vasodilatation, which leads to better glucose uptake of the peripheral tissue. This vascular action of insulin is mediated by nitric oxide (NO) derived by the endothelial cells of the vasculature. In order to enhance NO production, insulin must cross the endothelial barrier. Although it is not well understood yet, insulin probably reaches the endothelial cell by receptor-mediated internalization. Some studies of obese and T2D patients show evidence that damage of the endothelial barrier or longer transport time through the capillary bed interferes with insulin-induced local blood flow [82, 83].

According to recent findings, dysregulation of endothelial nitric oxide synthase (eNOS) is one of the key elements of IR. Moreover, glucose and lipid toxicity promote the production of reactive oxygen and nitrogen species, which reduce the available NO concentration [84, 85]. Chronic inflammation and a prothrombotic state are additional consequences of the activation of reactive oxygen species, which increases the local level of vascular and intercellular adhesion molecules (VCAM and ICAM), C-reactive protein, tumor necrosis factor α, interleukin 6, and endothelin-1 (ET-1) [83]. In addition, chronic inflammation triggers the migration and proliferation of vascular smooth muscle cells, which shifts vascular reactivity towards vasoconstriction in the absence of a sufficient amount of NO [86]. To determine whether the metabolic or mitogen insulin-signaling pathway coordinates NO release, endothelial cells and vascular smooth muscle cells harvested from healthy coronary arterioles were cultured in high-glucose, fatty acid, and insulin-containing media. Interestingly, mitogen signaling, including MAPK/ERC activation, was preserved or slightly augmented, whilst the metabolic pathway (PI3-K signaling) was reduced [86]. These results may prove that the metabolic effects of IR are responsible for the disadvantageous changes in arterial reactivity and that elevated CV risk is an indirect metabolic complication.

Regarding PCOS, several studies supported the theory of compromised arterial reactivity; however, it is not easy to distinguish between the impacts of IR and AE. In DHT-induced rodent models of PCOS, insulin-induced relaxation of the aorta was

significantly reduced [87]. Recent human studies showed that PCOS with or without the clinical features of IR and MetS elevates the level of reactive oxygen species, endoplasmic reticulum stress markers (GRP78, sXBP1, ATF6), and leukocyte rolling flux. [88]. Furthermore, a recent publication reported that 12 weeks of treatment with metformin improved endothelial function and significantly decreased the levels of ICAM-1, E-selectin, interleukin 6, and tumor necrosis factor α in PCOS patients [89]. Additionally, coronary artery and aortic calcification were increased in women with PCOS compared with healthy individuals, and age and body mass index were both determining factors for coronary artery calcification [90].

Figure 5 demonstrates a possible mechanism of vascular IR.

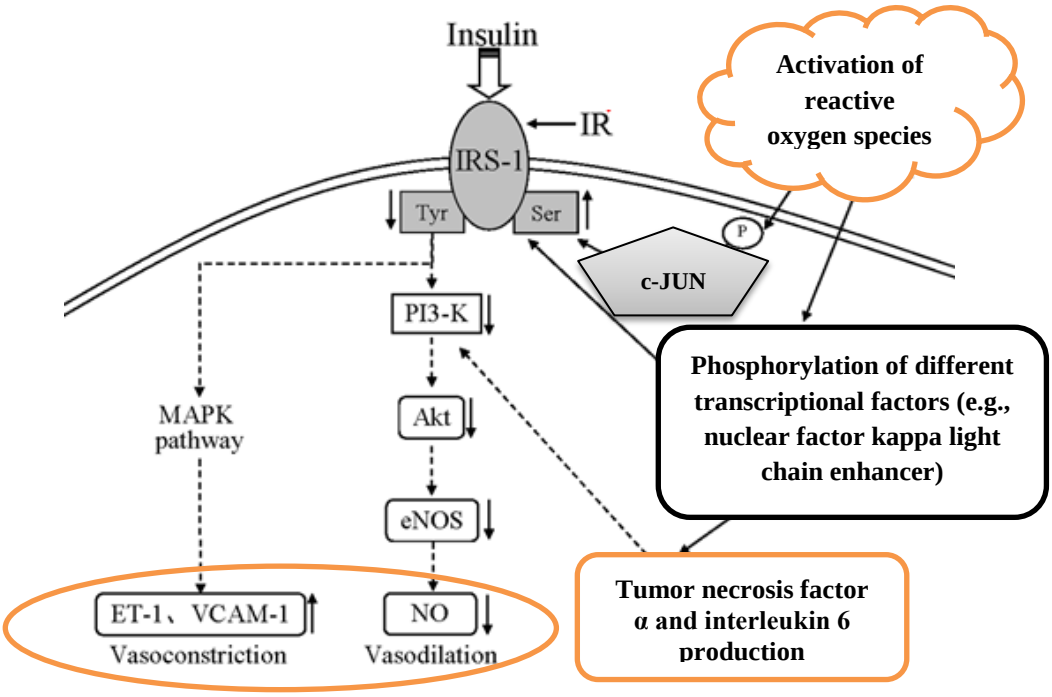

Figure 5. The effect of insulin resistance on vascular reactivity. Normally, insulin signaling leads to vasodilatation by PI3-K signaling and NO production. If the amount of reactive oxygen species is increased, downregulation of PI3-K signaling and upregulation of MAPK signaling are observed. As an end effect, NO production is decreased and vasoconstriction occurs. Abbreviations: IRS-1, insulin receptor substrate 1; MAPK, mitogen-activated kinase; ET-1, endothelin-1; VCAM-1, vascular adhesion molecule 1; PI3-K, phosphatidyl-inositol 3-kinase; Akt, protein kinase B; eNOS, endothelial nitric oxide synthase; NO, nitric oxide; eNOS, endothelial nitric oxide synthase; c-JUN, c-Jun N-terminal kinases. Adopted and modified from the article

“Tectorigenin attenuates palmitate-induced endothelial insulin resistance via targeting ROS-associated inflammation and IRS-1 pathway” [91].

1.3.2.3 Molecular effects of insulin resistance in PCOS

In addition to its well-known effects on glucose homeostasis, insulin affects lipid and protein metabolism, cell growth, and differentiation. Insulin signaling is mediated by insulin receptors, which are heterotetramers of α- and β-subunits. The extracellular α-subunit is responsible for ligand binding, whilst the β-subunit is activated by autophosphorylation. The cytoplasmic β-subunits have intrinsic protein tyrosine kinase activity. The classic insulin receptor shares substantial structural homology with the IGF-1 receptor and insulin-related receptor. Hence, insulin could induce autophosphorylation of different receptors. It was recently revealed that this autophosphorylation depends on insulin concentration [92] and that the physiological serum concentration promotes activation of the classic receptor.

The activated insulin receptor initiates tyrosine phosphorylation of intracellular substrates, like different insulin receptor substrates (IRS-1–4). Glucose uptake and metabolic effects are mediated by P-I3K, which then phosphorylates membrane phospholipids and phosphatidylinositol 4,5-bisphosphate, resulting in activation of the serine/threonine protein kinases (Akt) and atypical protein kinase C. These signaling pathways are responsible for transmembrane translocation of glucose transporter 4 or indirect activation of glycogen synthase. Protein synthesis and cellular nutrient sensing are also regulated by the PI3-K pathway via the mammalian target of rapamycin. The so-called mitogen pathway is regulated by the cascade of serine/threonine kinases and the enhancement of different MAPK kinases [93].

Because the metabolic and mitogen effects of insulin are regulated differently, impairments caused by them could develop separately. Metabolic IR is the cornerstone of PCOS. According to several studies, protein kinase C-mediated serine phosphorylation of the insulin receptor, serine phosphorylation of insulin receptor substrate 1, and increased insulin-independent serine phosphorylation are the most

important steps in the pathogenesis of metabolic IR in PCOS [67]. Presumably, downstream signaling pathways might be intact as Akt, protein kinase C, and B activation were unchanged in PCOS adipocytes [94]. However, a few studies suspected indirect regulation problems with Akt signaling [73, 93]. Increased extrinsic insulin-independent serine phosphorylation of the classic insulin receptors seems to be specific to PCOS, as it is not detectable in other IR-related diseases (i.e., obesity or T2D) [66]. In addition to the above-mentioned defects of insulin signaling, some data suggest that mitochondrial dysfunction of skeletal muscle cells plays a further role in PCOS [95].

1.3.3 Cardiovascular disease

The multiple metabolic complications caused by PCOS increase patients' CV risk. Women with hyperandrogenic PCOS have a relative risk of coronary heart disease at least two times higher than that of healthy controls [96, 97]. The rate of coronary artery calcification, an indicator of subclinical cardiovascular disease, was found to be present 40% of fertile-aged PCOS females (aged under 40) [98].

The prevalence of hypertension, which is one of the earliest consequences of atherosclerosis and reduced compliance of the vessel wall, was reported to be present in 65% of the premenopausal PCOS population. This proportion is even larger if the clinical picture involves IR, AE, and obesity or if patients are already in menopause [99].

Altered intima–media thickness of the vessel is considered to be a noninvasive marker of coronary and cerebrovascular events [100]. Premature atherosclerosis and higher intima–media thickness values (compared to healthy individuals) are frequently present in premenopausal PCOS women [100, 101]. This early stage of atherosclerosis in PCOS is often associated with elevated LDL serum levels or obesity [97].

Further cardiovascular abnormalities of PCOS patients include decreased cardiac systolic flow velocity, diastolic dysfunction, increased vascular stiffness, and endothelial dysfunction. Conventional echocardiography is still the easiest noninvasive

way to evaluate left ventricular function in PCOS patients, but the results are highly dependent on image quality, the assumption of left ventricular geometry, and the experience of the investigator. Some studies found evidence of a connection between early left ventricular impairment when mitral inflow deceleration time, isovolumetric relaxation time, and diastolic function were altered in the PCOS group [102]. Systolic blood flow velocity was also found to be decreased in PCOS, with an inverse correlation between systolic outflow parameters and fasting insulin levels [103].

Chronic activation of the sympathetic nervous system could lead to vascular dysfunction and hypertension. In PCOS, activation of the sympathetic nervous system and IR is a complex mechanism that is related to obesity. In PCOS patients, impairment of the sympathetic nervous system was demonstrated by an exaggerated systolic blood pressure response to exercise and delayed heart rate recovery [104]. Another study demonstrated that a high density of catecholaminergic nerve fibers is present in the ovaries of women with PCOS, which correlates with skeletal muscle and adipose tissue results [66].

1.3.3.1 The role of endothelial dysfunction

In PCOS, endothelial dysfunction is the source of further cardiovascular complications, and its severity is proportional to the level of androgens and IR. Hyperinsulinemia-induced endothelial dysfunction and hypertrophic remodeling occur due to its effects on vascular endothelial and smooth muscle cells as well as ET-1 production. ET-1 release is reported to be significantly increased in PCOS females, and this is also a sign of oxidative stress and altered vascular compliance [105]. Disturbed insulin-stimulated eNOS activation and NO release appear to negatively influence capillary network expansion, resulting in impaired microcirculation and blood flow regulation in metabolically active tissues.

Not only hyperinsulinemia but also an elevated level of circulating FFAs and chronic inflammation could enhance endothelial impairment by altering activation of the renin–angiotensin–aldosterone axis. The vascular effects of angiotensin II are mediated by two G-protein coupled receptor subtypes (subtype 1 and 2) with different

effects. Both receptors are expressed on the endothelial surface, but receptor subtype 1 is responsible for the well-known vasoconstrictor effects. PCOS rodent models revealed that reduced endothelial NO bioavailability, impaired insulin signaling, and IR are promoted by subtype 1 activation [106, 107]. Some recent clinical trials were able to prove the beneficial effects of selective angiotensin receptor subtype 1 blocking agents in PCOS females, such as improved cardiometabolic risk due to increased insulin sensitivity and prevention of T2D [107]. The effects mediated by angiotensin receptor subtype 2 include vasodilation and augmented insulin-mediated glucose disposal. These facts suggest a possible imbalance between the two receptor signaling mechanisms in PCOS, which could be indirectly improved by inhibition of angiotensin receptor subtype 1 [108].

Hormonal modulation failure of vascular reactivity plays an important role in impaired endothelial function. The two main effects of estrogens are eNOS phosphorylation due to activation of the PI3-K/Akt pathway and increased eNOS mRNA expression. In transgenic mice, the activation of estrogen receptor α was responsible for eNOS protein production [109]. In addition, estrogen regulates vascular endothelial growth factor production (via estrogen receptor α) in coronary circulation. These findings align with the flow-mediated vasodilatation results of healthy, premenopausal, and estrogen-deficient postmenopausal women [110].

Regarding the effects of androgens, the tissue-specific distribution of two key enzymes, aromatase and 5-α-reductase, must be taken into consideration. DHT is pure androgen, but T could be converted into estrogen and activate estrogen receptor α. Furthermore, T has complex vascular effects: it could relax coronary arteries by opening the large-conductance, calcium-activated potassium channels and up-regulating cyclooxygenase-2 activity, which in turn leads to increased prostacyclin formation [109]. The vascular effects of T may be gender-dependent, as flow-mediated vasodilatation was reduced in female-to-male transsexuals after administration of high concentrations of androgen. Animal studies of sexual transition suggest that T has a negative effect on eNOS-mediated vascular responses [111]. Androgens can also induce vasoconstriction by modulating the production of ET-1 or enhancing the production of arachidonic acid intermediates, including thromboxane A_2 and 20-hydroxyeicosatetraenoic acid. In female-to-male transsexuals and in postmenopausal

women, AE correlates well with ET-1 levels and subclinical cardiovascular risk [109, 112].

It was recently revealed that the levels of adipocytokines, such as visfatin, vascular endothelial growth factor, and matrix metalloprotease, can be used as specific indicators of endothelial dysfunction. Visfatin has insulin-mimicking effects and lowers blood sugar values. According to recent data, lower concentrations were found in PCOS females compared to controls with a similar body mass index. Increased vascular endothelial growth factor production is an indicator of chronic mild inflammation and is related to impaired vascular reactivity. Increased metalloprotease 9 concentrations predict excessive CV risk and extracellular matrix remodeling [113].

1.4 Vitamin D

VD is a fat-soluble vitamin that also acts as a steroid hormone. As a steroid hormone, VD is involved in mineral homeostasis, has immunomodulatory effects, and seems to have a protective role against MetS and cardiovascular disease.

VD is produced non-enzymatically under the skin upon exposure to ultraviolet sunlight, but dietary sources are important for a sufficient supply. Cytochrome p450 enzymes, namely CYP2R1, CYP27B1, CYP24A1, and CYP27B1, are involved in the metabolism of VD, which takes place in the liver and kidney. According to some estimations, more than 200 genes, most of which are responsible for cellular proliferation, differentiation, apoptosis, and angiogenesis, are directly or indirectly controlled by 1,25-hydroxyvitamin D. VD receptors (VDR) are reported to be present in brain, prostate, breast, colon, and pancreas tissue as well as in immune cells. Normal serum levels of VD are considered to be within the range of 30–100 ng/ml. Figure 6 shows the specific effects of VDR activation in different tissues.

VD insufficiency is a comorbidity that affects approximately 50% of the whole global population [114]. Very low levels of VD (<20 ng/ml) are reported to be present

in 67–85% of PCOS women. VDD could influence PCOS through hormonal and gene modulation, resulting in infertility, metabolic syndrome, and IR [115].

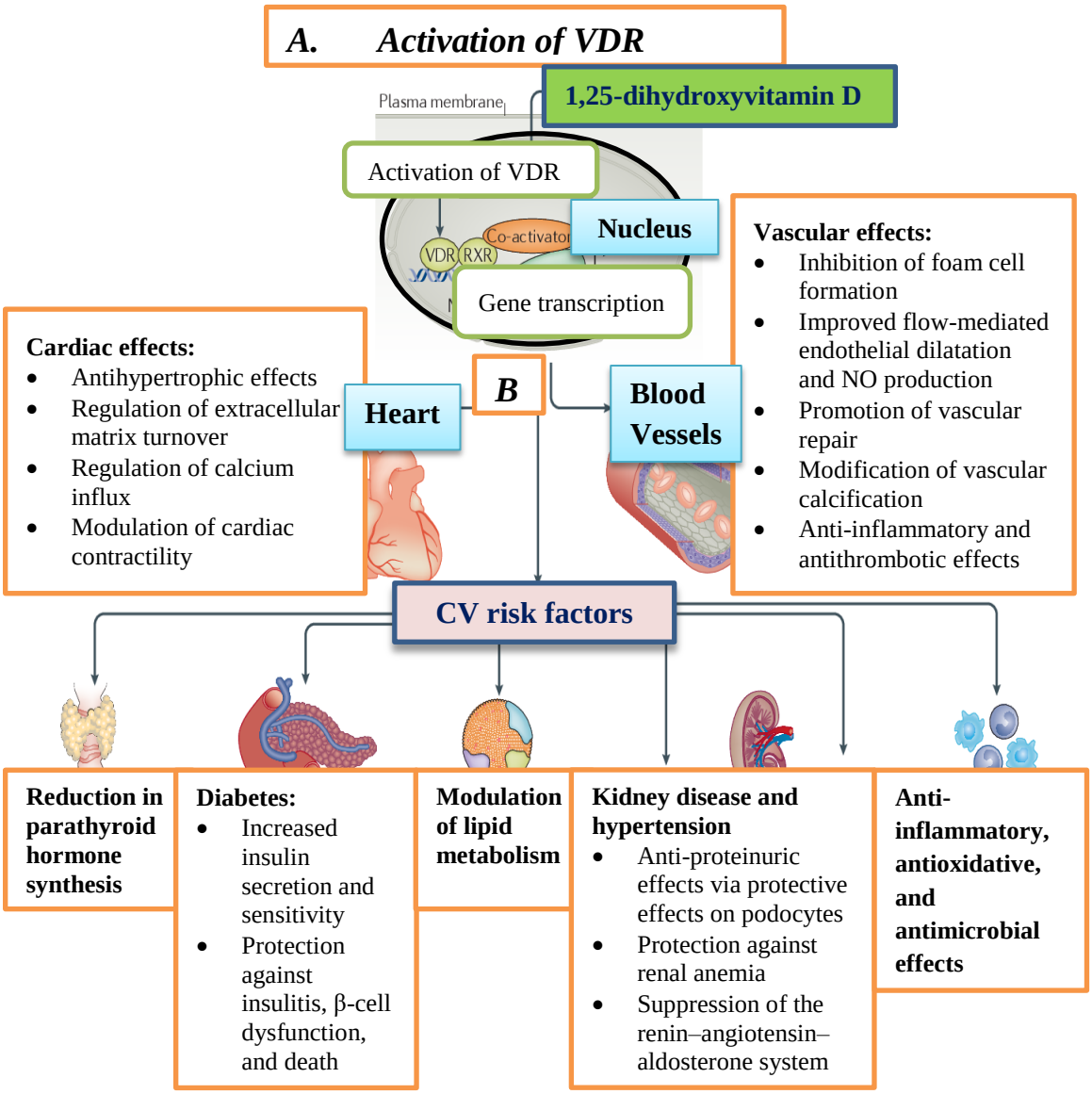

Figure 6. Effects of VDR activation in the human body, in special regard to cardiovascular risk factors. A. VDR activation in target cells. In the nucleus, VDR and retinoid X receptor form a heteromer, which promotes the transcription of several genes. **B.** VD-mediated effects in the heart and blood vessels. VD promotes vascular repair, improves flow-mediated endothelial relaxation, and modulates cardiac contractility. Further organ-specific positive effects on cardiovascular risk factors are shown below. Abbreviations: VDR, vitamin D receptor; RXR, retinoid X receptor; NO,

nitric oxide; CV risk, cardiovascular risk. Adopted and modified from the article "Vitamin D and cardiovascular disease prevention" [116].

1.4.1 Vitamin D and cardiovascular complications

The paracrine and autocrine actions of VD seem to be important for cardiovascular health. Cardiac inflammation, oxidative stress, energetic metabolic changes, cardiac hypertrophy, and alteration are just some of the complications observed in cases of VDD.

Left ventricular hypertrophy and negative inotropic changes were reported to be associated with low VD serum levels. In a rat model of T2D-induced left ventricular hypertrophy, VD successfully improved left ventricular mass by reducing TNF-α expression and inhibition of nuclear factor-kappa beta expression. VDD-induced chronic hypocalcemia could be a cause of dilated cardiomyopathy, which confirms the role of VDD. The ratio of serum $1,25(OH)_2D_3$ to parathyroid hormone could be a predictor of chronic heart failure and cardiovascular disease [117]. Not only endocrine but also genetic disorders in VDR signaling could lead to impairment in cardiac structure and function. Both whole-body VDR knockout and myocyte-specific VDR knockout mice exhibited reduced cardiac pump function due to cardiac remodeling and a higher prevalence of cardiac steatosis [118]. Another study with VDR knockout mice revealed significantly higher expression of collagen 1α1, collagen 3α1, matrix metalloproteinase 2, and osteopontin, which favor endothelial–mesenchymal transition and mediate cardiac fibrosis. If VD treatment is applied in isoproterenol-induced cardiomyopathic rats, the lower level of matrix metalloproteinase activity and diminution of endothelial cell transition are detected [119]. Some studies revealed that VDD could negatively influence postinfarction complications and cardiac remodeling in patients with myocardial infarction.

VD modulates the renin–angiotensin–aldosterone system and has direct effects on endothelial cells, calcium metabolism, and the growth of vascular smooth muscle cells

[120]. In obesity cases, perivascular adipose tissue affects smooth muscle contractility and endothelial function through local production of paracrine factors. According to some data, in VDD cases, the perivascular adipose tissue fails to suppress the enhanced contractile response of resistance arteries because angiotensin-induced contraction of mesenteric arteries was significantly increased. In a diabetic mice model of atherosclerosis, VDR and retinoid X receptor agonists (RXR) reduced atherosclerotic plaque formation and oxidative stress. Moreover, lower expression of VDR was detected within atherosclerotic plaque, which combined the expression alterations of VDR on M1 and M2 macrophages. VDD is followed by macrophage polarization (M1 versus M2) and intraplaque cholesterol efflux, which supports the role of VD in the early steps of atherosclerosis [117, 121]. Arterial aging and stiffness, atherosclerosis, and vascular calcification could also be related to low VD levels in peripheral arterial disease [120, 122, 123].

1.4.2 Vitamin D and insulin resistance

A low VD serum level seems to be a risk factor for the development of IR and diabetes (both type 1 and 2) by affecting insulin sensitivity or β-cell function. The prevalence of VDD is reported to be at least two times higher among patients with T2D compared to the healthy population. In T1D, the onset of disease often co-occurs with low VD serum levels, and the latter is reported to be a risk factor affecting the severity of later complications [124].

Genetic polymorphism of VDR, VD binding protein, and VD 1α-hydroxylase are responsible for inherited risk of IR. Several VDR polymorphisms have been found since the early 1990s, including Fok1, Apa1, Bsm1, and Taq1. Results from the Asian population indicate that Bsm1 polymorphism is associated with a significantly higher prevalence of T1D in adults. Another study from Germany suggested that a certain combination of Bsm1/Apa1/Taq1 polymorphisms increased the risk for T1D. Some electrophoretic variants of VD-binding proteins are suspected to promote prediabetes and T2D [125]. Two missense polymorphisms at codons 416 and 420 in exon 11 of the

VD-binding protein gene were reported to increase the prevalence of prediabetes in adults [126].

VD signaling pathways maintain balance in the inflammatory response by regulating both innate and adaptive immune reactions. On one hand, 1,25-dihydroxyvitamin D inhibits the adaptive immune response by affecting the capacity of antigen-presenting cells, which enhance T lymphocyte activation, proliferation, and cytokine secretion. On the other hand, 1,25-dihydroxyvitamin D regulates the innate immune system by modifying the maturation and differentiation of macrophages and dendritic cells and diminishing cytokine production. If this equilibrium of immune regulation is disturbed, β-cell degradation may occur due to overproduction of cytokines like interleukin-2 and 12 (which stimulate T-helper 1 cell development), interferon-γ, and tumor necrosis factor α (which stimulate inflammation) [126]. Moreover, macrophages and dendritic cells are able to produce 1,25-dihydroxyvitamin D with their own 1α-hydroxylase enzymes. Liver resident macrophages or Kupffer cells express the highest amount of VDR among non-parenchymal VDR-expressing cells. Their overactivation in a diet-induced obesity mice model triggered circulating macrophage recruitment in the liver, which led to chronic inflammation, impaired hepatic insulin sensitivity, and non-alcoholic fatty liver disease [127]

Insulin secretion from β-cell is reported to be directly stimulated by VD, but optimal calcium and parathyroid hormone levels are also essential. In a VDD rat, glucose-stimulated insulin secretion was significantly disturbed if hypocalcemia was also present. Parathyroid hormone not only controls the activation of 1α-hydroxylase but also decreases glucose uptake in the liver, muscle, and adipose cells. The pro-diabetic effect of parathyroid hormone is due to the inhibition of translocation of glucose transporters 1 and 4 in hepatic and skeletal muscle cells. As 1,25-hydroxyvitamin D suppresses parathyroid hormone production at the transcription level, higher parathyroid hormone plasma levels are secondarily connected to either an insufficient level of circulating VD level or receptor signaling failure [124].

1.4.3 Vitamin D and female fertility

It has been recently demonstrated that VD has multiple regulatory roles in reproductive tissue. Granulosa cells, the cumulus oophorus in human ovaries, the decidua and placenta, endometrium, and the pituitary gland all express VDR. In addition, human endometrium cells and the placenta exhibit 1α-hydroxylase activity.

VD regulates the expression of several cytochrome P450 enzymes involved in ovarian steroidogenesis. *In vitro* studies with human ovarian cell lines showed that calcitriol stimulated progesterone synthesis by 13%, estradiol synthesis by 9%, and estrone synthesis by 21% [128]. A study involving human granulosa cells ended with similar results; mRNA expression and activity of the enzyme 3β-hydroxysteroid-dehydrogenase were significantly upregulated after administration of calcitriol [129]. The mechanism of this regulation is not yet clear, but it was recently revealed that a VD response element is located in the promoter region of the aromatase enzyme, which is the key enzyme in the aromatization of androgens to estrogen in ovarian tissue. Calcitriol was also shown to have a direct effect on the signal transduction of adenosine-monophosphate-activated protein-kinase-induced phosphorylation, which is an essential step in enzyme expression associated with steroidogenesis [130]. In VDR and 1α-hydroxylase knockout female mice, infertility was found due to the combination of disturbed follicular maturation, reduced aromatase activity, and estrogen and progesterone deficit. In human granulosa cell lines from small primordial follicles (one of the characteristic features of PCOS), the level of VD in follicular fluid was two times lower compared to cells from normal-sized follicles. Moreover, VDR expression is significantly higher in the nuclei of granulosa cells from large follicles [129]. It seems that VD supports the selection and growth of follicles by adjusting L-type calcium channels and downregulating gap junction proteins in maturing follicles [131].

As was previously mentioned, the serum AMH level reflects the number of growing ovarian follicles and could be used a possible biomarker of PCOS. In human granulosa cells, calcitriol was not only able to decrease the level of AMH in small follicles but also reduced the expression of its highly specific receptor (type II) and the FSH receptor *in vitro* [129].

During pregnancy, calcium transport between trophoblasts and the endometrial decidua is regulated by locally synthetized calcitriol from the placenta. VD levels are

reported to be important for the sexual steroid synthesis of trophoblast cells and modulation of uterus tone and contraction in a calcium-dependent manner. Successful *in vitro* fertilization is more likely if VD serum levels are kept within a high normal range (at least 30–45 ng/ml) [132].

1.5 Evaluation of rodent models for PCOS

During the last three decades, many animal models have been tested to explore PCOS. The limitations of these models are mostly due to differences in ovulation patterns, released hormone profiles, sensitivity to hormones, behavioral characteristics, and organ anatomy. In addition, unlike humans, animals in nature very rarely develop AE and PCOS, although a PCOS-like syndrome with ovulation disorder is present in rats, pigs, cows, dogs, and monkeys [133]. Interestingly, in these animals, a hyperandrogen state is seldom part of the syndrome, but in primates, endocrine disorders are often involved in PCOS. In naturally hyperandrogen female rhesus monkeys, reduced fertility is combined with significantly increased serum levels of androstenedione, 17-hydroxyprogesterone, estradiol, LH, AMH, and cortisol [59].

PCOS-like animal models could be induced by androgens, including T propionate; dihydrotestosterone; dehydroepiandrosterone; or other hormonal agents, such as estradiol valerate, glucocorticoid, human chorionic gonadotropin, or AMH [60, 134-137]. Other studies used endocrine disruptors like letrozole (a P450 aromatase inhibitor) and bisphenol A to induce PCOS [138, 139]. Although such interventions and continuous light exposure could induce PCOS in rats [140], almost all of these non-hormonal methods were unable to reproduce dysfunctional ovulatory patterns and ovarian morphological changes such as a decreased amount of corpus luteum and an elevated number of antral and cystic follicles. Nevertheless, androgens are essential for inducing a hyperandrogenic state, as drugs with an estrogenic effect showed no or low impact on circulating androgen levels [133, 141]. Hence, hormonal interventions using androgens seem to be the most appropriate method for inducing a PCOS-like phenotype in animals, as they produce all the major characteristics of human PCOS [35]

In vivo rat and mouse models of human PCOS have several advantages over models involving other animals. First, these rodents possess stable genetic backgrounds, are easy to handle and maintain, and have shorter reproductive lifespan and generation times. Their short estrous cycles (4–5 days in both rats and mice) allow for fast evaluation of developing disturbances. In addition, the feasibility of genetic manipulation and affordability of rats and mice make them ideal for *in vivo* endocrine investigations. Their hormonal regulation of reproduction, hypothalamic–pituitary axis, and process of ovarian follicle development show well-conserved evolutionary patterns, similar to those in primates. In addition, rat and mice models demonstrate all the well-described hormonal and metabolic features of PCOS, including hyperandrogenism, elevated LH levels, ovulatory abnormalities, polycystic ovarian morphology, and altered insulin sensitivity [60, 142].

According to a great number of studies, timeframe and length of exposure to the chosen agent have a great influence on PCOS-like phenotypes. Postnatal treatment with androgens induces typical human PCOS features in rodents. If a single proportionate dose of T is administered to rats (1–5 days) and mice (1–3 days) after birth, the animals fail to ovulate later in adulthood. The best PCOS phenotype results were achieved with chronic treatment of T or its active metabolite, DHT (8–12 weeks) in adolescent animals (21 days old). In such cases, all the major PCOS symptoms are manifested, including estrus acyclicity, anovulation, polycystic ovaries, hyperandrogenism, and IR. Interestingly, if an excess of androgens arises during pre-adolescent (15–25 days old) female rats, none of the specific characteristics of PCOS appear [142].

Fetal or prenatal exposure to androgens led to conflicting results in rodents, but not in non-human primates. In rhesus monkeys, fetal encounter with T in the early to middle phase of gestation results in the most suitable phenotype for human PCOS models [38]. Abbott suggested a “two hit” theory regarding the manifestation of PCOS in early adulthood. The first “hit,” which is essential for later onset of AE, should occur in the prenatal phase. It was recently reported that the level of T in the umbilical vein of female infants born to hyperandrogen PCOS mothers is significantly elevated. Although there is currently no data regarding how many of these infants had PCOS as adults, the existence of prenatal T exposure in humans has been confirmed [143]. According to

Abbott's theory, hyperinsulinemia is the second "hit," which is facilitated by dysfunctional adipose-tissue-dependent lipid homeostasis and postnatal obesity.

In summary, previously reported data support the possibility of different vulnerable phases of AE after promoting the development of PCOS during adulthood. Rodent models are suitable for studying postnatal AE, as they are easy to reproduce and provoke hormonal and metabolic changes similar to those of human PCOS phenotypes.

1.6 Connections between the vascular effects of PCOS and vitamin D supply

The results of human studies involving subjects with PCOS showed a possible inverse association between serum VD levels, IR, and vascular function, but the potential beneficial vascular effects of VD supplementation are still under debate [115].

It was previously reported that VD supplementation improved the acetylcholine-induced relaxation of abdominal aorta and skeletal muscle resistance arterioles in female PCOS rats. The results from the same model also indicated that VD supplementation had a positive impact on the disadvantageous vascular and ovarian effects of nitrative stress [144-146]. Furthermore, noradrenalin-induced vasoconstriction in thoracic aorta rings from DHT-treated animals and VD-deficient animals was significantly enhanced and combined with impaired NO-dependent vasorelaxation. In this case, calcitriol administration was able to improve vascular relaxation capacities, but this effect was reduced by prostanoid-dependent vasoconstriction [145].

According to some studies, in hyperandrogen PCOS cases, vascular remodeling resulted in more rigid, less adaptive vessels, which was mostly interpreted as the first step towards a hypertensive state. If VD supplementation was applied to hyperandrogen PCOS rats, the negative effects of eutrophic remodeling were less pronounced [147].

Not only arterioles but also veins are affected by VDD, which suggests that VD plays a complex regulatory role in the vascular system. In rats with AE PCOS, veins showed the same remodeling patterns as varicose veins, and added VD resulted in beneficial effects.

The impacts of VDD and supplementation on remodeling and functional changes in coronary resistance arterioles in hyperandrogen PCOS cases have not yet been studied in parallel. Thus, we aimed to reveal the possible positive influence of VD supplementation and specific details about the damage to coronary resistance arterioles caused by hypovitaminosis D in hyperandrogen PCOS rats.

2 Aim of the study

Our aim was to create a new, easily reproducible hyperandrogen PCOS rat model to explore the use of transdermal T treatment. Rodent models are frequently used to study PCOS, but as mentioned previously, this is the first to induce AE with the use of a transdermal androgen hormone. We also aim to create a chronic model that could reproduce all the well-known reproductive, metabolic, and vascular alterations of PCOS.

Considering that PCOS and VDD are frequent comorbidities with similar cardiometabolic complication profiles, we aimed to examine their separate and joint impacts on the severity of metabolic complications, IR, and early alterations of the function of coronary resistance arteries.

The goal of the study was to investigate early and typical changes in coronary biomechanics that may put PCOS and VDD women at higher risk of cardiovascular disease. We assumed that IR is of great importance in both diseases due to its effects on functional disturbances, such as reduced dilatation capacity or coronary wall remodeling. It was also relevant for us to show whether there is any kind of interaction between VDD and AE in PCOS.

3 Materials and methods

3.1 Chemicals

Transdermal T gel (Androgel 1% from Lab. Besins International S.A, Paris, France) was used to induce a hyperandrogenic state. Cholecalciferol suspension (Vigantol oil 20,000 IU/ml from Merck/Merck Serono12, Mumbai, Maharashtra, India) was applied for oral VD supplementation. We used a normal Krebs-Ringer solution for *in vitro* studies, which contained the following (in mmol/l): NaCl 119, KCl 4.7, NaH_2PO_4 1.2, $MgSO_4$ 1.17, $NaHCO_3$ 24, $CaCl_2$ 2.5, glucose 5.5, and EDTA 0.034. To produce smooth muscle relaxation, we used a Ca-free Krebs solution containing the following (in mmol/l): NaCl 92, KCl 4.7, NaH_2PO_4 1.18, $MgCl_2$ 20, $MgSO_4$ 1.17, $NaHCO_3$ 24, glucose 5.5, EDTA 0.025, and EGTA 2. Solutions were kept at a fixed temperature (37 ºC) to stabilize pH they were bubbled with a gas mixture of O_2 (20%), CO_2 (5%), and N_2 (75%). U46619 (a thromboxane A_2 receptor agonist) was purchased from TOCRIS Bio-Techne (Bristol, UK), and adenosine (Adenocor) was purchased from Sanofi-Aventis (Madrid, Spain). Human-recombinant insulin (Actrapid pentafill 100 IU/ml) from Novo Nordisk was used for *in vitro* vascular tests. All chemicals were freshly prepared in normal Krebs solution on the day of the experiment.

For anesthesia, 45 mg/kg of intraperitoneal Nembutal (Phylaxia-Sanofi, Budapest, Hungary) was used at the end of the study procedure.

3.2 Animals

In total, 46 adolescent (21–28 days old) female Wistar rats weighing 90–110 g were provided by the Animal Facility of Semmelweis University in agreement with Charles River. The animals were supplied *ad libitum* with tap water and with normal or VD-deficient food (see below). Four to five rats were housed together with a constant light-dark (12:12 hours) cycle and controlled temperature (22 ± 1 ºC) and humidity

(56%). Starting from the 6th week, daily vaginal smear examinations were performed to assess ovulatory cycle changes. No medical or toxic complications were observed during the eight-week treatment period. The investigation conforms to the *Guide for the Care and Use of Laboratory Animals* published by the US National Institutes of Health (8th edition, 2011) and the Hungarian Law on Animal Care (XXVIII/1998). The Institutional Animal Care Commission and Hungarian authorities accepted the protocol (PEI/001/820-2/2015).

3.3 Chronic treatment

The study lasted eight weeks for each group. Rats were randomly selected into four groups. Twenty-four of the animals received a complete normal diet (ssniff Germany, SM rat/mouse complete diet containing 1,000 IU/kg vitamin D_3). To ensure optimal VD serum levels (serum 25-hydroxicholecalciferol of 30ng/ml), the above-mentioned animals received oral VD supplementation (see below). Twelve of the VD-supplemented rats composed the VD-supplemented, transdermal T-free group (VD+/T-, n = 12). The other 12 animals received regular transdermal T treatment as described below (VD+/T+ group, n = 12). To model VDD, 22 animals were put on a VD-free diet (ssniff Germany, EF rat/mouse complete VD-free diet containing < 5 IU/kg of vitamin D_3). Additional VD intake was excluded throughout the protocol period, which ensured severe VDD during the course of the study. Half of the animals were left without additional T treatment (VD-/T- group, n = 11), while the other half were given transdermal T (VD-/T+ group, n = 11).

Body weight was measured five times a week throughout the full study period. Body mass gain ratio (%) was calculated (final bodyweight/initial bodyweight *100%). Oral cholecalciferol administration proceeded as follows: at the beginning of the second week, 500 IU of vigantol oil was administered per os as a loading dose, and from the fourth week on, cholecalciferol was provided weekly up to 3000 NE/kg body weight (based on regular body weight measurements) to reach a higher range of normal VD serum levels.

Back skin was regularly shaved before transdermal T treatment. T gel was applied five times a week from the second day of treatment. The dose was 0.033 mg/g body weight[148], which ensured close to tenfold elevation of plasma T levels in treated female animals (see Table 1).

3.4 Oral glucose tolerance test and homeostatic assessment for insulin resistance

The oral glucose tolerance test (OGTT) was performed on the sixth week of treatment. After overnight fasting, a loading dose of 30% glucose solution (2g/ bodyweight kg glucose) was administered per os through a gauge [149]. Blood sugar levels were measured at 0'-60'-120' using a Decont Personal Accu-check (77 Electronics, Budapest, Hungary). Serum insulin levels at 0'-120' were detected using an enzyme-linked immunosorbent assay (ELISA) from Merck/Merck Millipore (Darmstadt, Germany/Budapest, Hungary). Homeostatic assessment for insulin resistance (HOMA-IR) was calculated as fasting plasma insulin (in milliunits per liter) × fasting plasma glucose (in millimoles per liter)/22.5.

3.5 Sexual steroid, leptin, and vitamin D plasma levels

Blood samples were taken on the eighth week of treatment from the tail vein. Serum samples were obtained and analyzed with high-performance liquid chromatography. The 5-dihydrotestosterone, 5-hydroxycholecalciferol, progesterone, and T levels were evaluated using a Flexar FX-10 ultra-performance liquid chromatograph coupled with a Sciex 5500 QTRAP tandem mass spectrometer operated in the positive electrospray ionization mode. DHT, 5-hydroxycholecalciferol, progesterone, and T were assayed in the same run. Reversed phase chromatographic

separation was performed using an octadecyl silica stationary phase. Detection was carried out with scheduled multiple reaction monitoring. A serum sample of 100–400 μL was spiked with 10 μL of internal standard solution (containing 200 ng/ml 13C3-T, 5 ng/ml D5-estradiol, and 2.5 μg/ml D6-25-hydroxycholecalciferol in acetonitrile) and diluted with 350–650 μL water and 250 μL methanol to obtain a 1 ml mixture, which was vortexed and extracted twice with 1 ml of ethyl-acetate. The organic phases were combined and evaporated to dryness under a stream of nitrogen. To assess DHT, 5-hydroxycholecalciferol, progesterone, and T levels, the residue was dissolved in a 50:50 v/v % mixture of water and methanol and was submitted for analysis [150]. Calibration was performed using the Chromsystems MassChrom® Steroids 6PLUS1® Multilevel Serum Calibrator Steroid Panel 2 (Abl&E-Jasco Magyarország Kft, Budapest, Hungary) with ranges of 0.47–1.34 ng/ml, 0.04–4.94 ng/ml, 0.17–25.6 ng/ml, and 0.05–11.8 ng/ml for DHT, progesterone, and T, respectively. Then, 25-hydroxycholecalciferol was calibrated using aqueous solutions containing 1.0–50 ng/ml 25-hydroxycholecalciferol. All calibrators were treated in the same way as test samples [150, 151].

3.6 Vaginal smear examination and ovarian morphology

Starting from the sixth week, for 14 days (until the end of the eighth week of treatment), daily vaginal smear examinations were performed to assess changes in the estrus cycles of the animals. Samples were dyed with 1% methylene blue solution. After microscopic analysis of the dominant cell types, a 4–5-day-long ovulatory cycle with at least three of four subsequent stages of the estrus cycle was regarded as normal.

The ovarian weight of each animal was measured upon termination of the study. Ovaries were collected for histological examination and fixed in formaldehyde solution. Four-μM longitudinal and serial sections of the ovarium were produced, and every tenth section was stained with hematoxylin–eosin. Representative samples of each treated group (n = 6) were analyzed to detect polycystic ovarian morphology. The total number, mean diameter, and total area of follicles and corpora lutea and the total area of ovarium

were measured with AxioVision Panoramic Viewer software (3DHISTECH Ltd., Budapest, Hungary).

3.7 Transthoracic echocardiography and invasive arterial blood pressure measurement

Transthoracic echocardiography was performed at the eighth week of treatment under pentobarbital anesthesia (intraperitoneal injection of 40 mg/kg). For this purpose, we used a SONOS 5500 ultrasound machine (Hewlett Packard) equipped with a high-frequency linear transducer (5–15 MHz). Long-axis B-mode images of the left ventricle were obtained to calculate end-diastolic volume and end-systolic volume from the left ventricular area (LVA) and left ventricular length (LVL) as $8(\mathrm{LVAd})^2/3\pi\mathrm{LVLd}$ and $8(\mathrm{LVAs})^2/3\pi\mathrm{LVLs}$, respectively (in the formulae, d and s stand for diastole and systole, respectively). Based on these parameters, the ejection fraction was calculated as 100(end-diastolic volume – end-systolic volume)/end-diastolic volume. Left ventricular short-axis echocardiograms were taken at the level of the papillary muscles to determine diastolic left ventricular wall thickness. In order to assess fractional shortening, short-axis images were used to measure left ventricular internal diameters in the diastole and systole (LVIDd and LVIDs, respectively). These parameters allowed for calculation of fractional shortening using the following formula: 100 (LVIDd-LVIDs)/LVIDd [152, 153].

Arterial blood pressure was invasively measured through an internal carotid artery catheter and was performed at the beginning of the experiment. Carotid artery catheter insertion was performed under aseptic conditions with the help of general surgical pentobarbital anesthesia [154].

3.8 Pressure arteriography of coronary arterioles

During the eighth week of treatment, animals were anesthetized as mentioned above. Under anesthesia, we performed heart ultrasound and invasive blood pressure measurement through carotid artery cannulation. Then, the chest was opened in order to extract the heart, which was perfused with a non-heparinized normal Krebs solution for two minutes. Heart weight was measured, followed by micropreparation of a coronary arteriole segment from the intramural network of the left anterior descendent coronary artery with an *in vivo* outer diameter of 100–150 μM. The coronary arteriole was microcannulated in normal Krebs solution in an organ chamber filled with saline and then oxygenized at a fixed temperature of 37 ºC. The microcannulas were connected to the servo pumps (Living Systems). Under no-flow conditions, the arteriole was intraluminally pressurized at 50 mmHg and extended to its normal *in vivo* length. The setup was positioned in the light path of an inversed Leica microscope to allow for evaluation of changes in the inner and outer diameters of the arteriole. With the aid of a digital histologic Leica video camera (DFC 320) and Leica QWin software, magnified pictures of the arteriole were obtained. Analysis of the vessel pictures was performed offline with the help of a Leica QWin image analyzing program.

The arteriole was allowed to equilibrate in oxygenized normal Krebs solution at a fixed pressure (50 mmHg) and temperature (37 ºC) for 30 minutes. During this incubation period, the arteriolar segments developed spontaneous tone. Their steady-state diameter was measured in this state. Pressure-diameter profile curves were obtained by training (0-150-0-150 mmHg intraluminal pressure) and performing fraction elevation (10 mmHg) of the intraluminal pressure from 0 mmHg to 150 mmHg. At the end of the 10-minute incubation period, when 50 mmHg intraluminal pressure was achieved, the resting diameter under intraluminal pressure was re-measured.

As the next step, an increasing dose of insulin (insulin concentrations of 30 mIU/ml, 100 mIU/ml, 300 mIU/ml, 600 mIU/ml; 1 IU = 0.035 mg insulin) was added to the bath and segments were incubated for eight minutes. After registration of each dose response, the drug was washed out from the bath of the organ chamber with a slow continuous flow of oxygenized and heated normal Krebs solution.

The vasoconstrictor biomechanical properties of the vessel were tested by a single high dose (10^{-6} M) of thromboxane A_2 receptor agonist (U46619). After five minutes of incubation, intraluminal pressure was gradually increased in 10 mmHg increments from 0 to 150 mmHg and alteration of the inner and outer diameters was registered. After resting for 10 minutes under 50 mmHg intraluminal pressure, the inner and outer diameters were recorded again.

Without washing out U46619, an elevating dose of adenosine (10^{-9} M, 10^{-8} M, 10^{-7} M, 10^{-6} M), a potent coronary relaxant agent, was added to the organ bath. Each dose was equilibrated for a three-minute period and changes in diameter were recorded.

The maximal smooth muscle relaxant potential of the vessel was evaluated by changing the organ chamber's solution to a calcium-free Krebs solution, which was both heated and oxygenized. After 20 minutes of incubation, the passive biomechanical properties of the vessel were examined based on changes in the inner and outer diameter under gradual elevation of intraluminal pressure (0 mmHg to 150 mmHg). The maximum relaxant diameters of the segments were obtained in calcium-free Krebs solution (warmed and oxygenized).

3.9 Biomechanical calculations

As mentioned above, the inner and outer diameters of the vessel were measured. The inner and outer radii were computed based on the diameter results (R_i = inner diameter/2, where R_i is the inner radius and R_o = the outer diameter/2, where R_o is the outer radius). Full contraction of the segment (T_{Full}) is described by the following equation: $T_{Full} = 100*(R_{cafree}-R_{U46619})/R_{cafree}$ (%), where R_{cafree} is the radius measured in calcium-free solution and R_{U46619} is the measured radius if thromboxane A_2 agonist was added to the organ chamber. Spontaneous (myogenic) tone was computed as follows: $T_{nKR} = 100*(R_{cafree}-R_{nKR})/R_{cafree}$ (%), where R_{nKR} is the radius of the coronary segment in normal Krebs solution. Adenosine-induced relaxation of the coronary arteriole segments was calculated with the help of the radius parameter (R_{Ade}), which was measured after an elevating concentration of adenosine was applied in the organ

chamber as follows: $T_{Ade} = 100 * (R_{Ade} – R_{u46619})/R_{cafree}$ (%). Tangential stress was calculated according to the Laplace equation: $Tg_{stress} = P*R_{i\ nKR}/h_{nKR}$, where Tg_{stress} is the tangential (circumferential) wall stress, P is the intraluminal pressure, Ri is the inner radius, and h_{nKR} is the wall thickness in normal Krebs solution. Wall thickness was calculated based on the following parameters: $h = R_o – R_i$. The circumferential incremental elastic modulus was computed with the following equation: $E_{inc} = (dP/dR_o) * 2(R_i * R_o^2)/(R_o^2 – R_i^2)$, where E_{inc} is the incremental elastic modulus and dR_o is the change in the outer radius in response to a change in dP upon intraluminal pressure. A cross-sectional area was calculated based on the inner and outer radii in a calcium-free solution: $A_{cs} = (R_{o\ cafree}^2 – R_{i\ cafree}^2) * \pi$. The remaining tone in insulin was expressed as a percent of the actual radius as a percent of passive (fully relaxed) radius: $T_{Ins} = 100 * (R_{cafree}-R_{Ins})/R_{cafree}$ (%), where R_{Ins} is the radius of the coronary arteriole if insulin was added to the organ chamber.

3.10 Histology

For histological examination, an intact and neighboring segment of the same vessel was removed from the coronary network. At first, the segment was fixed with formaldehyde and stained with hematoxylin-eosin and resorcin-fuchsin. Microscopic and morphometric pictures were taken, and elastic fiber density measurements were conducted on the scanned sections (Panoramic Viewer, 3DHISTECH Ltd., Budapest, Hungary) under identical conditions. RGB pictures of resorcin-fuchsin-stained segments were analyzed with Leica Qwin image analysis software. The software allows for identification, selection, and subtraction of structures of images based on spectrums of R (red), G (green), and B (blue) including 126 tones of red, 126 of green, and 126 of blue. The likelihood of separating structures within their limits is greater if higher numbers of red, green, and blue tones and combinations thereof are present in the studied tissue. Elastic fiber density was analyzed as follows: as the magenta color of the resorcin-fuchsine stain suppresses green, RGB green intensities (0–255) were measured in the radial direction starting at the endothelial luminal surface.

3.11 Immuno-histochemistry of coronary arterioles

Paraffin-embedded tissue sections were stained against insulin receptor beta and VDR using the BenchMark ULTRA Automated IHC/ISH slide staining system (Ventana Medical Systems, Inc., Tucson, AZ, USA) with monoclonal mouse anti-insulin receptor beta (Santa Cruz Biotechnology, Dallas, TX, USA) and polyclonal rabbit anti-VDR (Abcam, Cambridge, UK) antibodies. Visualization of specific labeling with diaminobenzidine as a colored substrate and hematoxylin counterstaining was performed with an UltraView Universal Diaminobenzidine Detection Kit (Ventana Medical Systems, Inc., Oro Valley, Arizona, USA), which is an indirect, biotin-free system for detecting mouse IgG, mouse IgM, and rabbit primary antibodies. The applied antibody concentrations and dilutions were 1:1000 for VDR and 1:100 for insulin receptor beta. For the negative control, we used the same tissue before applying the primary antibody (knockout tissue samples were not available). Insulin receptor beta connective tissue samples (fibroblasts expressing the receptor) were used as a positive control for VDR colon samples. Microscopic images of the stained vessels were taken by the Zeiss Axio Imager system (Zeiss, Oberkochen, Germany). The positively stained area was measured as the percentage of total tissue area in the intimal and medial layers of the vessel walls using ImageJ software (NIH, Bethesda, Maryland, USA).

3.12 Statistical analysis

For statistical analysis, we used GraphPad Prism 6.0 (GraphPad Software, Inc. San Diego, California, United States). A two-way repeated-measures analysis of variance (ANOVA) was used for statistical analysis of the curves (e.g., the cumulative concentration-diameter curve). Discrete parameters (e.g., bodyweight) were compared with one-way ANOVA. The Tukey test was used as a post-hoc test, and $p < 0.05$ was uniformly accepted as the threshold for statistical significance. Data are shown as mean ± SEM (Standard error of Mean).

4 Results

4.1 Bodyweight, heart weight, and body mass gain ratio

After eight weeks of treatment, regular transdermal T administration resulted in higher body weight ($p < 0.01$). VDD also provoked bodyweight changes. It resulted in significantly higher mass gain ratios in transdermal T-free animals ($p < 0.05$).

T treatment led to significantly higher heart weights ($p<0.01$) compared to VD-treated and transdermal T naïve rats. Without chronic transdermal T, VDD caused no further changes in heart weight values. Similarly, no significant differences in heart weight or body weight ratio were observed among the four groups. The results are shown in Table 1.

4.2 Serum hormone and leptin levels

A VDD diet produced serum 25-hydroxicholecalciferol levels about fivefold lower compared to the supplemented groups ($p < 0.01$). Oral VD supplementation led to normal VD levels and excluded hypovitaminosis D in the treated groups.

To prove the effectiveness of the transdermal T treatment, serum levels were tested on the eighth week of treatment. The levels of elevated serum T ($p < 0.01$) and its active metabolite, 5-DHT ($p < 0.05$), were detected in transdermally treated animals. Serum progesterone levels were reduced, leading to missing or disturbed luteinization. Both the above-mentioned features—hyperandrogen status and problems with luteinization—are typical in PCOS females. Serum leptin levels were significantly elevated as a result of T treatment (but only in the VD-supplemented group; $p < 0.05$). The above-mentioned results are shown in Table 1.

Table 1. Mean final bodyweights, body mass gain ratio, mean heart weight, steroid hormone, and leptin serum levels on the eighth week of treatment and the mean number of complete estrus cycles during the 14 days of the protocol in the four treatment groups. T-treated animals had significantly higher body and heart weights compared to double control animals. The treatment protocol resulted in appropriate sex hormone and VD serum levels. The highest leptin levels were detected in VD+/ T+ animals. Not only T treatment but also VDD had a significantly negative impact on the number of estrus cycles, which corresponds to the ovulatory pattern changes seen in PCOS cases. Groups of female animals: VD+, VD-supplemented; VD-, VD-deficient; T+, transdermal T-treated; T-, transdermal T non-treated. The significances are as follows: †, †† significant difference between T-treated and non-T-treated animals ($p < 0.05$ and $p < 0.01$, respectively); * significantly different from VD+/T- (double control) animals ($p < 0.05$); ‡ significantly different from corresponding animals kept on a VDD diet ($p < 0.01$). Results are shown as mean ± SEM.

	VD+/T- **n = 12**	**VD+/T+** **n = 12**	**VD-/T-** **n = 11**	**VD-/T+** **n = 11**
Final mean bodyweight (g)	282.58 ± 6.25	327.83 ± 8.32††	296.95 ± 3.94	321.55 ± 3.21††
Body mass gain ratio (%)	267.68 ± 6.51	305.98 ± 10.78††*	288.43 ± 3.78*	304.64 ± 5.83††*
Mean heart weight (g)	1.15 ± 0.05	1.46 ± 0.06*	1.27 ± 0.03	1.36 ± 0.03*
Testosterone (ng/ml)	0.31 ± 0.16	4.29 ± 0.56††	0.72 ± 0.16	5.49 ± 0.56††
5-dihydro-testosterone (ng/ml)	0.10 ± 0.01	0.62 ± 0.14†	0.12 ± 0.02	0.60 ± 0.16†
Progesterone (ng/ml)	19.20 ± 2.42	11.64 ± 1.47†	21.24 ± 3.71	10.91 ± 1.15††
25-hydroxi-cholecalciferol (ng/ml)	32.33 ± 4.49‡	33.11 ± 4.46‡	6.04 ± 0.63	6.01 ± 0.68
Leptin (ng/ml)	64.55 ± 9.53	153.88 ± 26.16†	118.97 ± 16.23	113.85 ± 28.47
Mean number of estrus cycles (days)	3.64 ± 0.15	0.90 ± 0.21††	2.00 ± 0.23*	0.36 ± 0.21††

4.1 Ovarian morphology and estrus cycle

After the eighth week of treatment, ovary morphology was examined and the total numbers of follicles and corpora lutea were counted. The mean area and total ovary area were also calculated in representative samples of each animal group (n = 6). According to observation of microscopic ovarian morphology, dominant follicles and corpora lutea were detectable only in VD-treated and transdermal T-free rats (Fig. 7).

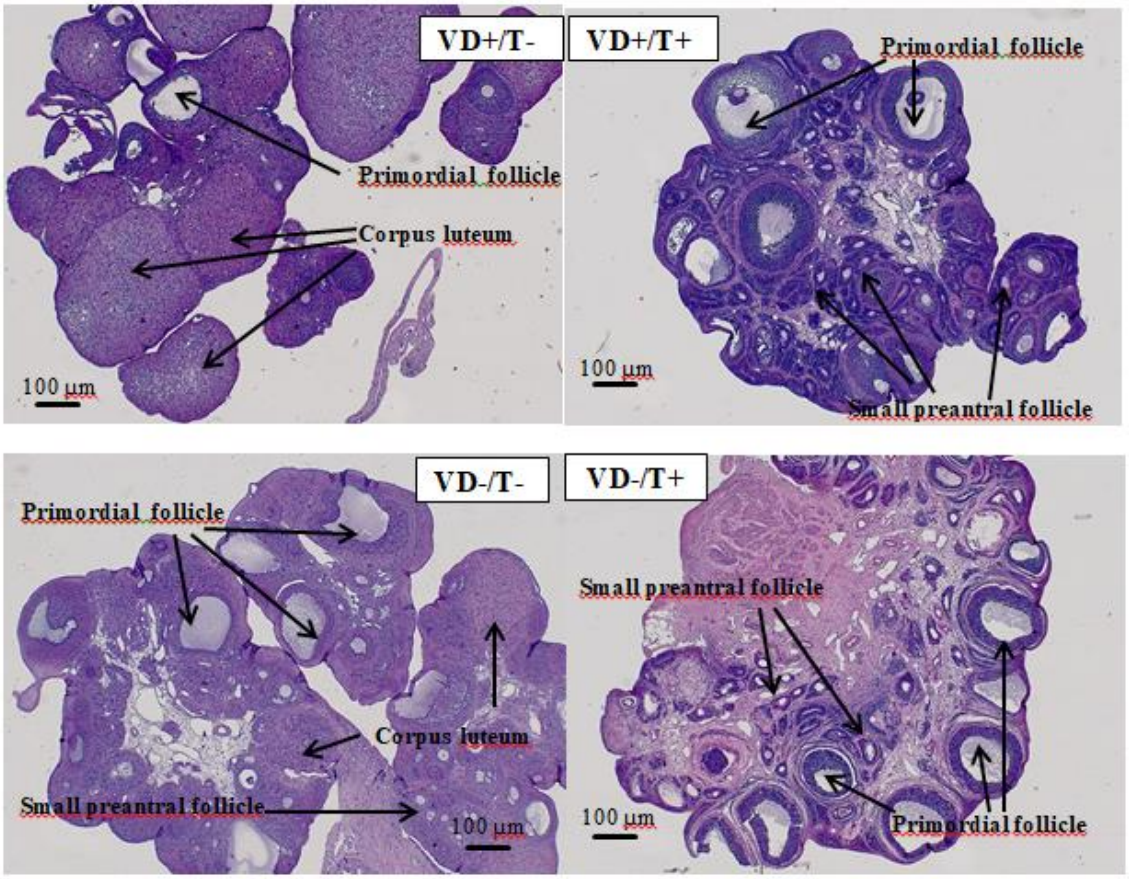

Figure 7. Representative hematoxylin-eosin stained pictures of the ovaries from each group. Only VD+/T- animals showed normal follicle development and a normal number of corpora lutea. Polycystic morphology was detectable after transdermal T treatment, but VDD alone caused similar changes and led to an elevated number of non-dominant (primordial) follicles.

Regarding the mean number of follicles, not only transdermal T treatment but also VDD led to a significantly increased number of follicles ($p < 0.05$ for all groups in comparison to the VD-supplemented, transdermal T-free group). Many small-sized primordial follicles were present in the samples, which is a typical feature in PCOS. The number of follicles and their area ratio were significantly higher in the T-treated groups compared to their counterparts ($p < 0.05$ for both comparisons; Figs. 8A and 8B). The corpus luteum was practically missing in T-treated animals, regardless of VD status, which issued in a significantly lower number of corpora lutea and mean area surface (T-treated vs. T-naïve, $p < 0.0001$, for both the VD-supplemented and VD-deficient group; Figs. 8C and 8D). Again, VDD alone reduced the number of corpora lutea and surface area ($p < 0.05$), contributing to polycystic ovary morphology.

Changes in the normal estrus cycle could be easily judged by daily vaginal smear examinations. The normal cycle lasts about 96 hours and consists of four phases. During proestrus, it is common for round and nucleated epithelial cells to be present. The estrus phase is characterized by non-nucleated, cornified epithelial cells. Metestrus features a low number of cells with many shattered cell parts, and diestrus is easy to identify due to the large amounts of lymphocytes and mucus. The mean number of estrus cycles observed during the last 14 days of the treatment period is shown in Table 1. Non-T-treated, VD-supplemented females had the highest number of intact estrus cycles. In VD-deficient, transdermal T-free animals, a significantly lower number of cycles was detected ($p < 0.05$ compared to counterparts; $n = 12$ in each group). If transdermal T treatment was applied, the normal number of estrus cycles was dramatically reduced ($p < 0.01$ in both comparisons; $n = 11$ for each group).

To briefly summarize the above data, PCOS morphology (high amount of small, primordial follicles or a missing or low number of corpora lutea) and irregular ovulation patterns could be observed not only in transdermal T-treated animals but also in VDD animals.

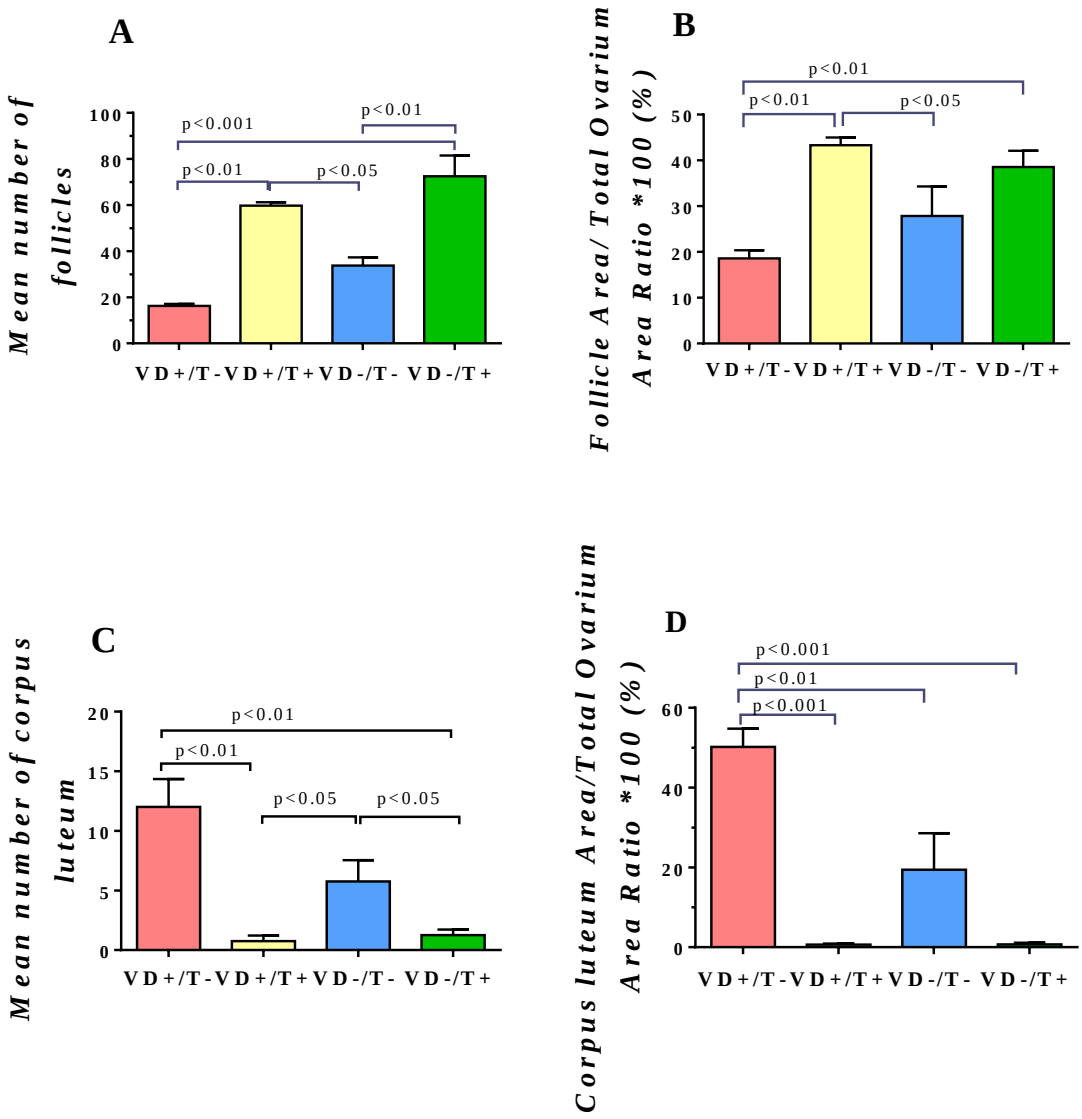

Figure 8. Mean numbers and total area ratio of follicles and corpora lutea. The bars show **(A and C)** the mean numbers of follicles and corpora lutea and **(B and D)** the mean percentages of the area ratio of follicle and corpora lutea compared to the total ovary area of each group. In PCOS cases, a high number of small primordial follicles and a low number of corpora lutea are typical. These typical changes were significantly detectable in both T-treated groups. The VD-supplemented, T-free group showed normal numbers of follicles and corpora lutea. Significances are shown above the bars. Data are shown with SEM in each group (n = 6) at the eighth week of treatment. Abbreviations: VD+, VD-supplemented; VD-, VD-deficient; T+, transdermal T-treated; T-, transdermal T-free animals.

4.2 Transthoracic echocardiography and blood pressure results

Transthoracic echocardiography was performed at the end of the study protocol to detect early changes in wall dimensions and cardiac pump function. The echocardiographic assessment revealed no significant difference in the left ventricle end diastolic volume or ejection fraction. No significant differences in parameters that were sensitive to left ventricular hypertrophic transformation (IVSD and end-diastolic volume of the left ventricle) were detected (Table 2). Blood pressure and heart rate values did not differ significantly among the four groups.

Table 2. Hemodynamic parameters, left ventricular dimensions, and *in vivo* pump functions of rats assessed by echocardiography at the eighth week of treatment (mean ± SEM). No significant changes were observed in the measured parameters among the four groups. IVSD(d): thickness of interventricular septum measured in a cross-sectional image at the level of the papillary muscles in diastole. All results shown as mean ± SEM.

	VD+/T- n = 12	**VD+/T+ n = 12**	**VD-/T- n = 11**	**VD-/T+ n = 11**
IVSD(d) (cm)	0.21 ± 0.01	0.20 ± 0.01	0.20 ± 0.03	0.22 ± 0.01
End-diastolic volume of the left ventricle (cm^3)	0.31 ± 0.01	0.29 ± 0.01	0.32 ± 0.02	0.27 ± 0.02
Ejection fraction (%)	69.2 ± 2.2	67.5 ± 3.2	66.9 ± 2.2	64.9 ± 2.0
Fractional shortening (%)	40.5 ± 1.4	40.4 ± 2.6	43.1 ± 1.4	38.9 ± 2.9
Cardiac output (cm^3/min)	83.8 ± 5.0	72.8 ± 4.1.6	86.3 ± 4.5	64.0 ± 4.6
Heart rate (beat/min)	378 ± 4	371 ± 4	401 ± 10	362 ± 9
Systolic blood pressure (mmHg)	133.2 ± 4.1	149.2 ± 3.6	133.8 ± 7.0	139.3 ± 5.3
Mean arterial blood pressure (mmHg)	110.5 ± 4.2	120.0 ± 4.2	106.2 ± 5.7	116.6 ± 6.0
Diastolic blood pressure (mmHg)	104.9 ± 4.4	110.1 ± 6.1	101.6 ± 5.2	111.5 ± 6.9

4.3 Geometry of the coronary arteriole

Coronary arterioles with similar outer diameters *in situ* underwent micropreparation and were used for further pressure angiography. After reaching a passive relaxation state in calcium-free solution after 50 mmHg of pressure, the inner and outer diameters of the vessel were measured. The inner and outer radii were computed based on the measured inner and outer diameter results as mentioned above.

VD-deficient groups had significantly higher wall thickness, narrower passive lumina and lower inner radii values ($p < 0.01$ in all comparison to VD-supplemented groups; Figs. 9A and 9B). The ratios of the outer radius and wall thickness showed the significant result that the VD-/T+ group had the smallest vessels with the thickest walls (Fig. 9C; $p < 0.05$ versus VD-/T-; $p < 0.01$ in comparison to both VD+ groups).

The significant effect of VD availability on morphological modeling of the coronary arteriole is revealed by alterations in the results of the cross-sectional area (i.e., the amount of wall material). While it was the highest in the double control group, VD-supplemented, T-free rats ($20.1 \pm 3.4\ 10^3 \mu m^2$), lower values ($11.4 \pm 1.1$ and $10.9 \pm 0.9\ 10^3\ \mu m^2$) were observed in the T-free and T-treated VD-deficient groups, respectively. Independently of VD supplementation, T treatment reduced the cross-sectional area results (to $14.3 \pm 1.6\ 10^3\ \mu m^2$ and $p < 0.01$ in all comparisons).

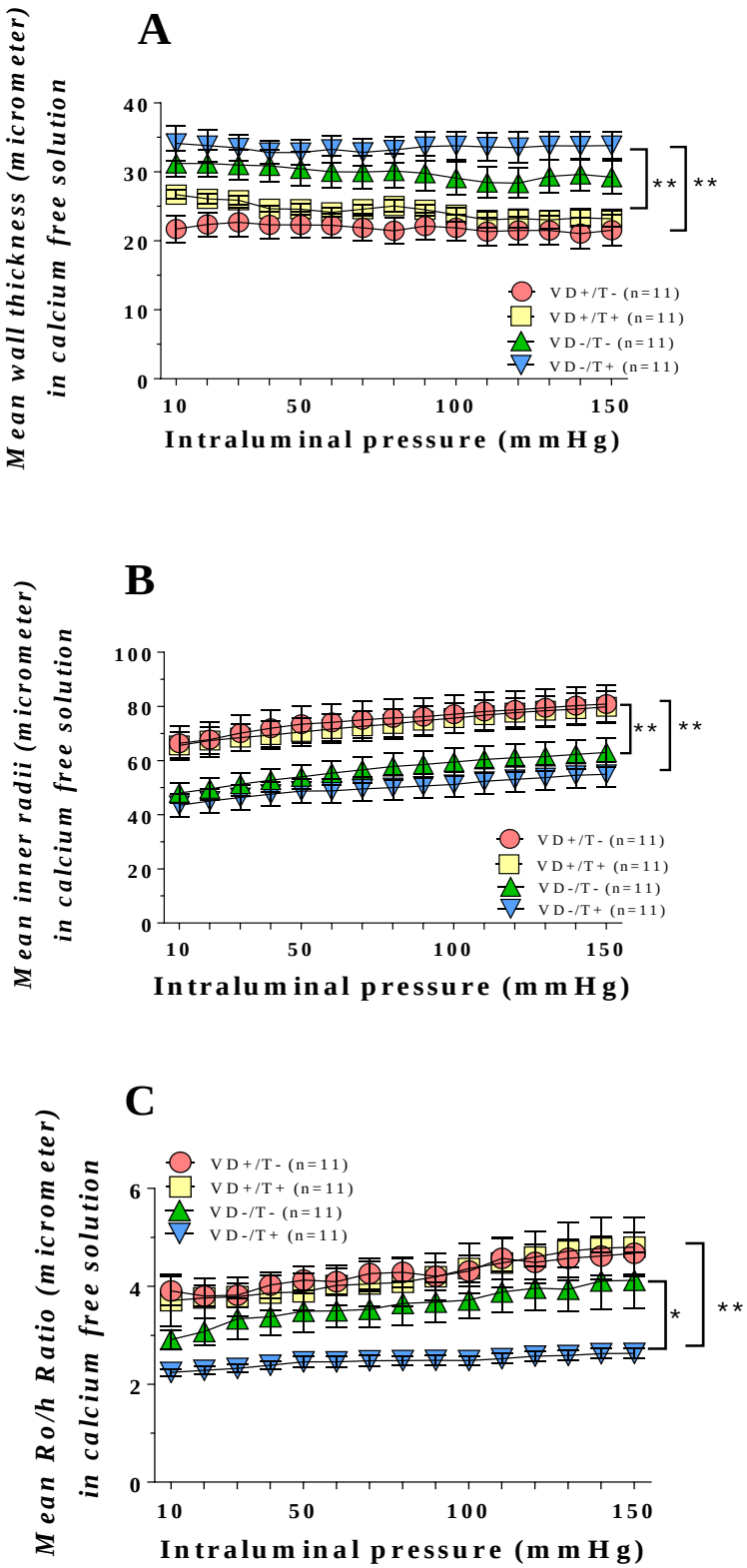

Figure 9. Geometric properties of intramural coronary resistance arteries from VD-supplemented and VD-deficient T-treated and untreated female rats. A. Wall

thickness as a function of intraluminal pressure in calcium-free solution (full relaxation). The wall thickness values of both VD- groups are significantly higher ($p < 0.01$ in both comparisons) than those of VD+ groups. **B.** Inner radius in the fully relaxed state as a function of intraluminal pressure. Here again, VDD caused significantly lower inner radii values in both groups compared to VD+ groups ($p < 0.01$ in both comparisons). **C.** Outer radius and wall thickness ratios in calcium-free solution. These results suggest that the coronary arterioles of the VD-/T+ group were the smallest vessels with the thickest wall. * VD-/T+ differs significantly from VD-/T- group ($p < 0.05$); ** VD-deficient group significantly differs from both VD-supplemented groups ($p < 0.01$). N = 11 for each group. Abbreviations: VD+, VD-supplemented; VD-, VD-deficient; T+ with transdermal T treatment; T-, without T treatment; VDD, vitamin D deficiency. The significances of the ANOVA tests are shown. All values are expressed as mean ± SEM.

4.4 Control of coronary arteriolar smooth muscle tone

Myogenic tone is essential for resistance artery function and autoregulation of local blood as well as protection against drastic intraluminal pressure changes. Alone or in combination, VDD and T treatment resulted in a significant reduction of myogenic tone compared to the double control (Fig. 10A; $p < 0.01$).

To examine how much additional substantial contraction could be achieved, a potent thromboxane A_2 agonist, U46619 (1 μmol/l at 50 mmHg) was used. In our "noxa-free" control group (VD-supplemented, transdermal T-free animals), 54.6 ± 3.2% contraction was recorded. According to our observations, T treatment did not affect the substantial contraction capacity (54.1 ± 4.1%). Developed tone was notably reduced in VDD: 26.7 ± 4.7% and 34.8 ± 1.9% of contraction were recorded in the VD-deficient T-free and T-treated groups, respectively ($p < 0.01$ in comparisons of VD-supplemented and VD-deficient groups).

After thromboxane A_2 agonist contraction, adenosine was used to induce endothelial-dependent relaxation of smooth muscle in arterioles. Our findings showed a clear connection between VD-supplemented groups, T administration, and endothelial-dependent relaxation capacities; the double control segments produced significantly better relaxation than the double noxa segments ($p < 0.01$; Fig. 10B).

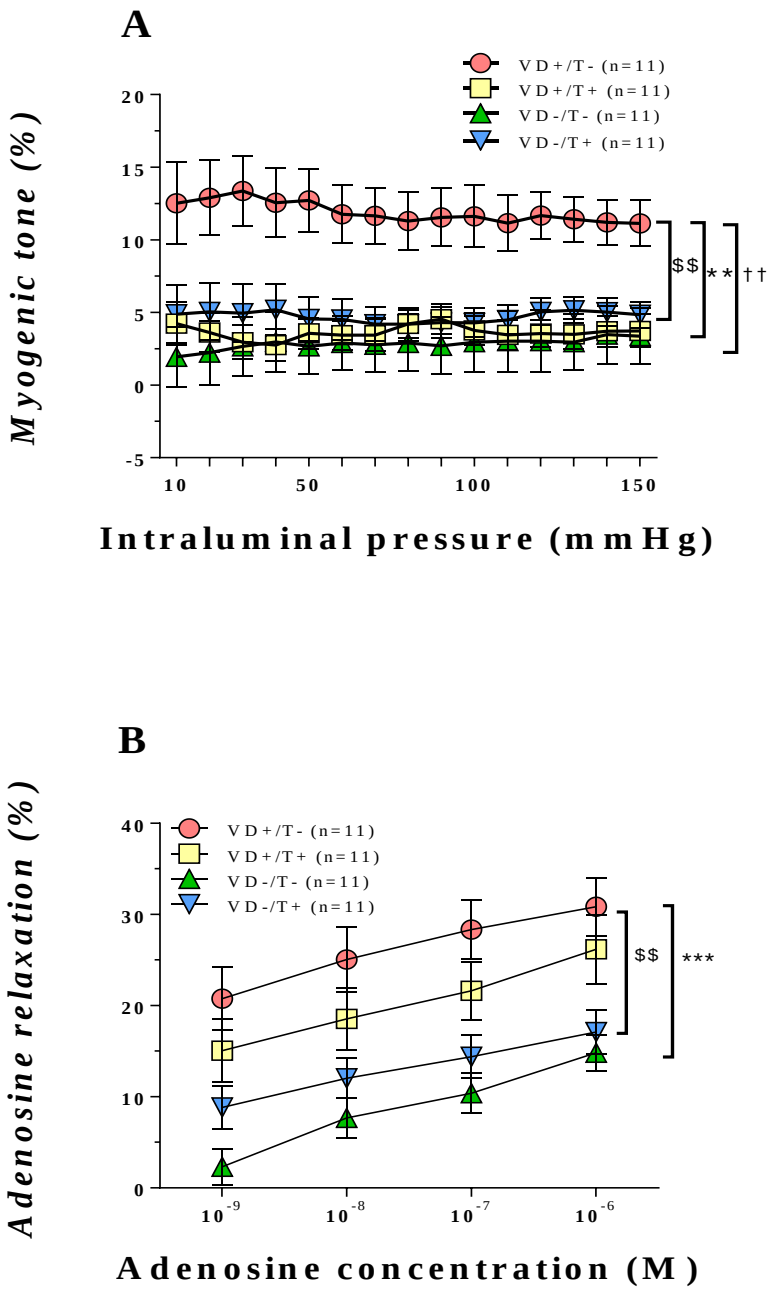

Figure 10. Contractile and relaxation properties of intramural coronary resistance arteries. A. Myogenic tone in nKR as a function of intraluminal pressure. In the

presence of any of the applied noxa, significant myogenic tone reduction compared to the noxa-free (VD+/T-) group was calculated. **B.** Relaxation induced by increasing concentrations of adenosine at 50 mmHg pressure. VD deficiency, alone or in combination with T treatment, resulted in diminished adenosine-induced relaxation of the arterioles compared to the double control group. **, *** VD-deficient group significantly differs from the corresponding VD-supplemented group ($p < 0.01$ or 0.001). $$ Double control (VD-supplemented, T treatment-free) animals were significantly different from animals with double noxa (VD-deficient, T-treated; $p < 0.01$). †† T-treated and T-free animals were significantly different ($p < 0.01$). Abbreviations: VD+, VD-supplemented; VD-, VD-deficient; T+, with transdermal T treatment; T-, without transdermal T treatment. The significances of ANOVA tests are shown. All values are expressed as mean ± SEM.

4.1 Elasticity of the coronary arteriolar wall

Tangential wall stress was measured in normal Krebs solutions (Fig. 11A). According to our findings, tangential wall stress was significantly diminished in both VD-deficient groups compared to the VD-supplemented groups, regardless of T treatment ($p < 0.001$ in all comparisons). To evaluate further elastic characteristics of the vessel wall, the tangential elastic modulus was calculated and plotted against tangential wall stress. With the help of these calculations, the elasticity of wall material could be judged independently based on geometrical properties.

Measured values of 25 kPa (high stress) are shown in Fig. 11B. A significantly reduced elastic modulus was found in the presence of VDD.

T treatment led to further value reduction, but this observation was only true in VD-deficient female rats (Fig. 11B). If the elastic modulus was plotted against intraluminal pressure (Fig. 11C), intraluminal-pressure-dependent differences were found. At low pressure ranges, all three treated groups differed significantly from our double controls (the VD-supplemented, transdermal T-free group; $p < 0.05$ in all three comparisons). Nonetheless, an increase in intraluminal pressure led to further significant value reduction in the case of the VD-deficient, transdermal T-treated group.

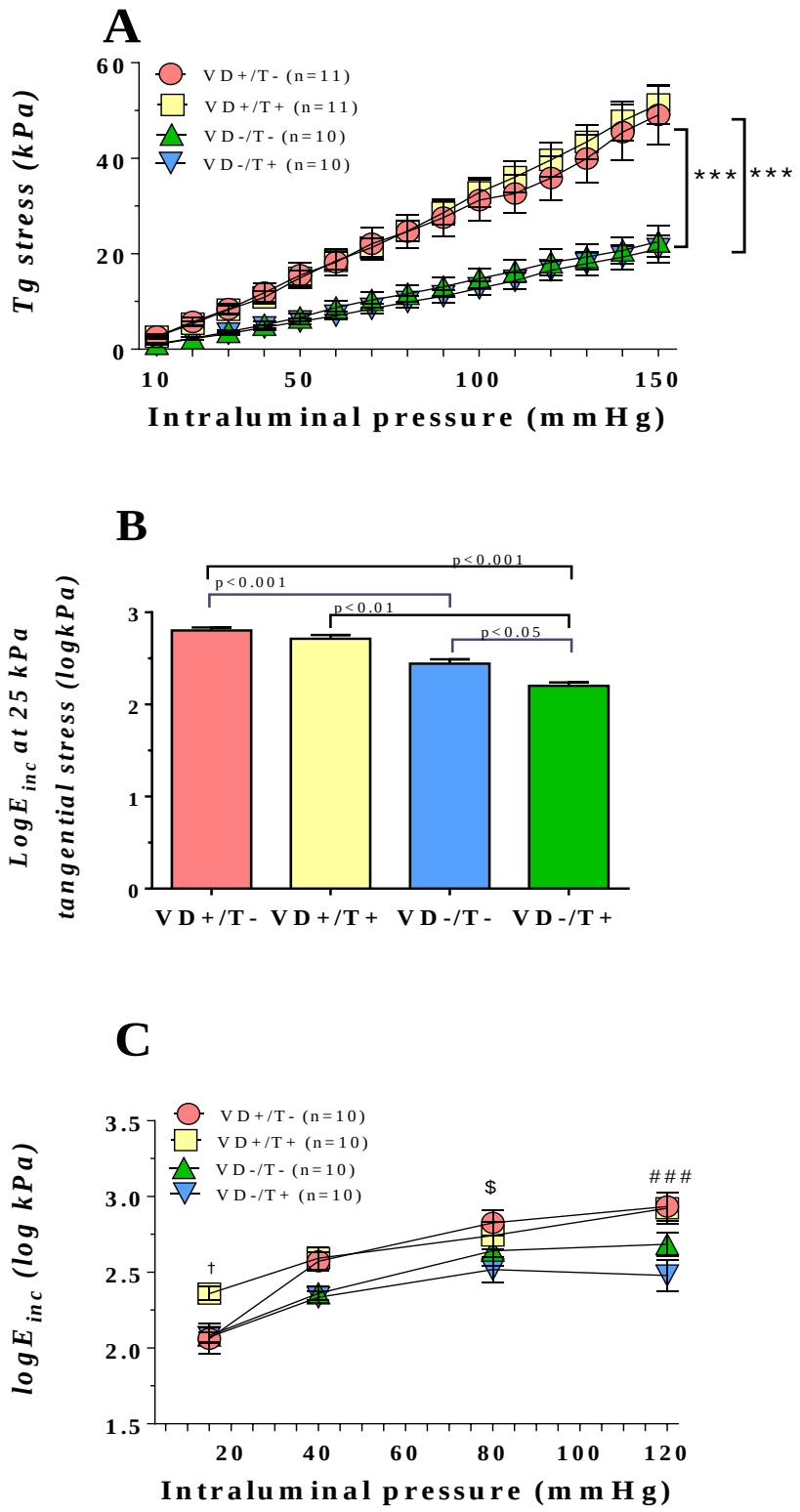

Figure 11. Tangential wall stress in normal Krebs solution and elastic properties of coronary arterioles. A. Tangential wall stress in normal Krebs solution. At

intraluminal pressures above 50 mmHg, both VD- groups differ significantly from both VD+ groups ($p < 0.001$ in all comparisons). **B.** Incremental elastic moduli ($logE_{inc}$) at tangential stress of 25 kPa. Both VD- groups had reduced incremental elastic moduli values compared to both VD+ groups. The significances of ANOVA tests are shown with numbers. **C.** Elastic modulus as a function of intraluminal pressure. At low pressure ranges, all three treated groups differed significantly from the double control ($p < 0.05$ in all three comparisons). At higher intraluminal pressure ranges, the VD-/T+ group showed further significant reduction than VD+ groups ($p < 0.001$). *** At intraluminal pressures above 50 mmHg, both VD-deficient groups statistically differ ($p < 0.001$ with ANOVA) from the VD-supplemented group. † VD-supplemented, transdermal T-free, and the other three groups significantly differ from each other ($p < 0.05$). $ Significant difference between VD-supplemented, transdermal T-free, and double noxa group ($p < 0.05$). ### Significant difference between VD-deficient, T-treated, and both VD-supplemented groups ($p < 0.001$). Abbreviations: VD+, VD-supplemented; VD-, VD-deficient; T+, with transdermal T treatment; T-, without transdermal T treatment; Tg stress, tangential wall stress of the arteriole; $logE_{inc}$, incremental elastic modulus of the vessel wall, $logE_{inc}$(logkPa), elastic modulus as a function of intraluminal pressure.

4.2 Elastica staining

A significant increase in the elastic components of the vessel wall occurred when either of the noxa was present. This observation could be quantitatively established by measuring the green density along a line that starts from the endothelial surface and is driven radially outward. The presence of fewer green components indicates a greater amount of elastic density because of its suppression by the magenta color of the elastica stain. In the vessel wall of double control animals (VD-supplemented, transdermal T-free), significantly fewer elastic components were detected (Fig. 12A, $p < 0.05$). On the other hand, both VDD and T treatment had an impact on elastic components, which can be demonstrated by significant changes in the quantity of the elastic components.

Figure 12B shows a representative picture of the resorcin-fuchsin stained vessel sections of each group.

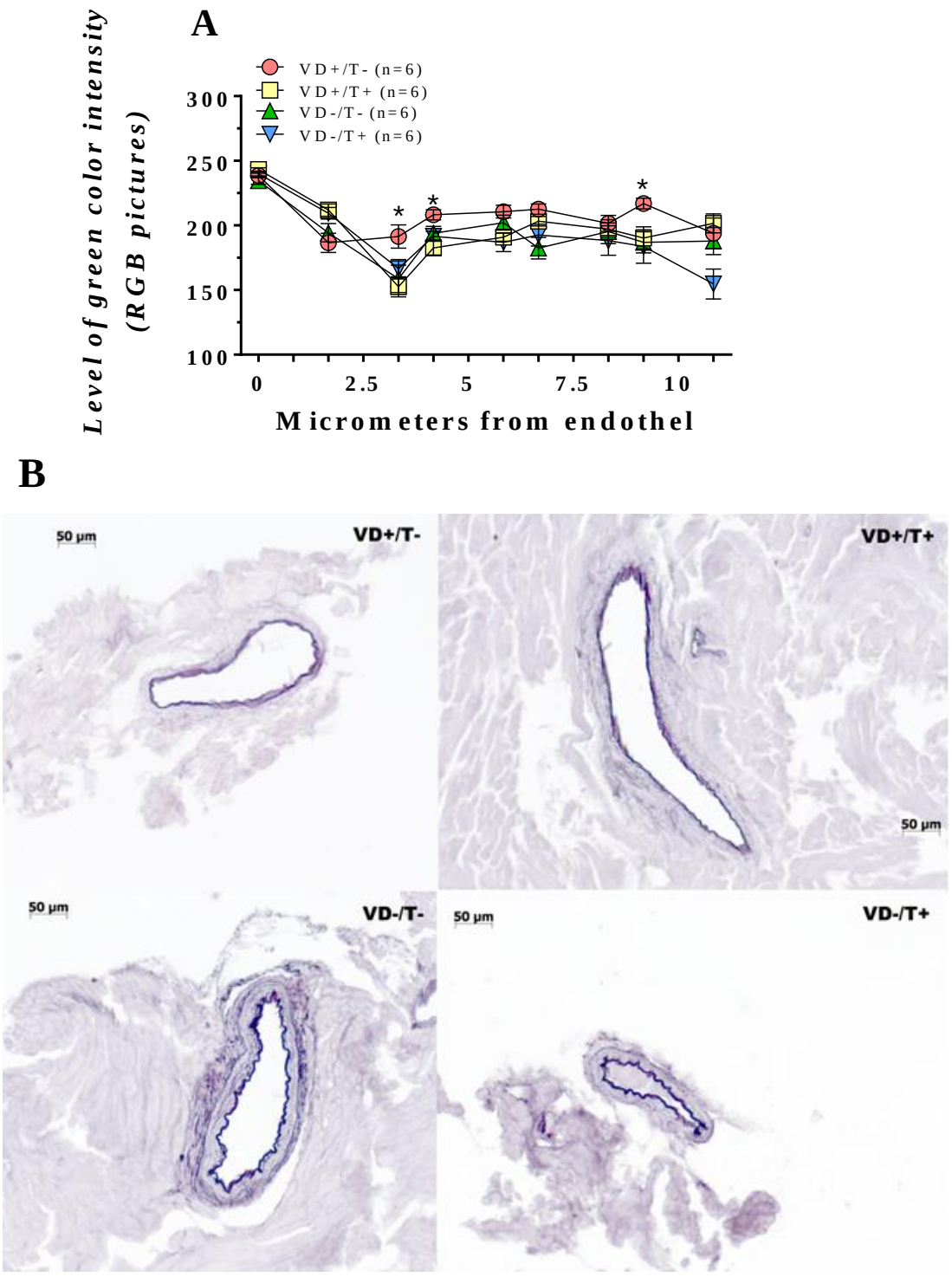

Figure 12. Density of elastic fiber and representative pictures of resorcin-fuchsin stained histological sections of intramural coronary resistance arteries from VD-supplemented and VD-deficient T-treated and untreated female rats. A. Density of

elastic fibers analyzed in RGB pictures of resorcin-fuchsin stained vessel sections. As magenta suppresses green, a low level of green color intensity is typical if elastic fibers are present. **B.** Representative picture of resorcin-fuchsin stained vessel sections of each group. Abbreviations: VD+, VD-supplemented; VD-, VD-deficient; T+, with transdermal T treatment; T-, without transdermal T treatment. The significances of ANOVA tests are shown. All values are expressed as mean ± SEM. * VD-supplemented, non-T-treated animals differ from all other groups ($p < 0.05$).

4.3 OGTT: plasma glucose, insulin and HOMA IR levels

Oral glucose tolerance levels are shown in Figure 13A. No significant difference in fasting glucose levels among the four groups could be detected. Considering the 60-minute post-load blood sugar levels, VD-supplemented, transdermal T-treated rats developed significantly higher blood sugar levels compared to the double control ($p < 0.05$). Nevertheless, T treatment altered 120-minute post-load values, which were significantly higher for the T-treated animals than for both groups of T-free animals ($p < 0.05$ and $p < 0.01$, respectively). Although the VD-deficient and transdermal T-treated group showed a slight elevation in 60-minute results, no significant difference could be detected during the OGTT protocol.

Regarding basal plasma insulin levels measured before OGTT, we observed no significant changes among the four groups. However, the 120-minute values of the VD-deficient, T-untreated group were significantly higher than those of their VD-supplemented double control counterparts (Fig. 13B, $p < 0.05$). Moreover, the computed HOMA IR results of both VD-deficient groups were significantly higher (Fig 13C, $p < 0.05$) than those of the VD-substituted double control animals. Mild elevation of HOMA IR was detected in the VD-supplemented, T-treated group, but this alteration was not significant.

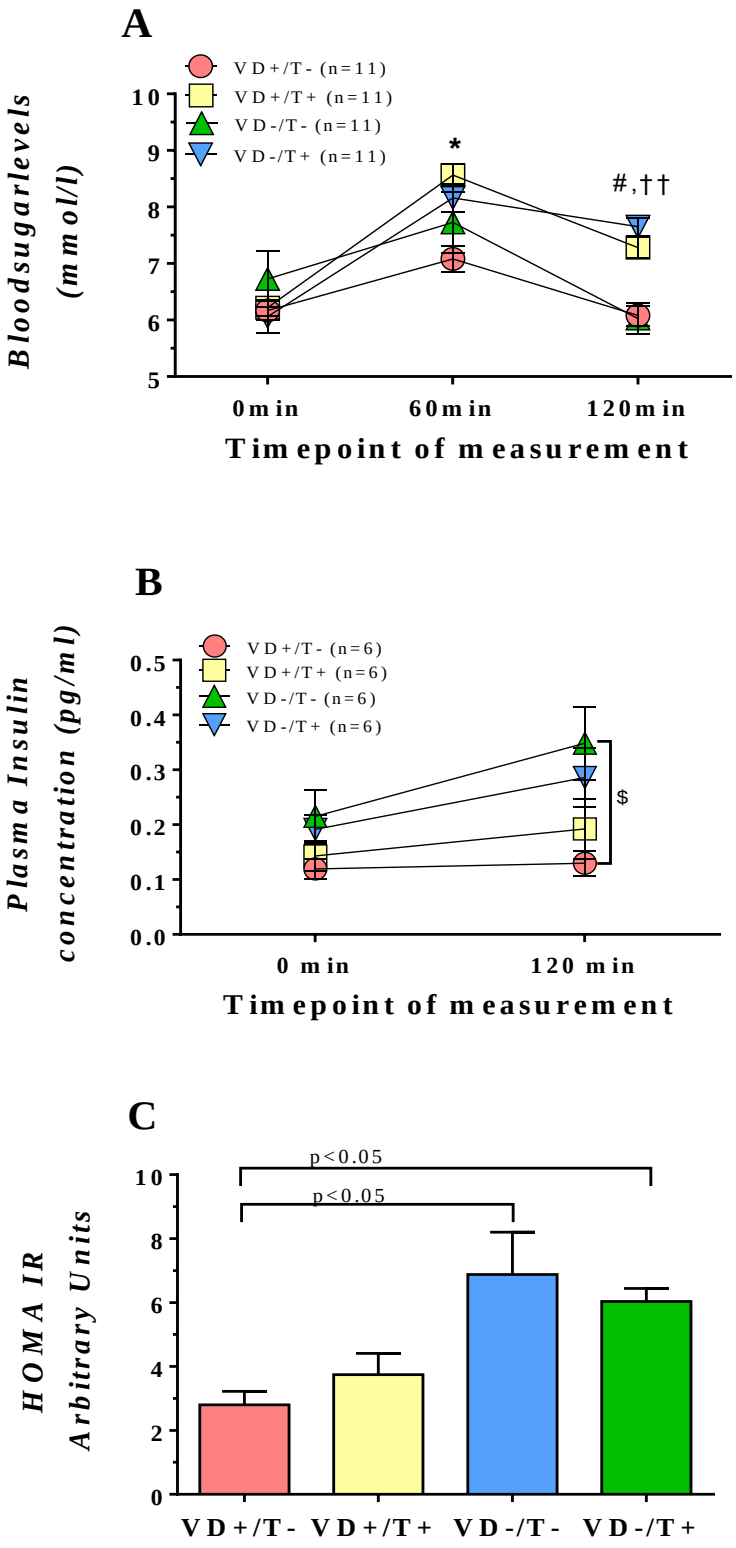

Figure 13. Results of OGTT: plasma glucose, insulin, and HOMA IR. A. Plasma glucose levels of the four groups following OGTT at the sixth week of treatment (n = 11

for each group). **B.** Plasma insulin levels following OGTT (n = 6). **C.** Calculated HOMA IR values (n = 11 for each group). Both T+ groups had significantly elevated 120-minute blood sugar levels compared to the T- groups ($p < 0.05$), but these results were not accompanied by significant plasma insulin concentration changes. The VD-/T- group had a significantly higher 120-minute plasma insulin concentration compared to the VD+/T- group. HOMA IR results revealed that both VD- groups had IR. Abbreviations: VD+, VD-supplemented; VD-, VD-deficient; T+, T-treated; T-, without T treatment. Significances of ANOVA tests are shown. * Significant difference between the VD-supplemented, T-treated and T-free (double control) animals ($p < 0.05$). #, †† Significant difference between T-treated and both non-treated animal groups ($p < 0.05$ and $p < 0.01$, respectively). $ VD-deficient, transdermal T-free animals significantly differ from corresponding animals kept on a VD diet ($p < 0.05$).

4.4 Insulin-induced relaxation in coronary arterioles

An increased concentration of insulin was added to the organ chamber to investigate its effects on coronary arteries (Fig. 14A). One of the two noxa was enough to significantly reduce insulin-induced relaxation ($p < 0.01$ in all three groups compared to the double control animals). At higher insulin concentrations, no relaxation could be observed at all.

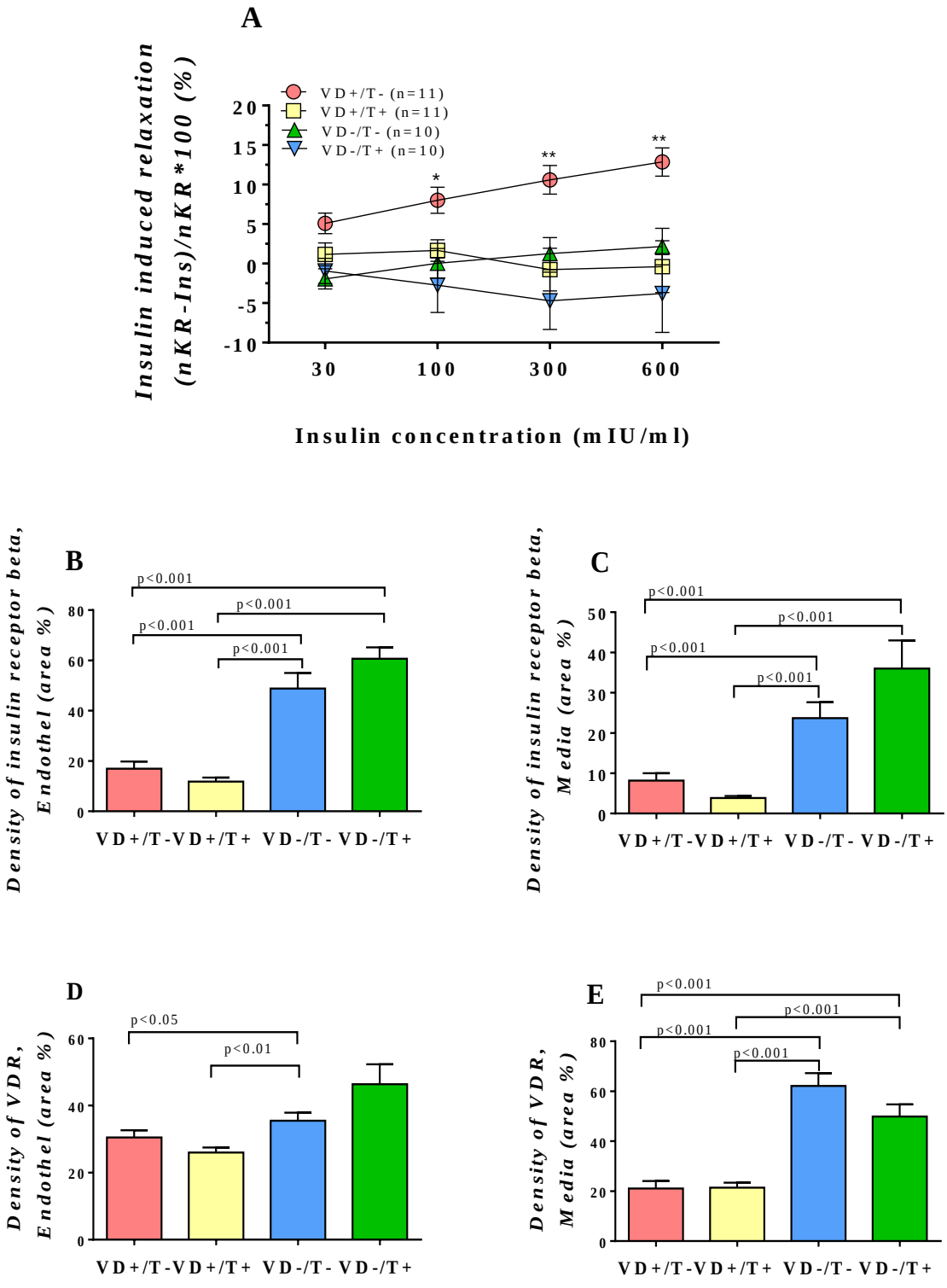

Fig 14. Insulin sensitivity and receptor expression in the walls of coronary arterioles. A. *In vitro* relaxation of intramural coronary arterioles in response to elevated concentrations of insulin. **B and C.** Immunohistochemical density of insulin receptor in the endothelium and media, respectively. **D and E.** Immunohistochemical

density of VDR in the endothelium and media, respectively. **B–E.** Total area ratio percentages (n = 6 in all groups). Insulin-induced relaxation capacities were significantly reduced in VDD and hyperandrogenism if an elevated concentration of insulin was added to the organ chamber. The insulin receptor beta and VDR density across the vessel wall was significantly elevated in both VD- groups (significance values are shown above the bars). Abbreviations: VD+: VD-supplemented; VD-: VD-deficient; T+: treatment with T; T-: no T treatment. **A–E.** Means ± SEM. Significances of ANOVA tests are shown. *, ** All the other groups were significantly different from the VD-supplemented and T-treatment-free (VD+/T-, double control) group ($p < 0.01$ and $p < 0.001$, respectively). Other significances are indicates by numbers in the diagrams.

4.5 Insulin and vitamin D receptor density in coronary arteriolar tissue

To reveal insulin receptor and VDR density through the coronary arteriole wall, we used immunohistochemistry. According to our findings, VDD affects the expression of the insulin receptor in the endothelial and media layers. In both groups, regardless of T treatment, we measured significantly higher insulin receptor density (Figs. 14B and 14C; $p < 0.001$ in all VD-supplemented comparisons). Additionally, greater VDR density was found in VDD female animals (Figs. 14D and 14E; $p < 0.01$ and 0.001). This difference was more pronounced in the media layer, and T treatment resulted in no further differences between the two groups. Figures 15A and 15B show representative images of insulin and VD receptor density in vessel sections.

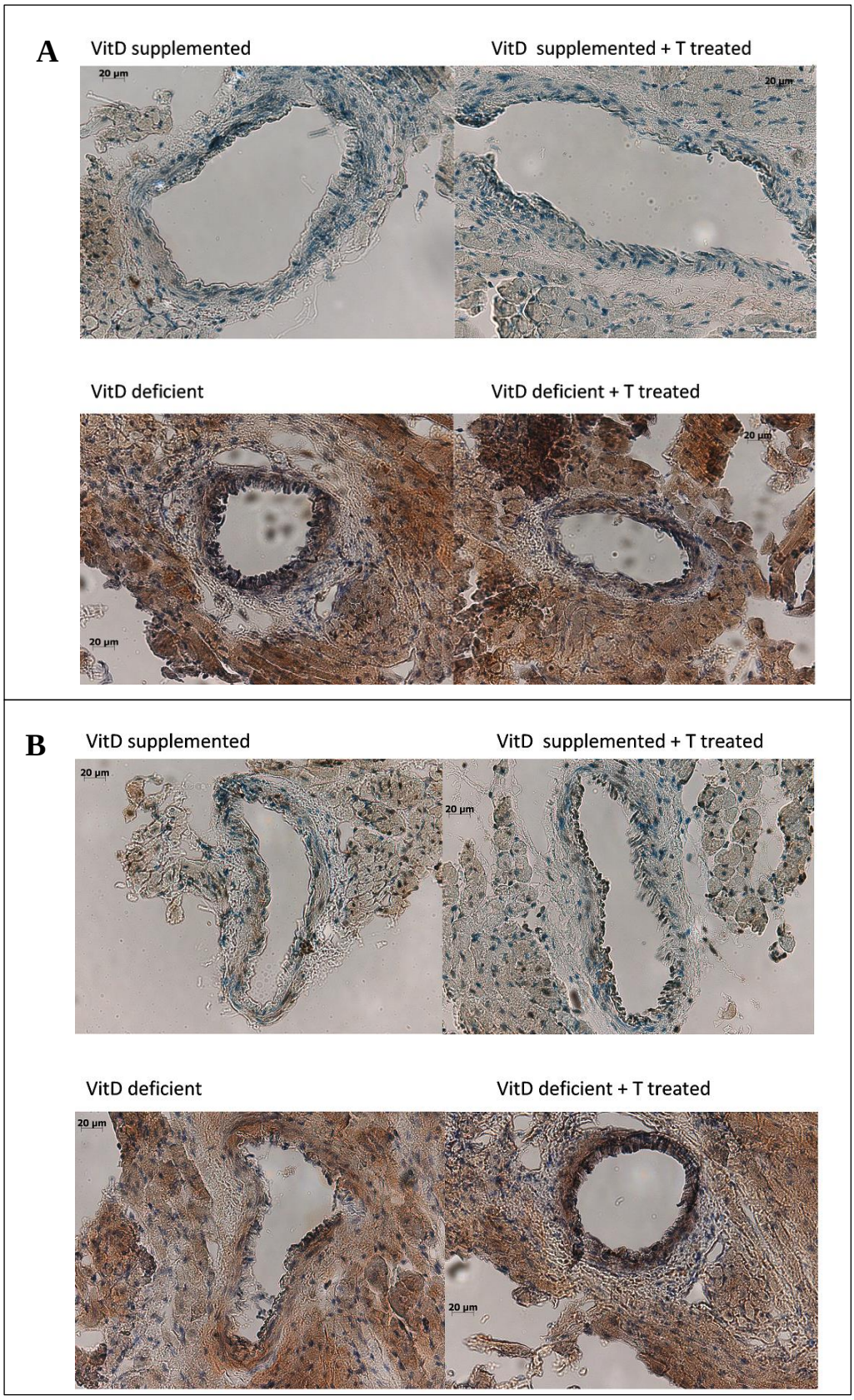

Fig 15. Representative pictures of insulin (A) and VD (B) receptor density in vessel sections. Abbreviations: VD+, VD-supplemented; VD-, VD-deficient; T+, treatment with T; T-, no T treatment.

5 Discussion

5.1 Phenotypical and cardiometabolic changes after transdermal testosterone treatment with and without vitamin D deficiency

According to some estimations, VDD affects 67–85% of the hyperandrogenic female population worldwide [115]. It serves as an aggravating risk factor for cardiovascular and metabolic diseases, such as stroke, acute coronary syndrome, or diabetes mellitus [6, 145, 155-158]. Additionally, AE and low VD serum levels could trigger the occurrence of IR and coronary disease. Our aim was to reveal the possible interplay of these factors and the effect of this interplay on coronary microvascular damage in PCOS with or without VDD.

In our model, transdermal T was applied to provoke AE. T gel was introduced in the early 2000s as a treatment for the hypogonadic state in males [159]. As this application results in good bioavailability, quickly achieves steady-state plasma levels (within the first 48 hours after administration), and is easy to use, it is an ideal agent to investigate androgen state alterations in rodents [160]. As far as we know, this was the first time that hyperandrogen PCOS was induced by chronic transdermal T gel administration.

According to the latest recommendations of the Androgen Excess and PCOS (AE-PCOS) Society [161, 162], clinical or biochemical hyperandrogenism is crucial to diagnose PCOS in humans, and the oligo-anovulatory PCO form of ovulatory dysfunction is required. At the end of our study protocol, markedly elevated levels of serum T and its active metabolite, DHT, were measured in treated animals (Table 1). In contrast, untreated animals maintained normal sex steroid levels, proving the efficiency of our transdermal T regime. Hyperandrogen female rats developed phenotypic changes in PCOS, including higher body weight and body mass gain ratio, similar to the changes observed in human PCOS patients (Table 1).

The goal VD status was achieved in specific groups. Oral VD supplementation ensured high normal levels, while VD-deficient nutrition resulted in VDD (Table 1). We concluded that our study successfully reproduced a range of VD serum levels in rodents similar to those observed in various human studies investigating the level of VDD in the adult PCOS female population [158, 163].

In addition to hyperandrogenism, the gonadal features of PCOS include chronic ovulation irregularities and ultrasound diagnosis of polycystic ovary morphology. Transdermal T-treated female rats failed to develop regular estrus cycles, which led to both a low follicle rate and a remarkable reduction in the number of corpora lutea. We detected that VD-deficient animals without hyperandrogenism had irregular estrus cycle patterns, an elevated number of follicles, and a reduced number of corpora lutea. These findings could be explained by the multiple regulatory roles of VD in ovarian follicular development and luteinization. As VD affects the signal transduction of AMH, FSH sensitivity, and progesterone production of granulosa cells, PCOS-like ovarian morphology and ovulation disturbances are often observed in VDD cases [164]. The linkage between AMH levels and VD could explain follicular arrest in VDD cases. Whilst AMH inhibits primordial follicular recruitment and decreases the FSH sensitivity of growing follicles, the two- to threefold higher AMH serum levels in PCOS females could play an essential role in ovulatory dysfunction [165]. AMH also negatively controls aromatase activity in granulosa cells and reduces estradiol transformation, resulting in higher androgen serum levels. *In vitro*, the AMH gene is regulated by VD through functional VD response elements that bind the VDR [166]. Since both hormones show the same seasonal variability and an inverse correlation between VD and AMH was proven to exist in fertile females (with low circulating VD and high AMH levels), this could be a key element for understanding the effect of VD action on ovulatory function [167].

Regarding metabolic consequences, our findings revealed that both hormonal disturbances could provoke IR. Recently, some human studies pointed out that approximately 80% of the PCOS population suffers from IR, but this appears to be multifactorial [168]. The correlation between the prevalence of IR and VDD has already been investigated [163, 169, 170]. Although there was no difference between fasting glucose values in our study, transdermal T treatment led to elevated blood sugar levels

(after 60 min and 120 min), which was not followed by greater insulin secretion (Figs. 13A and 13B). In VDD cases, higher insulin output was recorded, but glucose levels remained unchanged (Fig. 13B). Interestingly, there was no additional effect between VDD and the hyperandrogenic state (i.e., the presence of both noxa did not result in worse IR values). These observations suggest that two different paths toward IR could be present at one time. In the case of T treatment, serum insulin levels were unable to prevent the development of hyperglycemia. This could be due to decreased beta-cell sensitivity, which may lead to worsening of hyperglycemia. If VDD is present, higher insulin levels could be able to normalize blood glucose levels. In addition, the measured HOMA IR values revealed that VDD was enough on its own to provoke IR. If the serum levels of VD were optimal, the HOMA IR results of T treated animals were unaltered in comparison to transdermal T-free ones (Fig. 13C). When the two noxa were combined, a marked elevation in plasma glucose levels were recorded despite higher 120 min insulin levels. In the double noxa group, HOMA IR and elevated plasma glucose levels indicated disturbed insulin homeostasis.

Leptin, which is an anorexigenic hormone, has multiple roles in the development of obesity, metabolic syndrome, and IR. Leptin receptors are present in various tissues, including hypothalamus, liver, stomach, adipose, and ovary tissue. In PCOS patients, hyperleptinemia combined with IR is frequently present, among other hormone disturbances [171]. In our study, we observed that both T treatment (regardless of VD status) and VDD led to higher serum leptin levels (Table 1). On one hand, this could be interpreted as a consequence of VDR upregulation in adipose tissue [172]. On the other hand, leptin is involved in ovarian steroid genesis, suggesting a strong relation between higher circulating T levels and hyperleptinemia. In PCOS cases, just like in T2D cases, dysfunctional adipocytes are involved in higher activation of anti-apoptotic pathways, resulting in higher body mass index and obesity [173]. The higher amount of malfunctioning fatty tissue could be responsible for higher leptin levels, which could be accompanied by leptin resistance [174]. Recently, some studies pointed out that considering the leptin/adiponectin ratio allows for better evaluation of the long-term metabolic complications in both the lean and obese PCOS populations. According to these data, altered hormone secretion in adipose tissue could be more important for determining metabolic risk than obesity alone [175].

According to recent guidelines, screening for cardiovascular risk factors should be implemented early in young fertile females with PCOS [162]. In PCOS women with or without actual cardiovascular risk factors, regular check-ups that include measurements of blood pressure and lipid profile control are recommended on a yearly basis.

At the end of our study, we observed slight elevation of the systolic, diastolic, and mean arterial blood pressure values in both T-treated groups. In humans, these results might be regarded as early alterations and regular follow-ups would be necessary according to recent guidelines. Although the cardiac output results were mildly reduced in both T-treated groups, all of the other echocardiographic parameters remained unchanged (compared to our double controls). Although hypertension and changes in cardiac pump function are considered to be late-onset cardiovascular complications, their predicting factors have been reported to be present in the early stage of human PCOS. Humoral factors, such as high normal aldosterone serum levels (excluding primary hyperaldosteronism), could be one of the first steps toward dysregulation of the renin–angiotensin aldosterone axis [176]. Evaluation of atherogenesis based on carotid intima-media thickness or the circulating levels of insulin, total cholesterol, LDL-C, C reactive protein, and serum interleukin-18 could be also useful for predicting subclinical cardiovascular disease [98].

5.2 Biomechanical and pharmacological changes of the coronary arterioles

We observed that not only hyperandrogen status (transdermal T treatment) but also chronic VD withdrawal alone resulted in fundamental changes in arteriolar geometry. Smaller inner radii and greater wall thickness was observed in both VD-deficient groups. Interestingly, if both conditions were present (VDD and AE), no further aggravation (greatest wall thickness and smaller lumina) could have been detected (Figs. 9A and 9B). These findings suggest that accompanying VDD would have an early and strong influence on vascular geometry changes in PCOS females.

The antiatherosclerotic role of VDR signaling in leukocytes/macrophages was described recently. VD is involved in antiatherosclerotic mechanisms, which inhibit the activation of the local renin-angiotensin system in macrophages and in the atherosclerotic lesion itself [177]. On the other hand, VDD leads to remodeling triggered by the migration of leukocytes into the vessel wall, early vessel wall calcification, and activation of endothelial cells and pericytes [178]. In PCOS patients, androgen-induced hypertension is the first step toward long-term changes in vessel biomechanics [179]. As reported previously, this complex phenomenon causes inward hypertrophic remodeling in peripheral resistance vessels, in which the media thickens to the disadvantage of the lumen, resulting in an increased cross-sectional area and media-to-lumen ratio [147]. Moreover, higher intima media thickness values have been reported in human muscular arteries among PCOS patients [180, 181]. In our study, coronary arteriole geometry did not correlate with blood pressure, as could have been expected based on Folkow's law [182]. Nevertheless, VD had indisputably trophic effects on the coronary arteriolar wall, as VDD is accompanied by increased wall thickness and luminal reduction. On the other hand, T-induced alterations were not detected as expected, and arteriole wall mass was decreased in hyperandrogen female rats. In light of these findings, we assume that T might have some kind of inhibitory effect on female coronary arteriolar wall trophism. This observation is supported by some recent data regarding the hormone-dependent activation of specific matrix metalloproteinase subfamilies. These enzymes play a key role in vascular smooth muscle cell migration and remodeling. It was shown that male (T and DHT) and female (estrogen and progesterone) sexual steroids maintain a balance between matrix metalloproteinases in vascular smooth muscle cells [183] in a gender-dependent manner.

Myogenic tone is essential for arteries to maintain optimal blood flow during hypo- and hypertension. In coronary arterioles, this ability is crucial to optimize ventricular blood flow and maintain constant perfusion for myocardium. According to our findings, both VDD and hyperandrogen states resulted in a reduction in the substantial spontaneous myogenic tone of the examined coronary segments (Fig. 10A). This observation supports the above-mentioned theory regarding altered vascular smooth muscle cell migration, as spontaneous myogenic tone involves a contraction initiated by the smooth muscle cell itself. In VDD cases, vascular smooth muscle tone

could be damaged by different mechanisms, as VD has direct regulatory effects on vascular smooth muscle growth and calcification. Under normal circumstances, VD inhibits the proliferation of vascular smooth muscle cell by acute influx of calcium into the cell and increases cellular calcification. In addition, cardiomyocytes express VDRs, which enables the conversion of calcidiol to calcitriol. In this regard, VDD could be plausible for alterations in vascular smooth muscle cell trophism [120].

Thromboxane A_2 agonist-induced maximum contraction and adenosine-induced vasodilation were decreased in the presence of VDD (Fig. 10B). On one hand, VD supplementation in AE was able to compensate for both the maximal contraction and relaxation capacities. On the other hand, VDD attenuated the adaption capacity of coronary arterioles, although T was mainly responsible for changes in relaxation capacity. We conclude that both noxa deteriorate the vessel's capability to adjust local ventricular flow to meet higher metabolic demand. If such vascular tone disturbances persist in small coronary arterioles, alterations in myocardium trophism and higher CV risk could be long-term consequences.

Tangential stress is the stress surrounding the circumference of a pipe due to a pressure gradient. As blood flow is normally laminar through most of the circulatory system, tangential wall stress is important for judging the stress profile of arteriolar walls. *In vivo*, low tangential stress or changing shear stress direction can be found in conditions of turbulent flow, which is typical in bifurcations or the presence of atherosclerosis. These mechanisms could promote endothelial shape changes, proliferation, and apoptosis. Turbulent flow also triggers the secretion of vasoconstrictive agents, coagulation, and platelet aggregation. Advanced atherosclerotic lesions with arterial stiffening and reduced flow-mediated dilatation have already been described among patients with VDD and chronic renal failure [184]. Our results could suggest a possible imbalance in laminar and turbulent flow, as tangential stress values were significantly reduced in both VD-deficient groups (Fig. 11A).

The elastic properties of the coronary arterioles are useful indicators to evaluate possible vascular remodeling. In both VD-deficient groups, the elastic modulus parameters were reduced under the same tangential wall stress (high wall shear stress value: 25 kPa, Fig. 11B). The lowest values were observed when VDD and a hyperandrogen state were present at the same time ($p < 0.01$ and 0.05, respectively). We plotted the elastic modulus against intraluminal pressure (Fig. 11C). In the lower blood

pressure range, T treatment resulted in a significant elevation in our values ($p < 0.05$), but in the high blood pressure range, VD caused a significant reduction ($p < 0.001$). To determine which wall component is responsible for the above-mentioned changes, we measured elastic density in the vessel wall (Figs. 12A and 12B). Our elastica staining results correlated well with the changes in vessel biomechanics, and corresponding significant alterations were found under the above-mentioned circumstances. Based on our results, we could conclude that VDD and AE could be responsible for the early steps of remodeling, as the elastic components of the vessel wall were altered by both noxa.

5.3 Insulin resistance of the coronary arterioles

The effects of insulin can be divided into two groups: metabolic effects, which are supposed to maintain glucose homeostasis, and non-metabolic effects, including regulation of mitogenesis and cell growth. In the vasculature, insulin is responsible for eNOS-mediated vasodilation. In the short term, this vasodilatation aids glucose distribution and promotes capillary recruitment. As a general consequence, it also improves blood flow, which protects against vascular aging and atherosclerosis. It is clear that some kind of dysregulation of insulin-dependent vasodilation could serve as an independent risk factor for cardiovascular events.

The action of insulin is mediated by two different receptors: the “classic” insulin receptor and the related IGF-1 receptor [185]. As both receptors are ligand-activated tyrosine kinases, they could initiate several phosphorylation cascades. The main characteristics of the two insulin receptors are different in some ways. On one hand, they are both expressed on cell surfaces, including endothelial cells. On the other hand, their insulin-mediated activation is concentration-specific. It was recently reported in human cells that insulin in physiological concentrations (<10 nM) selectively enhances autophosphorylation of the classic receptor. If the supraphysiological insulin concentration (>10 nM) is applied, autophosphorylation of the IGF-1 dominated over the classic receptor [92]. As hyperinsulinemia is typical in IR, the above-mentioned findings suggest that IGF-1 receptor-mediated signaling is involved in damaged

vasodilatation and eNOS activation. A recent investigation aimed to identify in bovine and porcine aortic endothelial cells which receptor pathway is a determinant of eNOS activation. Interestingly, the classic insulin receptor seems to play a key role, as high insulin dose and IGF-1 receptor inhibitors had no or little impact on eNOS activation [186, 187]. Based on these findings, we speculated that any type of dysfunction in the "classic" insulin receptor-mediated cascade might result in disturbances in insulin-mediated vasodilatation.

It has already been noted that the metabolic features of IR were present in both the hyperandrogen and VD-deficient groups due to our treatment. Our results indicated the possibility of two different, but not additive, IR mechanisms: after OGTT in VD cases, hyperinsulinemia was detected with normal blood sugar levels, and in a hyperandrogen state, high blood sugar levels were combined with slightly elevated serum insulin levels. We tested insulin-induced relaxation with an elevated concentration of insulin, as our aim was to investigate the effect of hyperinsulinemia on the typical state of IR. Some reduction in relaxation was detected after administration of a physiologic concentration of insulin (which would be normal under intact *in vivo* circumstances). After applying the supraphysiological insulin concentration (similar to hyperinsulinemia), more expressed reduction was observed, which turned into vasocontraction (negative dilatation values) at peak concentrations (Fig. 14A).

According to our immunohistology results, we suggest the following possible explanations for the observed phenomena. In hyperandrogen females with normal serum VD levels, T alone attenuated insulin-induced relaxation (Fig. 14A) but had no impact on the number of insulin receptors in the vessel wall (Figs. 14B and 14C), as the double control group had similar values. It is important to add that the HOMA IR index (Fig. 13C) was also elevated in this group, but the values could not reach significance. Therefore, the key element of IR is probably not a changed number of receptors, but specific signaling pathways of vascular insulin receptors.

One possible reason for such disturbances could be the downregulation of PI3-K-dependent insulin signaling. Normally, in the vasculature, activation of insulin receptors could maintain a balance between the PI3-K-dependent pathways, which regulate endothelial NO production, and the MAPK-dependent insulin signaling pathways, which trigger secretion of the vasoconstrictor ET-1. Another important effect of PI3-K is the stimulation of glucose uptake in insulin-responsive tissues. If PI3-K-dependent

pathways are suppressed, other pathways would dominate the microvascular response to insulin, affecting vasoconstriction (as was observed in our study) and causing hyperglycemia [188]. It was already revealed that, *in vivo*, elevated ET-1 activity is typical in coronary vessels with vulnerable or obstructive atherosclerosis. Interestingly, in porcine coronary artery rings from both genders, thromboxane A_2- and ET-1-mediated vasoconstriction was elevated by low doses of T. In parallel, endothelium-dependent relaxation of the coronary rings was diminished in not only males but also females. Transcription (actinomycin D) and translation (cycloheximide) blocking agents as well as anti-androgens (flutamide and cyproterone acetate) were unable to completely antagonize these effects, supporting the modulatory action theory of T [189].

Selective vascular IR could be a plausible reason for reduced relaxation capacities. Vascular endothelium insulin receptor knock-out mice possess normal glucose metabolism and blood pressure under normal circumstances, but if a cardiovascular risk factor arises, the characteristics of selective vascular IR will appear. The hypothesis was verified by a high salt diet challenge, after which knockout mice developed hypertension, endothelial dysfunction, and vascular IR [190]. This finding suggests that in IR cases, loss of eNOS activation is probably more important than ET-1-triggered vasoconstriction, as both mechanisms are disturbed in vascular endothelium insulin receptor knockout mice. Recent studies showed that not only NO production but also its bioavailability are diminished in IR cases, mainly due to the increased generation of reactive oxygen species and local activation of the renin–angiotensin system [191, 192]. Expression of eNOS mRNA and protein expression in transgenic mice with endothelium-targeted overexpression of a dominant-negative mutant human insulin receptor did not differ from the wild type. Furthermore, in this study, these transgenic animals were normotensive and normoglycemic, but insulin failed to produce relaxation on the thoracic aorta rings. Simultaneous overexpression of nicotinamide adenine dinucleotide phosphate oxidase isoform (Nox2 and Nox4) mRNA occurred, which could blunt the bioavailability of NO to the target cells [193]. According to recent data, T has modulatory effects on reactive oxygen species as well. In spontaneously hypertensive, ovariectomized female rats, chronic T supplementation increased the generation of reactive oxygen species throughout the activation of cytosolic nicotinamide adenine dinucleotide phosphate oxidase subunit $p47^{phox}$ and antagonized the protective action of estrogen on angiotensin II contraction and

endothelial function [194]. In this regard, chronic elevation of circulating T levels could be a plausible explanation for different insulin signaling disturbances.

In addition, VDD alone provoked altered insulin relaxation (Fig. 14A) and increased the number of vascular insulin receptors (Figs. 14B and 14C). It seems that reduced insulin receptor sensitivity could be responsible for higher HOMA IR values (Fig. 13C) and only higher insulin levels can keep postprandial glucose levels within a normal range (Fig. 13A). As an end effect, the typical characteristics of IR (hyperinsulinemia combined with receptor upregulation and functional alterations) were present in VDD cases. Within the double noxa group, the most pronounced damage was detected for insulin-induced relaxation, which was combined with the highest insulin receptor density. In this group, all features of metabolic syndrome, including increased body weight (Table 1), high postprandial glucose levels (Fig. 13A), and pronounced IR (elevated HOMA IR; Fig. 13C), were simultaneously present.

VD has several modulatory function *in vivo*, but VD supplementation has no further positive effect if serum levels are already within the normal range. On the other hand, it is well reported that VDD could lead to IR by triggering chronic inflammation. VDD promotes the upregulation of pro-inflammatory cytokines like tumor necrosis factor α, nuclear factor κB, and specific interleukins, which could trigger c-JUN *N*-terminal kinase and the inhibitor of κB kinase. These kinases can target insulin receptor substrates 1 for serine phosphorylation, which inhibits insulin receptor signaling and leads to IR [195].

In our study, VDRs were present in the vessel walls and showed similar density patterns to insulin receptors (Figs. 14D and 14E). Recent data suggests that VD could modulate insulin sensitivity, and a functional VDR element has been identified in the promoter region of the insulin receptor. This promoter region of the insulin receptor gene contains one VD response element that is activated by the VDR and RXR heterocomplex [196]. In this manner, VD levels could directly regulate insulin receptor expression through genomic interactions.

6 Conclusions

We studied the metabolic and vascular effects of hyperandrogen PCOS with and without VD deficiency in a rat model of PCOS. We also investigated the cardiometabolic effects of VD deficiency without additional AE.

I would like to briefly summarize our results below:

- ***A new hyperandrogen-deficient and VDD PCOS rat model was successfully created***

  The applied transdermal T treatment successfully produced the phenotypical changes required for diagnosis of the classic PCOS phenotype. Although VD supplementation in rats with AE partially restored ovulatory patterns, polycystic ovary morphology was still present. Meanwhile, disturbed ovarian morphology as well as estrus cycle irregularities and a reduced amount of corpus luteum could be detected among both VD-deficient groups. Although VDD alone did not affect the measured sexual steroid serum levels, changes in ovarian morphology were still present, as in the oligo-anovulatory polycystic PCOS phenotype without AE. Moreover, VDD combined with AE produced the lowest estrus cycle rates, highlighting the importance of VD supplementation in hyperandrogen PCOS women with a history of problems with conception.

- ***Major metabolic changes in VDD and AE could be observed at the same time***

  Our study revealed that both factors (in combination or alone) were able to induce the major symptoms of metabolic syndrome as well as IR. We concluded that AE had a very important role in body weight changes, as supported by the fact that 75% of obese PCOS patient suffer from AE. Neither VD supplementation nor VDD had any relevant impact on body weight gain ratio in our study. In line with some findings showing that body mass index has an inverse correlation with circulating VD levels, it is tempting to speculate that VD insufficiency might be responsible for the development of dysfunctional adipose tissue and obesity. However, recent *in vivo* studies presume the opposite: it is obesity and increased

VD uptake and reduced release across abdominal subcutaneous adipose tissue that might be responsible for lower levels of circulating VD.

- ***VDD and T treatment induced morphological and elastic remodeling of the vessel wall***

  Narrower passive inner lumina and greater wall thickness were detected in cases of VD deficiency, and the presence of T treatment worsened wall properties. Although we speculated that T treatment would provoke wall hypertrophism, our findings confirmed the opposite for coronary arterioles. One possible explanation for the AE-induced hypotrophic remodeling is the activation of different matrix metalloprotease subtypes and vascular smooth muscle cell migration rate. In addition, the contractile–relaxation range of the arterioles was reduced by VDD and AE. Damaged vascular adaptation range has a negative impact on ventricular tissue blood flow if a sudden adjustment is needed to alter metabolic needs. Reduced spontaneous tone and increased wall rigidity were characteristics of VD-deficient and T-treated vessels. The presence of both noxa led to the most disadvantageous changes in maximal relaxation capacity. Alteration of the vessel's elastic components was observed in cases of both VDD and AE, which supports the existence of early wall remodeling.

- ***VDD and AE provoked IR with different mechanisms***

  In cases of T treatment and VD supplementation, AE elevated postprandial sugar but generated neither hyperinsulinemia nor HOMA IR elevation. Insulin-induced relaxation of the coronary arterioles was also diminished, despite the fact that insulin receptor expression was unaltered. VDD, regardless of T treatment, resulted in higher postprandial insulin concentrations, elevated HOMA IR values, and reduced the insulin-induced vascular response. Moreover, in cases of VD, an elevated number of vascular insulin receptors was detected in both the endothelial and media layers of the vessel wall. This type of alteration in the number of receptors was also measurable in VDR, but the detected changes were much more significant at the media layer. Therefore, we conclude that there might be two different ways to develop IR, and when combined, they significantly worsen the vascular response to insulin.

Our results confirmed that both AE and VD could provoke undesirable vascular and metabolic alterations to coronary resistance arteries. However, we must admit that this study aimed to demonstrate early changes, and hence possible long-term interactions should be considered in further research. Our findings support previous reports suggesting the importance of treating both AE and hypovitaminosis D in PCOS in order to minimize the prevalence of metabolic and vascular complications.

7 Summary

Polycystic ovary syndrome (PCOS) affects 8–12% of fertile reproductive-aged women. Vitamin D deficiency (VDD) is a common comorbidity in hyperandrogen PCOS females (67–85%). Our aim was to study early biomechanical and metabolic alterations to the coronary resistance arterioles in hyperandrogen PCOS and VDD cases. Forty-six, 4-week-old female Wistar rats weighing 90–110 g were grouped into four groups. Twenty-four were kept on a VD-supplemented diet, and 12 of these animals received transdermal testosterone (T). Twenty-two animals went on a VDD diet, 11 of which were treated with T. Oral cholecalciferol was administered from the second week on. Sexual steroid and VD hormone levels were measured at the sixth and eighth weeks. On the sixth week, the OGTT was performed and plasma insulin and glucose levels were measured. From the sixth week on, a vaginal smear was collected and the estrus cycle was examined daily. At the end of the protocol, pressure arteriography was performed with coronary segments (diameters of 200 μm) taken from the left anterior descendent coronary artery. The inner and outer radii were measured with video microscopy. Normal myogenic tone, insulin-induced vascular reactivity, and maximal passive relaxation and constriction were calculated and statistically analyzed. Insulin receptor and VD receptor (VDR) expression were tested based on immunohistochemistry. Transdermal T treatment, VDD, and a supplemented diet resulted in appropriate hormonal changes. Rats with AE showed significant phenotypical changes in PCOS. VDD and AE had a significant impact on the wall thickness, inner lumina, maximal passive relaxant potential, thromboxane-induced contraction capacity, and myogenic tone. T treatment resulted in impaired glucose tolerance and significantly reduced insulin-induced coronary relaxation without hyperinsulinemia and reduction in the number of insulin receptors. VDD led to high postprandial insulin levels, altered HOMA IR, diminished insulin-induced relaxation, and increased the number of VDR and insulin receptors. Combination of VDD and AE resulted in the most disadvantageous vascular alterations. Insulin resistance is present both in VDD and AE, although their pathomechanisms are different. Therefore, treating AE and VDD at the same time could have cardiovascular benefits in PCOS females.

8 Összefoglalás

A policisztás ovárium szindróma (PCOS) a fogamzó képes korú nők 8-12% - át érinti; az androgén túlsúlyos betegek 67-85 %-a pedig D-vitaminhiányos is. Célunk a koszorúserek rezisztencia arterioláinak korai biomechanikai és adaptációs változásainak tanulmányozása volt a fenti állapotokban. Negyvenhat, 4 hetes, 90-110 gramm súlyú nőstény Wistar patkányt 4 csoportra osztottunk. Huszonnégy D-vitamin pótolt, míg 22 D-vitaminhiányos étrendben részesült. Mindkét csoport fele heti ötször transzdermális tesztoszteron (T) kezelést kapott. A 2. héttől a fenti étrendet orális D-vitaminpótlással egészítettük ki. A 6. héten OGTT vizsgálat, plazma inzulin és glükóz mérés történt. A 6. és 8. kezelési heten a szexuál szteroid és a D-vitamin szérum koncentrációkat megmértük. A 6. héttől napi hüvelyváladék vizsgálatot és ösztrusz cikluselemzést végeztünk. A 8. héten *in vitro* nyomás angiográfiás méréseket végeztünk a bal koszorúsér elülső leszálló ágának vég- és oldalágainak 200 mikrométeres külső átmérőjű szegmenseivel. Az erek belső és külső átmérőjét videomikroszkópos technikával mértük. Az eredményekből spontán miogén tónust, maximális passzív relaxációt és konstrikciót, valamint inzulin indukált ér reaktivitást számítottunk. Az erek inzulin és D-vitamin receptor sűrűségét immunhisztokémiai vizsgálattal határoztuk meg. A kapott eredményeket statisztikailag elemeztük. A transzdermális T kezelés és a D-vitaminmentes illetve pótolt táplálás a várt hormonális változásokat okozta. A D-vitaminhiány és az androgén túlsúly egyaránt negatívan hatott az erek falvastagságára, csökkentette belső keresztmetszetük, maximális passzív relaxációjuk, kontrakciójuk és spontán tónusuk. A T kezelés az OGTT alatt magas vércukor és normál plazma inzulin szintet okozott, melyet az erek csökkent inzulin relaxációja és változatlan inzulin receptor sűrűsége kísért. D-vitaminhiányban a normál vércukorszinthez magas posztprandiális inzulin értékek társultak, melyhez megnövekedett inzulin és D vitamin receptor sűrűsége és károsodott inzulin relaxáció párosult. A D-vitaminhiány és az androgén túlsúly együttes fennállása a koszorúsér arteriolák biomechanikai adaptációs képességeit károsítja és az érfal remodelingjét okozza. Mind a D-vitaminhiány, mind az androgén túlsúly inzulin rezisztenciát okoz, azonban feltehetőleg más mechanizmussal. A D-vitaminhiány és az androgén túlsúly egyidejű kezelése kedvezően hat a kardiovaszkuláris szövődmények kialakulására a PCOS-ben szenvedő betegekben.

9 References

1. Wolf WM, Wattick RA, Kinkade ON, Olfert MD. (2018) Geographical prevalence of polycystic ovary syndrome as determined by region and race/ethnicity. Int J Environ Res Public Health, 15(11): 2589–2602.
2. Bonora E. (2006) The metabolic syndrome and cardiovascular disease. Ann Med, 38(1): 64–80.
3. Geer EB, Shen W. (2009) Gender differences in insulin resistance, body composition, and energy balance. Gend Med, 6(Suppl 1): 60–75.
4. Moran A, Jacobs DR Jr., Steinberger J, Steffen LM, Pankow JS, Hong CP, Sinaiko AR. (2008) Changes in insulin resistance and cardiovascular risk during adolescence: establishment of differential risk in males and females. Circulation, 117(18): 2361–2368.
5. Naderpoor N, Shorakae S, Abell SK, Mousa A, Joham AE, Moran LJ, Stepto NK, Spritzer PM, Teede HJ, de Courten B. (2018) Bioavailable and free 25-hydroxyvitamin D and vitamin D binding protein in Polycystic Ovary Syndrome: Relationships with obesity and insulin resistance. J Steroid Biochem Mol Biol, 177: 209–215.
6. Wehr E, Pilz S, Schweighofer N, Giuliani A, Kopera D, Pieber TR, Obermayer-Pietsch B. (2009) Association of hypovitaminosis D with metabolic disturbances in polycystic ovary syndrome. Eur J Endocrinol, 161(4): 575–582.
7. Speca S, Napolitano C, Tagliaferri G. (2007) The pathogenetic enigma of polycystic ovary syndrome. J Ultrasound, 10(4): 153–160.
8. Azziz R, Adashi EY. (2016) Stein and Leventhal: 80 years on. Am J Obstet Gynecol, 214(2): 247 e1–247 e11.
9. Azziz R, Carmina E, Chen Z, Dunaif A, Laven JS, Legro RS, Lizneva D, Natterson-Horowtiz B, Teede HJ, Yildiz BO. (2016) Polycystic ovary syndrome. Nat Rev Dis Primers, 2: 16057: 1-18.
10. Goodman NF, Cobin RH, Futterweit W, Glueck JS, Legro RS, Carmina E. (2015) American Association of Clinical Endocrinologists, American College of Endobrinology, and Androgen Excess and PCOS Society disease state clinical

review: guide to the best practices in the evaluation and treatment of polycystic ovary syndrome—part 1. Endocr Pract, 21(11): 1291–1300.

11. Azziz R. (2018) Polycystic ovary syndrome. Obstet Gynecol, 132(2): 321–336.
12. Dumesic DA, Oberfield SE, Stener-Victorin E, Marshall JC, Laven JS, Legro RS. (2015) Scientific statement on the diagnostic criteria, epidemiology, pathophysiology, and molecular genetics of polycystic ovary syndrome. Endocr Rev, 36(5): 487–525.
13. Zhao XM, Ni RM, Huang J, Huang LL, Du SM, Ma MJ, Lin DY, Yang DZ. (2013) Study on the facial and body terminal hair growth in women in Guangdong by using modified Ferriman-Gallwey scoring system. Zhonghua Fu Chan Ke Za Zhi, 48(6): 427–431.
14. DeUgarte CM, Woods KS, Bartolucci AA, Azziz R. (2006) Degree of facial and body terminal hair growth in unselected black and white women: toward a populational definition of hirsutism. J Clin Endocrinol Metab, 91(4): 1345–1350.
15. Zhao X, Ni R, Li L, Mo Y, Huang J, Huang M, Azziz R, Yang D. (2011) Defining hirsutism in Chinese women: a cross-sectional study. Fertil Steril, 96(3): 792–796.
16. Vogeser M, Parhofer KG. (2007) Liquid chromatography tandem-mass spectrometry (LC-MS/MS)—technique and applications in endocrinology. Exp Clin Endocrinol Diabetes, 115(9): 559–570.
17. Demers LM. (2008) Testosterone and estradiol assays: current and future trends. Steroids, 73(13): 1333–1338.
18. Bui HN, Struys EA, Martens F, de Ronde W, Thienpont LM, Kenemans P, Verhoeven MO, Jakobs C, Dijstelbloem HM, Blankenstein MA. (2010) Serum testosterone levels measured by isotope dilution-liquid chromatography-tandem mass spectrometry in postmenopausal women versus those in women who underwent bilateral oophorectomy. Ann Clin Biochem, 47(Pt 3): 248–252.
19. Brennan K, Huang A, Azziz R. (2009) Dehydroepiandrosterone sulfate and insulin resistance in patients with polycystic ovary syndrome. Fertil Steril, 91(5): 1848–1852.

20. Huang A, Brennan K, Azziz R. (2010) Prevalence of hyperandrogenemia in the polycystic ovary syndrome diagnosed by the National Institutes of Health 1990 criteria. Fertil Steril, 93(6): 1938–1941.
21. Dewailly D, Robin G, Peigne M, Decanter C, Pigny P, Catteau-Jonard S. (2016) Interactions between androgens, FSH, anti-Müllerian hormone and estradiol during folliculogenesis in the human normal and polycystic ovary. Hum Reprod Update, 22(6): 709–724.
22. Dilaver N, Pellatt L, Jameson E, Ogunjimi M, Bano G, Homburg R, Mason H D, Rice S. (2019) The regulation and signalling of anti-Müllerian hormone in human granulosa cells: relevance to polycystic ovary syndrome. Hum Reprod, 34(12): 2467–2479
23. Abbara A, Eng PC, Phylactou M, Clarke SA, Hunjan T, Roberts R, Vimalesvaran S, Christopoulos G, Islam R, Purugganan K, Comninos AN, Trew GH, Salim R, Hramyka A, Owens L, Kelsey T, Dhillo WS. (2019) Anti-Müllerian hormone (AMH) in the diagnosis of menstrual disturbance due to polycystic ovarian syndrome. Front Endocrinol (Lausanne), 10: 656: 1-11.
24. Lie Fong S, Laven JSE, Duhamel A, Dewailly D. (2017) Polycystic ovarian morphology and the diagnosis of polycystic ovary syndrome: redefining threshold levels for follicle count and serum anti-Müllerian hormone using cluster analysis. Hum Reprod, 32(8): 1723–1731.
25. Hassa H, Tanir HM, Yildiz Z. (2006) Comparison of clinical and laboratory characteristics of cases with polycystic ovarian syndrome based on Rotterdam's criteria and women whose only clinical signs are oligo/anovulation or hirsutism. Arch Gynecol Obstet, 274(4): 227–232.
26. McGovern PG, Legro RS, Myers ER, Barnhart HX, Carson SA, Diamond MP, Carr BR, Schlaff WD, Coutifaris C, Steinkampf MP, Nestler JE, Gosman G, Leppert PC, Giudice LC. (2007) Utility of screening for other causes of infertility in women with "known" polycystic ovary syndrome. Fertil Steril, 87(2): 442–454.
27. Adams J, Polson DW, Franks S. (1986) Prevalence of polycystic ovaries in women with anovulation and idiopathic hirsutism. Br Med J (Clin Res Ed), 293(6543): 355–359.

28. Jonard S, Robert Y, Cortet-Rudelli C, Pigny P, Decanter C, Dewailly D. (2003) Ultrasound examination of polycystic ovaries: is it worth counting the follicles? Hum Reprod, 18(3): 598–603.
29. Carmina E, Oberfield SE, Lobo RA. (2010) The diagnosis of polycystic ovary syndrome in adolescents. Am J Obstet Gynecol, 203(3): 201 e1–201 e5.
30. Johnstone EB, Rosen MP, Neril R, Trevithick D, Sternfeld B, Murphy R, Addauan-Andersen C, McConnell D, Pera RR, Cedars MI. (2010) The polycystic ovary post-Rotterdam: a common, age-dependent finding in ovulatory women without metabolic significance. J Clin Endocrinol Metab, 95(11): 4965–4972.
31. Xu S, Hu S, Yu X, Zhang M, Yang Y. (2017) 17alphahydroxylase/17,20lyase deficiency in congenital adrenal hyperplasia: a case report. Mol Med Rep, 15(1): 339–344.
32. Yao K, Bian C, Zhao X. (2017) Association of polycystic ovary syndrome with metabolic syndrome and gestational diabetes: aggravated complication of pregnancy. Exp Ther Med, 14(2): 1271–1276.
33. Franks S. (2008) Polycystic ovary syndrome in adolescents. Int J Obes (Lond), 32(7): 1035–1041.
34. Agapova SE, Cameo T, Sopher AB, Oberfield SE. (2014) Diagnosis and challenges of polycystic ovary syndrome in adolescence. Semin Reprod Med, 32(3): 194–201.
35. Abbott DH, Dumesic DA, Franks S. (2002) Developmental origin of polycystic ovary syndrome—a hypothesis. J Endocrinol, 174(1): 1–5.
36. Crowley JW, Hall JE, Martin KA, Adams J, Taylor AE. (1993) An overview of the diagnostic considerations in polycystic ovarian syndrome. Ann N Y Acad Sci, 687: 235–241.
37. Kumar TR, Agno J, Janovick JA, Conn PM, Matzuk MM. (2003) Regulation of FSHbeta and GnRH receptor gene expression in activin receptor II knockout male mice. Mol Cell Endocrinol, 212(1–2): 19–27.
38. Abbott DH, Tarantal AF, Dumesic DA. (2009) Fetal, infant, adolescent and adult phenotypes of polycystic ovary syndrome in prenatally androgenized female rhesus monkeys. Am J Primatol, 71(9): 776–784.

39. van Rooyen D, Gent R, Barnard L, Swart AC. (2018) The in vitro metabolism of 11beta-hydroxyprogesterone and 11-ketoprogesterone to 11-ketodihydrotestosterone in the backdoor pathway. J Steroid Biochem Mol Biol, 178: 203–212.
40. Ali Hassan H, El-Gezeiry D, Nafaa TM, Baghdady I. (2001) Improved responsiveness of PCOS patients to clomiphene after CYP17a inhibitor. J Assist Reprod Genet, 18(11): 608–611.
41. Asagami T, Holmes TH, Reaven G. (2008) Differential effects of insulin sensitivity on androgens in obese women with polycystic ovary syndrome or normal ovulation. Metab: Clin Exp, 57(10): 1355–1360.
42. Allahbadia GN, Merchant R. (2011) Polycystic ovary syndrome and impact on health. Middle East Fertil Soc J, 16(1): 19–37.
43. Dumesic DA, Oberfield SE, Stener-Victorin E, Marshall JC, Laven JS, Legro RS. (2015) Scientific statement on the diagnostic criteria, epidemiology, pathophysiology, and molecular genetics of polycystic ovary syndrome. Endocr Rev, 36(5): 487–525.
44. Rutkowska AZ, Diamanti-Kandarakis E. (2016) Polycystic ovary syndrome and environmental toxins. Fertil Steril, 106(4): 948–958.
45. Mapanga RF, Essop MF. (2016) Damaging effects of hyperglycemia on cardiovascular function: spotlight on glucose metabolic pathways. Am J Physiol Heart Circ Physiol, 310(2): H153–H173.
46. Deligeoroglou E, Vrachnis N, Athanasopoulos N, Iliodromiti Z, Sifakis S, Iliodromiti S, Siristatidis C, Creatsas G. (2012) Mediators of chronic inflammation in polycystic ovarian syndrome. Gynecol Endocrinol, 28(12): 974–988.
47. Al-Jefout M, Alnawaiseh N, Al-Qtaitat A. (2017) Insulin resistance and obesity among infertile women with different polycystic ovary syndrome phenotypes. Sci Rep, 7(1): 5339: 1-9.
48. Barber TM, McCarthy MI, Wass JA, Franks S. (2006) Obesity and polycystic ovary syndrome. Clin Endocrinol (Oxf), 65(2): 137–145.
49. Cerda C, Pérez-Ayuso RM, Riquelme A, Soza A, Villaseca P, Sir-Petermann T, Espinoza M, Pizarro M, Solis N, Miquel JF. (2007) Nonalcoholic fatty liver disease in women with polycystic ovary syndrome. J Hepatol, 47(3): 412–417.

50. Spritzer PM. (2014) Polycystic ovary syndrome: reviewing diagnosis and management of metabolic disturbances. Arq Bras Endocrinol Metabol, 58(2): 182–187.
51. Cooney LG, Milman LW, Hantsoo L, Kornfield S, Sammel MD, Allison KC, Epperson CN, Dokras A. (2018) Cognitive-behavioral therapy improves weight loss and quality of life in women with polycystic ovary syndrome: a pilot randomized clinical trial. Fertil Steril, 110(1): 161–171 e1.
52. Hiam D, Moreno-Asso A, Teede HJ, Laven JSE, Stepto NK, Moran LJ, Gibson-Helm M. (2019) The genetics of polycystic ovary syndrome: an overview of candidate gene systematic reviews and genome-wide association studies. J Clin Med, 8(10): 1606: 1-17.
53. Bajuk Studen K, Pfeifer M. (2018) Cardiometabolic risk in polycystic ovary syndrome. Endocr Connect, 7(7): R238–R251.
54. Laakso M, Kuusisto J. (2014) Insulin resistance and hyperglycaemia in cardiovascular disease development. Nat Rev Endocrinol, 10(5): 293–302.
55. Hallajzadeh J, Khoramdad M, Karamzad N, Almasi-Hashiani A, Janati A, Ayubi E, Pakzad R, Sullman MJM, Safiri S. (2018) Metabolic syndrome and its components among women with polycystic ovary syndrome: a systematic review and meta-analysis. J Cardiovasc Thorac Res, 10(2): 56–69.
56. Ghaffarzad A, Amani R, Mehrzad Sadaghiani M, Darabi M, Cheraghian B. (2016) Correlation of serum lipoprotein ratios with insulin resistance in infertile women with polycystic ovarian syndrome: a case control study. Int J Fertil Steril, 10(1): 29–35.
57. Berneis K, Rizzo M, Hersberger M, Rini G, Di Fede G, Pepe I, Spinas G, Carmina E. (2009) Atherogenic forms of dyslipidaemia in women with polycystic ovary syndrome. Int J Clin Pract, 63(1): 56–62.
58. Roe A, Hillman J, Butts S, Smith M, Rader D, Playford M, Mehta NN, Dokras A. (2014) Decreased cholesterol efflux capacity and atherogenic lipid profile in young women with PCOS. J Clin Endocrinol Metab, 99(5): E841–E847.
59. Abbott DH, Rayome BH, Dumesic DA, Lewis KC, Edwards AK, Wallen K, Wilson ME, Appt SE, Levine JE. (2017) Clustering of PCOS-like traits in naturally hyperandrogenic female rhesus monkeys. Hum Reprod, 32(4): 923–936.

60. Manneras L, Cajander S, Holmang A, Seleskovic Z, Lystig T, Lonn M, Stener-Victorin E. (2007) A new rat model exhibiting both ovarian and metabolic characteristics of polycystic ovary syndrome. Endocrinology, 148(8): 3781–3791.
61. Ryan GE, Malik S, Mellon PL. (2018) Antiandrogen treatment ameliorates reproductive and metabolic phenotypes in the letrozole-induced mouse model of PCOS. Endocrinology, 159(4): 1734–1747.
62. Manneras-Holm L, Leonhardt H, Kullberg J, Jennische E, Oden A, Holm G, Hellstrom M, Lonn L, Olivecrona G, Stener-Victorin E, Lonn M. (2011) Adipose tissue has aberrant morphology and function in PCOS: enlarged adipocytes and low serum adiponectin, but not circulating sex steroids, are strongly associated with insulin resistance. J Clin Endocrinol Metab, 96(2): E304–E311.
63. Kupreeva M, Diane A, Lehner R, Watts R, Ghosh M, Proctor S, Vine D. (2019) Effect of metformin and flutamide on insulin, lipogenic and androgen-estrogen signaling, and cardiometabolic risk in a PCOS-prone metabolic syndrome rodent model. Am J Physiol Endocrinol Metab, 316(1): E16–E33.
64. Bhattacharya SM, Jha A. (2011) Prevalence and risk of metabolic syndrome in adolescent Indian girls with polycystic ovary syndrome using the 2009 ‘joint interim criteria’. J Obstet Gynaecol Res, 37(10): 1303–1307.
65. Nohara K, Laque A, Allard C, Munzberg H, Mauvais-Jarvis F. (2014) Central mechanisms of adiposity in adult female mice with androgen excess. Obesity (Silver Spring), 22(6): 1477–1484.
66. Diamanti-Kandarakis E, Dunaif A. (2012) Insulin resistance and the polycystic ovary syndrome revisited: an update on mechanisms and implications. Endocr Rev, 33(6): 981–1030.
67. Cassar S, Misso ML, Hopkins WG, Shaw CS, Teede HJ, Stepto NK. (2016) Insulin resistance in polycystic ovary syndrome: a systematic review and meta-analysis of euglycaemic-hyperinsulinaemic clamp studies. Hum Reprod, 31(11): 2619–2631.
68. Robert JJ. (1995) Methods for the measurement of insulin resistance. Hyperinsulinemic euglycemic clamp. Presse Med, 24(15): 730–744.

69. Holte J, Bergh T, Berne C, Wide L, Lithell H. (1995) Restored insulin sensitivity but persistently increased early insulin secretion after weight loss in obese women with polycystic ovary syndrome. J Clin Endocrinol Metab, 80(9): 2586–2593.
70. Stassek J, Erdmann J, Ohnolz F, Berg FD, Kiechle M, Seifert-Klauss V. (2017) C-peptide, baseline and postprandial insulin resistance after a carbohydrate-rich test meal—evidence for an increased insulin clearance in PCOS patients? Geburtshilfe Frauenheilkd, 77(1): 59–65.
71. Vicini P, Zachwieja JJ, Yarasheski KE, Bier DM, Caumo A, Cobelli C. (1999) Glucose production during an IVGTT by deconvolution: validation with the tracer-to-tracee clamp technique. Am J Physiol, 276(2): E285–E294.
72. Mishra JS, More AS, Kumar S. (2018) Elevated androgen levels induce hyperinsulinemia through increase in Ins1 transcription in pancreatic beta cells in female rats. Biol Reprod, 98(4): 520–531.
73. Baptiste CG, Battista MC, Trottier A, Baillargeon JP. (2010) Insulin and hyperandrogenism in women with polycystic ovary syndrome. J Steroid Biochem Mol Biol, 122(1–3): 42–52.
74. Benrick A, Chanclon B, Micallef P, Wu Y, Hadi L, Shelton JM, Stener-Victorin E, Wernstedt Asterholm I. (2017) Adiponectin protects against development of metabolic disturbances in a PCOS mouse model. Proc Natl Acad Sci U S A, 114(34): E7187–E7196.
75. Spranger J, Mohlig M, Wegewitz U, Ristow M, Pfeiffer AF, Schill T, Schlosser HW, Brabant G, Schofl C. (2004) Adiponectin is independently associated with insulin sensitivity in women with polycystic ovary syndrome. Clin Endocrinol (Oxf), 61(6): 738–746.
76. Cheng X, Guo J, Xie J. (2014) Association between levels of serum leptin and insulin resistance in patients with polycystic ovary syndrome. Zhonghua Liu Xing Bing Xue Za Zhi, 35(12): 1389–1391.
77. Cerf ME. (2013) Beta cell dysfunction and insulin resistance. Front Endocrinol (Lausanne), 4: 37. 1-12
78. Samson SL, Garber AJ. (2014) Metabolic syndrome. Endocrinol Metab Clin North Am, 43(1): 1–23.

79. Rojas J, Chavez M, Olivar L, Rojas M, Morillo J, Mejias J, Calvo M, Bermudez V. (2014) Polycystic ovary syndrome, insulin resistance, and obesity: navigating the pathophysiologic labyrinth. Int J Reprod Med, 2014: 719050.
80. Mukherjee S, Maitra A. (2010) Molecular & genetic factors contributing to insulin resistance in polycystic ovary syndrome. Indian J Med Res, 131: 743–760.
81. Book CB, Dunaif A. (1999) Selective insulin resistance in the polycystic ovary syndrome. J Clin Endocrinol Metab, 84(9): 3110–3126.
82. Wang N, Tan AWK, Jahn LA, Hartline L, Patrie JT, Lin S, Barrett EJ, Aylor KW, Liu Z. (2020) Vasodilatory actions of glucagon-like peptide 1 are preserved in skeletal and cardiac muscle microvasculature but not in conduit artery in obese humans with vascular insulin resistance. Diabetes Care, 43(3): 634–642.
83. Cersosimo E, DeFronzo RA. (2006) Insulin resistance and endothelial dysfunction: the road map to cardiovascular diseases. Diabetes Metab Res Rev, 22(6): 423–436.
84. Neunteufl T, Katzenschlager R, Hassan A, Klaar U, Schwarzacher S, Glogar D, Bauer P, Weidinger F. (1997) Systemic endothelial dysfunction is related to the extent and severity of coronary artery disease. Atherosclerosis, 129(1): 111–118.
85. Zeng G, Quon MJ. (1996) Insulin-stimulated production of nitric oxide is inhibited by wortmannin. Direct measurement in vascular endothelial cells. J Clin Invest, 98(4): 894–908.
86. Cersosimo E, Xu X, Upala S, Triplitt C, Musi N. (2014) Acute insulin resistance stimulates and insulin sensitization attenuates vascular smooth muscle cell migration and proliferation. Physiol Rep, 2(8): e12123: 1-10.
87. Masszi G, Buday A, Novak A, Horvath EM, Tarszabo R, Sara L, Revesz C, Benko R, Nadasy GL, Benyo Z, Hamar P, Varbiro S. (2013) Altered insulin-induced relaxation of aortic rings in a dihydrotestosterone-induced rodent model of polycystic ovary syndrome. Fertil Steril, 99(2): 573–578.
88. Banuls C, Rovira-Llopis S, Martinez de Maranon A, Veses S, Jover A, Gomez M, Rocha M, Hernandez-Mijares A, Victor VM. (2017) Metabolic syndrome enhances endoplasmic reticulum, oxidative stress and leukocyte-endothelium interactions in PCOS. Metabolism, 71: 153–162.

89. Dube R. (2016) Does endothelial dysfunction correlate with endocrinal abnormalities in patients with polycystic ovary syndrome? Avicenna J Med, 6(4): 91–102.
90. Talbott EO, Zborowski JV, Rager JR, Boudreaux MY, Edmundowicz DA, Guzick DS. (2004) Evidence for an association between metabolic cardiovascular syndrome and coronary and aortic calcification among women with polycystic ovary syndrome. J Clin Endocrinol Metab, 89(11): 5454–5461.
91. Wang Q, Cheng XL, Zhang DY, Gao XJ, Zhou L, Qin XY, Xie GY, Liu K, Qin Y, Liu BL, Qin MJ. (2013) Tectorigenin attenuates palmitate-induced endothelial insulin resistance via targeting ROS-associated inflammation and IRS-1 pathway. PLoS One, 8(6): e66417: 1-10.
92. Li G, Barrett EJ, Wang H, Chai W, Liu Z. (2005) Insulin at physiological concentrations selectively activates insulin but not insulin-like growth factor I (IGF-I) or insulin/IGF-I hybrid receptors in endothelial cells. Endocrinology, 146(11): 4690–4706.
93. Carvalho LML, Dos Reis FM, Candido AL, Nunes FFC, Ferreira CN, Gomes KB. (2018) Polycystic ovary syndrome as a systemic disease with multiple molecular pathways: a narrative review. Endocr Regul, 52(4): 208–221.
94. Ciaraldi TP, Aroda V, Mudaliar S, Chang RJ, Henry RR. (2009) Polycystic ovary syndrome is associated with tissue-specific differences in insulin resistance. J Clin Endocrinol Metab, 94(1): 157–163.
95. Skov V, Glintborg D, Knudsen S, Jensen T, Kruse TA, Tan Q, Brusgaard K, Beck-Nielsen H, Hojlund K. (2007) Reduced expression of nuclear-encoded genes involved in mitochondrial oxidative metabolism in skeletal muscle of insulin-resistant women with polycystic ovary syndrome. Diabetes, 56(9): 2349–2355.
96. Blagojevic IP, Eror T, Pelivanovic J, Jelic S, Kotur-Stevuljevic J, Ignjatovic S. (2017) Women with polycystic ovary syndrome and risk of cardiovascular disease. J Med Biochem, 36(3): 259–269.
97. Meyer ML, Malek AM, Wild RA, Korytkowski MT, Talbott EO. (2012) Carotid artery intima-media thickness in polycystic ovary syndrome: a systematic review and meta-analysis. Hum Reprod Update, 18(2): 112–126.

98. Osibogun O, Ogunmoroti O, Michos ED. (2019) Polycystic ovary syndrome and cardiometabolic risk: opportunities for cardiovascular disease prevention. Trends Cardiovasc Med, S1050–1738(19): 30128–30138.
99. Doroszewska K, Milewicz T, Mrozinska S, Janeczko J, Rokicki R, Janeczko M, Warzecha D, Marianowski P. (2019) Blood pressure in postmenopausal women with a history of polycystic ovary syndrome. Prz Menopauzalny, 18(2): 94–98.
100. Allameh Z, Rouholamin S, Adibi A, Mehdipour M, Adeli M. (2013) Does carotid intima-media thickness have relationship with polycystic ovary syndrome? Int J Prev Med, 4(11): 1266–1270.
101. Luque-Ramírez M, Mendieta-Azcona C, Alvarez-Blasco F, Escobar-Morreale HF. (2007) Androgen excess is associated with the increased carotid intima-media thickness observed in young women with polycystic ovary syndrome. Hum Reprod, 22(12): 3197–3203.
102. Erdoğan E, Akkaya M, Bacaksız A, Tasal A, Turfan M, Kul Ş, Sönmez O, Vatankulu MA, Ertaş G, Batmaz G. (2013) Subclinical left ventricular dysfunction in women with polycystic ovary syndrome: an observational study. Anatol J Cardiol, 13(8): 784–790.
103. Prelevic GM, Beijic T, Balint-Peric L, Ginsburg J. (1995) Cardiac flow velocity in women with the polycystic ovary syndrome. Clin Endocrinol, 43(6): 677–681.
104. Bentley-Lewis R, Seely E, Dunaif A. (2011) Ovarian hypertension: polycystic ovary syndrome. Endocrinol Metab Clin North Am, 40(2): 433–449, ix–x.
105. Diamanti-Kandarakis E, Alexandraki K, Piperi C, Protogerou A, Katsikis I, Paterakis T, Lekakis J, Panidis D. (2006) Inflammatory and endothelial markers in women with polycystic ovary syndrome. Eur J Clin Invest, 36(10): 691–707.
106. Muniyappa R, Yavuz S. (2013) Metabolic actions of angiotensin II and insulin: a microvascular endothelial balancing act. Mol Cell Endocrinol, 378(1–2): 59–69.
107. Connolly A, Leblanc S, Baillargeon JP. (2018) Role of lipotoxicity and contribution of the renin-angiotensin system in the development of polycystic ovary syndrome. Int J Endocrinol, 2018: 4315413: 1-13.
108. Horiuchi M, Mogi M, Iwai M. (2006) Signaling crosstalk angiotensin II receptor subtypes and insulin. Endocr J, 53(1): 1–5.

109. Chistiakov DA, Myasoedova VA, Melnichenko AA, Grechko AV, Orekhov AN. (2018) Role of androgens in cardiovascular pathology. Vasc Health Risk Manag, 14: 283–290.
110. Stanhewicz AE, Wenner MM, Stachenfeld NS. (2018) Sex differences in endothelial function important to vascular health and overall cardiovascular disease risk across the lifespan. Am J Physiol Heart Circ Physiol, 315(6): H1569–H1588.
111. Chatrath R, Ronningen KL, Severson SR, LaBreche P, Jayachandran M, Bracamonte MP, Miller VM. (2003) Endothelium-dependent responses in coronary arteries are changed with puberty in male pigs. Am J Physiol Heart Circ Physiol, 285(3): H1168–H1176.
112. Polderman KH, Stehouwer CD, van Kamp GJ, Dekker GA, Verheugt FW, Gooren LJ. (1993) Influence of sex hormones on plasma endothelin levels. Ann Intern Med, 118(6): 429–432.
113. Dambala K, Paschou SA, Michopoulos A, Siasos G, Goulis DG, Vavilis D, Tarlatzis BC. (2019) Biomarkers of endothelial dysfunction in women with polycystic ovary syndrome. Angiology, 70(9): 797–801.
114. Adams JS, Hewison M. (2010) Update in vitamin D. J Clin Endocrinol Metab, 95(2): 471–478.
115. Thomson RL, Spedding S, Buckley JD. (2012) Vitamin D in the aetiology and management of polycystic ovary syndrome. Clin Endocrinol (Oxf), 77(3): 343–350.
116. Pilz S, Verheyen N, Grübler MR, Tomaschitz A, März W. (2016) Vitamin D and cardiovascular disease prevention. Nat Rev Cardiol, 13(7): 404–417.
117. Rai V, Agrawal DK. (2017) Role of vitamin D in cardiovascular diseases. Endocrinol Metab Clin North Am, 46(4): 1039–1059.
118. Rai V, Sharma P, Agrawal S, Agrawal DK. (2017) Relevance of mouse models of cardiac fibrosis and hypertrophy in cardiac research. Mol Cell Biochem, 424(1–2): 123–145.
119. Glenn DJ, Cardema MC, Gardner DG. (2016) Amplification of lipotoxic cardiomyopathy in the VDR gene knockout mouse. J Steroid Biochem Mol Biol, 164: 292–298.

120. Mozos I, Marginean O. (2015) Links between vitamin D deficiency and cardiovascular diseases. Biomed Res Int, 2015: 109275: 1-13.
121. Gupta GK, Agrawal T, Rai V, Del Core MG, Hunter WJ 3rd, Agrawal DK. (2016) Vitamin D supplementation reduces intimal hyperplasia and restenosis following coronary intervention in atherosclerotic swine. PLoS One, 11(6): e0156857: 1-15.
122. Cheng S, Massaro JM, Fox CS, Larson MG, Keyes MJ, McCabe EL, Robins SJ, O'Donnell CJ, Hoffmann U, Jacques PF, Booth SL, Vasan RS, Wolf M, Wang TJ. (2010) Adiposity, cardiometabolic risk, and vitamin D status: the Framingham Heart Study. Diabetes, 59(1): 242–258.
123. Huang T, Afzal S, Yu C, Guo Y, Bian Z, Yang L, Millwood IY, Walters RG, Chen Y, Chen N, Gao R, Chen J, Clarke R, Chen Z, Ellervik C, Nordestgaard BG, Lv J, Li L. (2019) Vitamin D and cause-specific vascular disease and mortality: a Mendelian randomisation study involving 99,012 Chinese and 106,911 European adults. BMC Med, 17(1): 160–192.
124. Teegarden D, Donkin SS. (2009) Vitamin D: emerging new roles in insulin sensitivity. Nutr Res Rev, 22(1): 82–92.
125. Pani MA, Knapp M, Donner H, Braun J, Baur MP, Usadel KH, Badenhoop K. (2000) Vitamin D receptor allele combinations influence genetic susceptibility to type 1 diabetes in Germans. Diabetes, 49(3): 504–507.
126. Sung CC, Liao MT, Lu KC, Wu CC. (2012) Role of vitamin D in insulin resistance. J Biomed Biotechnol, 2012: 634195: 1-11.
127. Dong B, Zhou Y, Wang W, Scott J, Kim KH, Sun Z, Guo Q, Lu Y, Gonzales NM, Wu H, Hartig S, York RB, Yang F, Moore DD. (2019) Vitamin D receptor activation in liver macrophages ameliorates hepatic inflammation, steatosis, and insulin resistance in mice. Hepatology. 2019 Sep 11. doi: 10.1002/hep.30937. Online ahead of print.
128. Parikh G, Varadinova M, Suwandhi P, Araki T, Rosenwaks Z, Poretsky L, Seto-Young D. (2010) Vitamin D regulates steroidogenesis and insulin-like growth factor binding protein-1 (IGFBP-1) production in human ovarian cells. Horm Metab Res, 42(10): 754–767.

129. Merhi Z, Doswell A, Krebs K, Cipolla M. (2014) Vitamin D alters genes involved in follicular development and steroidogenesis in human cumulus granulosa cells. J Clin Endocrinol Metab, 99(6): E1137–E1145.
130. Bakhshalizadeh S, Amidi F, Alleyassin A, Soleimani M, Shirazi R, Shabani Nashtaei M. (2017) Modulation of steroidogenesis by vitamin D3 in granulosa cells of the mouse model of polycystic ovarian syndrome. Syst Biol Reprod Med, 63(3): 150–161.
131. Lee CT, Wang JY, Chou KY, Hsu MI. (2014) 1,25-Dihydroxyvitamin D3 increases testosterone-induced 17beta-estradiol secretion and reverses testosterone-reduced connexin 43 in rat granulosa cells. Reprod Biol Endocrinol, 12(1): 90: 1-12.
132. Lerchbaum E, Rabe T. (2014) Vitamin D and female fertility. Curr Opin Obstet Gynecol, 26(3): 145–150.
133. Paixao L, Ramos RB, Lavarda A, Morsh DM, Spritzer PM. (2017) Animal models of hyperandrogenism and ovarian morphology changes as features of polycystic ovary syndrome: a systematic review. Reprod Biol Endocrinol, 15(1): 12: 1-11.
134. Wu XY, Li ZL, Wu CY, Liu YM, Lin H, Wang SH, Xiao WF. (2010) Endocrine traits of polycystic ovary syndrome in prenatally androgenized female Sprague-Dawley rats. Endocr J, 57(3): 201–209.
135. Tyndall V, Broyde M, Sharpe R, Welsh M, Drake AJ, McNeilly AS. (2012) Effect of androgen treatment during foetal and/or neonatal life on ovarian function in prepubertal and adult rats. Reproduction, 143(1): 21–33.
136. Familiari G, Toscano V, Motta PM. (1985) Morphological studies of polycystic mouse ovaries induced by dehydroepiandrosterone. Cell Tissue Res, 240(3): 519–528.
137. Billiar RB, Richardson D, Anderson E, Mahajan D, Little B. (1985) The effect of chronic and acyclic elevation of circulating androstenedione or estrone concentrations on ovarian function in the rhesus monkey. Endocrinology, 116(6): 2209–2220.
138. Kafali H, Iriadam M, Ozardali I, Demir N. (2004) Letrozole-induced polycystic ovaries in the rat: a new model for cystic ovarian disease. Arch Med Res, 35(2): 103–108.

139. Fernandez M, Bourguignon N, Lux-Lantos V, Libertun C. (2010) Neonatal exposure to bisphenol a and reproductive and endocrine alterations resembling the polycystic ovarian syndrome in adult rats. Environ Health Perspect, 118(9): 1217–1222.
140. Kang X, Jia L, Shen X. (2015) Manifestation of hyperandrogenism in the continuous light exposure-induced PCOS rat model. Biomed Res Int, 2015: 943694:11-24.
141. Ryu Y, Kim SW, Kim YY, Ku SY. (2019) Animal models for human polycystic ovary syndrome (PCOS) focused on the use of indirect hormonal perturbations: a review of the literature. Int J Mol Sci, 20(11): 2720–2747.
142. Walters KA, Allan CM, Handelsman DJ. (2012) Rodent models for human polycystic ovary syndrome. Biol Reprod, 86(5): 149: 1–12.
143. Barry JA, Kay AR, Navaratnarajah R, Iqbal S, Bamfo JEAK, David AL, Hines M, Hardiman PJ. (2010) Umbilical vein testosterone in female infants born to mothers with polycystic ovary syndrome is elevated to male levels. J Obstet Gynaecol, 30(5): 444–446.
144. Masszi G, Benko R, Csibi N, Horvath EM, Tokes AM, Novak A, Beres NJ, Tarszabo R, Buday A, Repas C, Bekesi G, Patocs A, Nadasy GL, Hamar P, Benyo Z, Varbiro S. (2013) Endothelial relaxation mechanisms and nitrative stress are partly restored by vitamin D3 therapy in a rat model of polycystic ovary syndrome. Life Sci, 93(4): 133–138.
145. Masszi G, Novak A, Tarszabo R, Horvath EM, Buday A, Ruisanchez E, Tokes AM, Sara L, Benko R, Nadasy GL, Revesz C, Hamar P, Benyo Z, Varbiro S. (2013) Effects of vitamin D3 derivative—calcitriol on pharmacological reactivity of aortic rings in a rodent PCOS model. Pharmacol Rep, 65(2): 476–483.
146. Sara L, Nadasy GL, Antal P, Monori-Kiss A, Szekeres M, Masszi G, Monos E, Varbiro S. (2012) Pharmacological reactivity of resistance vessels in a rat PCOS model—vascular effects of parallel vitamin D(3) treatment. Gynecol Endocrinol, 28(12): 961–964.
147. Sara L, Nadasy G, Antal P, Szekeres M, Monori-Kiss A, Horvath EM, Tokes AM, Masszi G, Monos E, Varbiro S. (2012) Arteriolar biomechanics in a rat

polycystic ovary syndrome model—effects of parallel vitamin D3 treatment. Acta Physiol Hung, 99(3): 279–288.

148. Kim MK, Lee CH, Kim DD. (2000) Skin permeation of testosterone and its ester derivatives in rats. J Pharm Pharmacol, 52(4): 369–375.

149. Huang-Doran I, Franks S. (2016) Genetic rodent models of obesity-associated ovarian dysfunction and subfertility: insights into polycystic ovary syndrome. Front Endocrinol (Lausanne), 7: 53. 1-10.

150. Nelson RE, Grebe SK, O'Kane DJ, Singh RJ. (2004) Liquid chromatography-tandem mass spectrometry assay for simultaneous measurement of estradiol and estrone in human plasma. Clin Chem, 50(2): 373–384.

151. Wang Q, Bottalico L, Mesaros C, Blair IA. (2015) Analysis of estrogens and androgens in postmenopausal serum and plasma by liquid chromatography-mass spectrometry. Steroids, 99(Pt A): 76–83.

152. Baumann M, Janssen BJ, Hermans JJ, Peutz-Kootstra C, Witzke O, Smits JF, Struijker Boudier HA. (2007) Transient AT1 receptor-inhibition in prehypertensive spontaneously hypertensive rats results in maintained cardiac protection until advanced age. J Hypertens, 25(1): 207–215.

153. Miklos Z, Kemecsei P, Biro T, Marincsak R, Toth BI, Op den Buijs J, Benis E, Drozgyik A, Ivanics T. (2012) Early cardiac dysfunction is rescued by upregulation of SERCA2a pump activity in a rat model of metabolic syndrome. Acta Physiol (Oxf), 205(3): 381–393.

154. Parasuraman S, Raveendran R. (2012) Measurement of invasive blood pressure in rats. J Pharmacol Pharmacother, 3(2): 172-177.

155. Joham AE, Teede HJ, Cassar S, Stepto NK, Strauss BJ, Harrison CL, Boyle J, de Courten B. (2016) Vitamin D in polycystic ovary syndrome: relationship to obesity and insulin resistance. Mol Nutr Food Res, 60(1): 110–118.

156. Krul-Poel YH, Snackey C, Louwers Y, Lips P, Lambalk CB, Laven JS, Simsek S. (2013) The role of vitamin D in metabolic disturbances in polycystic ovary syndrome: a systematic review. Eur J Endocrinol, 169(6): 853–865.

157. Kotsa K, Yavropoulou MP, Anastasiou O, Yovos JG. (2009) Role of vitamin D treatment in glucose metabolism in polycystic ovary syndrome. Fertil Steril, 92(3): 1053–1068.

158. Mishra S, Das AK, Das S. (2016) Hypovitaminosis D and associated cardiometabolic risk in women with PCOS. J Clin Diagn Res, 10(5): BC01–BC04.
159. Lakshman KM, Basaria S. (2009) Safety and efficacy of testosterone gel in the treatment of male hypogonadism. Clin Interv Aging, 4: 397–412.
160. Ainbinder D, Touitou E. (2005) Testosterone ethosomes for enhanced transdermal delivery. Drug Deliv, 12(5): 297–303.
161. Azziz R, Carmina E, Dewailly D, Diamanti-Kandarakis E, Escobar-Morreale HF, Futterweit W, Janssen OE, Legro RS, Norman RJ, Taylor AE, Witchel SF. (2009) The Androgen Excess and PCOS Society criteria for the polycystic ovary syndrome: the complete task force report. Fertil Steril, 91(2): 456–488.
162. Teede HJ, Misso ML, Costello MF, Dokras A, Laven J, Moran L, Piltonen T, Norman RJ. (2018) Recommendations from the international evidence-based guideline for the assessment and management of polycystic ovary syndrome. Hum Reprod, 33(9): 1602–1618.
163. Irani M, Merhi Z. (2014) Role of vitamin D in ovarian physiology and its implication in reproduction: a systematic review. Fertil Steril, 102(2): 460–468 e3.
164. Kokanali D, Karaca M, Ozaksit G, Elmas B, Engin Ustun Y. (2019) Serum vitamin D levels in fertile and infertile women with polycystic ovary syndrome. Geburtshilfe Frauenheilkd, 79(5): 510–516.
165. Pigny P, Merlen E, Robert Y, Cortet-Rudelli C, Decanter C, Jonard S, Dewailly D. (2003) Elevated serum level of anti-Müllerian hormone in patients with polycystic ovary syndrome: relationship to the ovarian follicle excess and to the follicular arrest. J Clin Endocrinol Metab, 88(12): 5957–5962.
166. Irani M, Minkoff H, Seifer DB, Merhi Z. (2014) Vitamin D increases serum levels of the soluble receptor for advanced glycation end products in women with PCOS. J Clin Endocrinol Metab, 99(5): E886–E890.
167. Cappy H, Giacobini P, Pigny P, Bruyneel A, Leroy-Billiard M, Dewailly D, Catteau-Jonard S. (2016) Low vitamin D3 and high anti-Müllerian hormone serum levels in the polycystic ovary syndrome (PCOS): is there a link? Ann Endocrinol (Paris), 77(5): 593–599.

168. DeUgarte CM, Bartolucci AA, Azziz R. (2005) Prevalence of insulin resistance in the polycystic ovary syndrome using the homeostasis model assessment. Fertil Steril, 83(5): 1454–1460.
169. Pal L, Zhang H, Williams J, Santoro NF, Diamond MP, Schlaff WD, Coutifaris C, Carson SA, Steinkampf MP, Carr BR, McGovern PG, Cataldo NA, Gosman GG, Nestler JE, Myers E, Legro RS. (2016) Vitamin D status relates to reproductive outcome in women with polycystic ovary syndrome: secondary analysis of a multicenter randomized controlled trial. J Clin Endocrinol Metab, 101(8): 3027–3035.
170. Jukic AM, Upson K, Harmon QE, Baird DD. (2016) Increasing serum 25-hydroxyvitamin D is associated with reduced odds of long menstrual cycles in a cross-sectional study of African American women. Fertil Steril, 106(1): 172–179 e2.
171. Gambineri A, Laudisio D, Marocco C, Radellini S, Colao A, Savastano S. (2019) Female infertility: which role for obesity? Int J Obes Suppl, 9(1): 65–72.
172. Kong J, Chen Y, Zhu G, Zhao Q, Li YC. (2013) 1,25-dihydroxyvitamin D3 upregulates leptin expression in mouse adipose tissue. J Endocrinol, 216(2): 265–271.
173. Savastano S, Valentino R, Di Somma C, Orio F, Pivonello C, Passaretti F, Brancato V, Formisano P, Colao A, Beguinot F, Tarantino G. (2011) Serum 25-hydroxyvitamin D levels, phosphoprotein enriched in diabetes gene product (PED/PEA-15) and leptin-to-adiponectin ratio in women with PCOS. Nutr Metab (Lond), 8: 84–105.
174. Farr OM, Gavrieli A, Mantzoros CS. (2015) Leptin applications in 2015: what have we learned about leptin and obesity? Curr Opin Endocrinol Diabetes Obes, 22(5): 353–359.
175. Oda N, Imamura S, Fujita T, Uchida Y, Inagaki K, Kakizawa H, Hayakawa N, Suzuki A, Takeda J, Horikawa Y, Itoh M. (2008) The ratio of leptin to adiponectin can be used as an index of insulin resistance. Metabolism, 57(2): 268–273.
176. Macut D, Mladenovic V, Bjekic-Macut J, Livadas S, Stanojlovic O, Hrncic D, Rasic-Markovic A, Milutinovic DV, Andric Z. (2020) Hypertension in polycystic ovary syndrome: novel insights. Curr Hypertens Rev, 16(1): 55–60.

177. Legarth C, Grimm D, Wehland M, Bauer J, Kruger M. (2018) The impact of vitamin D in the treatment of essential hypertension. Int J Mol Sci, 19(2): 455–483.
178. Bozic M, Alvarez A, de Pablo C, Sanchez-Nino MD, Ortiz A, Dolcet X, Encinas M, Fernandez E, Valdivielso JM. (2015) Impaired vitamin D signaling in endothelial cell leads to an enhanced leukocyte-endothelium interplay: implications for atherosclerosis development. PLoS One, 10(8): e0136863: 1-20
179. Torres Fernandez ED, Adams KV, Syed M, Maranon RO, Romero DG, Yanes Cardozo LL. (2018) Long-lasting androgen-induced cardiometabolic effects in polycystic ovary syndrome. J Endocr Soc, 2(8): 949–964.
180. Lakhani K, Hardiman P, Seifalian AM. (2004) Intima-media thickness of elastic and muscular arteries of young women with polycystic ovaries. Atherosclerosis, 175(2): 353–359.
181. Lakhani K, Leonard A, Seifalian AM, Hardiman P. (2005) Microvascular dysfunction in women with polycystic ovary syndrome. Hum Reprod, 20(11): 3219–3224.
182. Folkow B. (1995) Hypertensive structural changes in systemic precapillary resistance vessels: how important are they for in vivo haemodynamics? J Hypertens, 13(12 Pt 2): 1546–1559.
183. Grandas OH, Mountain DJ, Kirkpatrick SS, Rudrapatna VS, Cassada DC, Stevens SL, Freeman MB, Goldman MH. (2008) Effect of hormones on matrix metalloproteinases gene regulation in human aortic smooth muscle cells. J Surg Res, 148(1): 94–99.
184. Davies MR, Hruska KA. (2001) Pathophysiological mechanisms of vascular calcification in end-stage renal disease. Kidney Int, 60(2): 472–479.
185. Duckles SP, Miller VM. (2010) Hormonal modulation of endothelial NO production. Pflugers Arch, 459(6): 841–851.
186. Kuboki K, Jiang ZY, Takahara N, Ha SW, Igarashi M, Yamauchi T, Feener EP, Herbert TP, Rhodes CJ, King GJ. (2000) Regulation of endothelial constitutive nitric oxide synthase gene expression in endothelial cells and in vivo: a specific vascular action of insulin. Circulation, 101(6): 676–681.

187. Fisslthaler B, Benzing T, Busse R, Fleming I. (2003) Insulin enhances the expression of the endothelial nitric oxide synthase in native endothelial cells: a dual role for Akt and AP-1. Nitric Oxide, 8(4): 253–261.

188. Muniyappa R, Sowers JR. (2013) Role of insulin resistance in endothelial dysfunction. Rev Endocr Metab Disord, 14(1): 5–12.

189. Teoh H, Quan A, Man RY. (2000) Acute impairment of relaxation by low levels of testosterone in porcine coronary arteries. Cardiovasc Res, 45(4): 1010–1018.

190. Vicent D, Ilany J, Kondo T, Naruse K, Fisher SJ, Kisanuki YY, Bursell S, Yanagisawa M, King GL, Kahn CR. (2003) The role of endothelial insulin signaling in the regulation of vascular tone and insulin resistance. J Clin Invest, 111(9): 1373–1380.

191. Picchi A, Gao X, Belmadani S, Potter BJ, Focardi M, Chilian WM, Zhang C. (2006) Tumor necrosis factor-alpha induces endothelial dysfunction in the prediabetic metabolic syndrome. Circ Res, 99(1): 69–77.

192. Watt NT, Gage MC, Patel PA, Viswambharan H, Sukumar P, Galloway S, Yuldasheva NY, Imrie H, Walker AMN, Griffin KJ, Makava N, Skromna A, Bridge K, Beech DJ, Schurmans S, Wheatcroft SB, Kearney MT, Cubbon RM. (2017) Endothelial SHIP2 suppresses Nox2 NADPH oxidase-dependent vascular oxidative stress, endothelial dysfunction, and systemic insulin resistance. Diabetes, 66(11): 2808–2821.

193. Duncan ER, Crossey PA, Walker S, Anilkumar N, Poston L, Douglas G, Ezzat VA, Wheatcroft SB, Shah AM, Kearney MT. (2008) Effect of endothelium-specific insulin resistance on endothelial function in vivo. Diabetes, 57(12): 3307–3314.

194. Costa TJ, Ceravolo GS, dos Santos RA, de Oliveira MA, Araujo PX, Giaquinto LR, Tostes RC, Akamine EH, Fortes ZB, Dantas AP, Carvalho MH. (2015) Association of testosterone with estrogen abolishes the beneficial effects of estrogen treatment by increasing ROS generation in aorta endothelial cells. Am J Physiol Heart Circ Physiol, 308(7): H723–H732.

195. Chagas CE, Borges MC, Martini LA, Rogero MM. (2012) Focus on vitamin D, inflammation and type 2 diabetes. Nutrients, 4(1): 52–67.

196. Zaulkffali AS, Md Razip NN, Syed Alwi SS, Abd Jalil A, Abd Mutalib MS, Gopalsamy B, Chang SK, Zainal Z, Ibrahim NN, Zakaria ZA, Khaza'ai H.

(2019) Vitamins D and E stimulate the PI3K-AKT signalling pathway in insulin-resistant SK-N-SH neuronal cells. Nutrients, 11(10): 2525–2560.

10 Publications

The thesis is based on the following publications:

1. **Hadjadj L**, Monori-Kiss A, Horváth EM, Heinzlmann A, Magyar A, Sziva RE, Miklós Z, Pál É, Gál J, Szabó I, Benyó Z, Nádasy GL, Várbíró S. (2019) Geometric, elastic and contractile-relaxation changes in coronary arterioles induced by Vitamin D deficiency in normal and hyperandrogenic female rats. Microvasc Res, 122: 78–84 . IF: 2,604

2. **Hadjadj L,** Várbíró S, Horváth EM, Monori-Kiss A, Pál É, Karvaly GB, Heinzlmann A, Magyar A, Szabó I, Sziva RE, Benyó Z, Buday M, and Nádasy GL. (2018) Insulin resistance in an animal model of polycystic ovary disease is aggravated by vitamin D deficiency: Vascular consequences. Diab Vasc Dis Res, 15(4): 294-301 IF: 2,357

Other publications:

Hadjadj L, Pál É, Monori-Kiss A, Sziva RE, Korsós-Novák Á, Horváth EM, Benkő R, Magyar A, Magyar P, Benyó Z, Nádasy GL and Várbíró S. (2019) Vitamin D deficiency and androgen excess result eutrophic remodeling and reduced myogenic adaptation in small cerebral arterioles in female rats. Gynecol Endocrinol, 35(6): 529–534. IF: 1,406

Lajtai K, Nagy CT, Tarszabó R, Benkő R, **Hadjadj L**, Sziva RE, Gerszi D, Bányai B, Ferdinandy P, Nádasy GL, Giricz Z, Horváth EM, Várbíró S. (2019) Effects of vitamin D deficiency on proliferation and autophagy of ovarian and liver tissues in a rat model of polycystic ovary syndrome. Biomolecules, 9(9): 471-485. IF: 4,694

Pál É*, **Hadjadj L***, Fontányi Z, Monori-Kiss A, Lippai N, Horváth EM, Magyar A, Horváth E, Monos E, Nadasy GL, Benyó Z, Várbíró S. (2019)

Gender, hyperandrogenism and vitamin D deficiency related functional and morphological alterations of rat cerebral arteries. PLoS One, 14(5): e0216951: 1-13. IF: 2,776

Pál É, **Hadjadj L**, Fontányi Z; Monori-Kiss A; Mezei Z; Lippai N; Magyar A; Heinzlmann A, Karvaly GB, Monos, E, Nádasy GL, Várbíró S. (2018) Vitamin D deficiency causes inward hypertrophic remodeling and alters vascular reactivity of rat cerebral arterioles. PLoS One, 13(2): e0192480, 1-16. IF: 2,776

11 Acknowledgements

This study was carried out at the Institute of Human Physiology and Clinical Experimental Research, Semmelweis University, Budapest, in 2014 and 2015.

I want to express my thanks to my project leader, ***Szabolcs Várbíró***, Associate Professor of the 2nd Department of Obstetrics and Gynecology, who managed my studies and provided me his valuable professional support. He was always ready to discuss my technical and theoretical questions and sacrifice his spare time for the purpose of the study.

I want to express my thanks to ***György L. Nádasy***, Associate Professor of the Department of Physiology, who taught me the methods of vessel micropreparation and introduced me to special methods of microangiometric measurement and experimental processes. His help was invaluable during the study and evaluation of the results.

I wish to thank to ***Professor Zoltán Benyó***, Director of the Institute of Human Physiology and Clinical Experimental Research, for helping to design and finish this study.

I am very grateful to ***Professor Emil Monos*** for giving us the opportunity to carry out this project in his laboratory.

I want to express my thanks to ***Anna Monori-Kiss***, who was always there to help when technical and methodological questions occurred and showed me the methods of pressure angiometric measurements.

I want to convey my thanks to ***Eszter M. Horváth*** for her help, kind advice, professional support, and help with technical problems.

I am really thankful to ***Professor János Gál***, Director of the Department of Anesthesiology and Intensive Therapy, Semmelweis University, who permitted me to be a full-time PhD student for two years.

I wish to express my gratitude to ***Ildikó Murányi*** for her devoted efforts to solve technical problems during the laboratory work.

I am very grateful to ***Éva Pál***, ***Réka E. Sziva***, ***Attila Magyar***, ***Andrea Heinzlmann***, ***Anna Buday***, ***Lilla Lénárt***, ***Mária Szekeres***, ***Zsuzsanna Miklós***, ***Gellért B. Karvaly***, ***Attila Patócs***, ***Marianna Buday***, ***Anna-Mária Tőkés***, ***Ágnes Korsós-Novák, Péter Magyar***, and ***Rita Benkő*** for their help and effort.

I express my gratitude and thanks to my beloved husband, ***András***, who spent hours in the lab with me, supported me emotionally, and showed me patience and love. I wish to thank my beautiful daughter, ***Elisa***, who was born during my PhD studies. I am thankful for my mother, ***Andrea***, who gave me a love for physiology as a teenager, and my stepfather ***Lajos***, who sadly passed away before the end of my studies. I would also like to say thank you to my sister, ***Amina***, and my colleagues for their encouragement and support during my work.